# MECHANISMS OF THE MRTF-A CONTROLLED MYOFIBROBLASTIC DIFFERENTIATION AND ITS INFLUENCE ON THE TUMOUR PROPAGATING FUNCTION OF MESENCHYMAL STROMAL CELLS

Dissertation

submitted in partial fulfilment of the requirements for the degree of „Doctor rerum naturalium” (Dr. rer. nat.) at the

**Faculty of Natural Sciences I**

- Life Sciences -

of Martin-Luther-University Halle-Wittenberg

Doctoral defence: 12.05.2025

**Sara Werner**

[redacted]

Reviewers:

Prof. Dr. Guido Posern

apl. Prof. Lutz P. Müller

Prof. Dr. med. Dr. rer. nat. Wolfgang Wagner

Zörbig, Oktober 2024

# Copyright notification

# TABLE OF CONTENTS

# I SUMMARY

Tumour growth and metastasis are complex processes in cancer development, significantly influenced by the tumour stroma across all cancer types. Among the several components of the tumour microenvironment, cancer-associated fibroblasts (CAF) play a crucial role by secreting extracellular matrix proteins, cytokines, and proteases. Multipotent mesenchymal stromal cells (MSC) are considered precursors of CAF, residing in a perivascular niche, and have been shown to promote the growth of colorectal cancer (CRC). Tumour-cell-derived factors, like cytokines e.g. transforming growth factor β1 (TGF-β1), have been hypothesised to induce the myofibroblastic differentiation of precursor cells like MSC into CAF. This differentiation process is associated with significant actin remodelling and increased expression of marker genes. In this thesis, I demonstrate that primary human bone marrow-derived MSC from different donors differentiate into CAF when stimulated with TGF-β1 or tumour-conditioned medium (TCM) within 48 h. The TCM was conditioned by HCT8 colorectal cancer cells. Both recombinant TGF-β1 and TCM increased the expression of myofibroblastic marker genes, including alpha-smooth muscle actin (α-SMA), Calponin 1, and collagen 1A1 (COL1A1), at both mRNA and protein levels. The effect of TCM on MSC was shown to involve Alk5 receptor kinase activity, as evidenced by SMAD2 (Mothers against decapentaplegic homolog 2) western blot analysis using Repsox, an ALK5 (Activin A receptor type II-like protein kinase) inhibitor. Most importantly, the myocardin-related transcription factor A (MRTF-A) was identified as a key regulator of myofibroblastic MSC to CAF differentiation in vitro. MRTF-A activation during differentiation was confirmed by fluorescence microscopy translocation assays and luciferase reporter assays, both of which showed comparable activation upon stimulation with TGF-β1 and TCM. The luciferase reporter construct was designed as part of the thesis. Further MRTF-A knockdown experiments using siRNA and shRNA revealed that MRTF-A is essential for TGF-β1 and TCM-induced expression of α-SMA and Calponin 1, but not COL1A1. Additionally, in vivo experiments showed that MRTF-A knockdown reduced xenograft growth of CRC. The results suggest a critical role for MRTF-A in the functional differentiation of MSC to CAF and their subsequent support of CRC tumour growth in vivo. However, MRTF-A knockdown did not completely abolish xenograft growth, indicating that other mechanisms beyond MRTF-A may also contribute to MSC to CAF differentiation and tumour growth. Future studies should focus on investigating additional signalling pathways, particularly those regulating COL1A1, to fully understand the role of MSC in early tumour support.

# II ZUSAMMENFASSUNG

Tumorwachstum und Metastasierung sind komplexe Prozesse der Karzinogenese, die maßgeblich vom Tumorstroma beeinflusst werden. Unter den vielfältigen Komponenten des Tumormikromilieus spielen vor allem Krebs-assoziierte Fibroblasten (CAF) eine große Rolle, da sie extrazelluläre Matrixproteine, Zytokine und Proteasen sekretieren. Multipotente mesenchymale Stromazellen (MSC) gelten als Vorläufer von CAF. Sie überdauern in einer perivaskulären Nische und fördern nachweislich das Wachstum von kolorektalen Karzinomzellen (CRC). Tumor sekretierte Zytokine, wie beispielsweise *transforming growth factor β1* (TGF-β1), wurden als mögliche Induktoren der myofibroblastären Differenzierung von Vorläuferzellen wie MSC zu CAF beschrieben. Dieser Prozess ist mit signifikanten Umbauprozessen des Aktinzytoskeletts und einer erhöhten Expression von Markern verbunden. Die vorliegende Dissertation zeigt, dass sich MSC bei der Stimulation mit TGF-β1 oder HCT8 tumorkonditioniertem Medium (TCM) innerhalb von 48 h in CAF differenzieren. Sowohl rekombinantes TGF-β1 als auch TCM erhöhten die Markerexpression auf mRNA- und Proteinebene, darunter *alpha-smooth muscle actin* (α SMA), Calponin 1 und Kollagen 1A1 (COL1A1). Die TCM-Wirkung auf MSC ist mit der Aktivität der Alk5-Rezeptorkinase verbunden, wie durch eine SMAD2-Western-Blot-Analyse unter Verwendung von Repsox, einem ALK5-Inhibitor (*Activin A receptor type II-like protein kinase*), nachgewiesen wurde. Besonders hervorzuheben ist, dass MRTF-A (*myocardin-related transcription factor A*) als Schlüsselregulator der Differenzierung von MSC zu CAF *in vitro* identifiziert wurde. Die Aktivierung von MRTF-A wurde durch Fluoreszenzmikroskopie und Luciferase-Reporter-Analysen bestätigt. Nach Stimulation mit TGF-β1 oder TCM zeigten beide Experimente eine vergleichbare Aktivierung von MRTF-A. Die Erstellung des Luciferase-Reporterkonstrukts war Teil dieser Dissertation. Weiterführende MRTF-A-*Knockdown*-Experimente mit si- und shRNA zeigten, dass MRTF-A essenziell für die TGF-β1- und TCM-induzierte Expression von α-SMA und Calponin 1 ist, COL1A1 davon jedoch unbeeinflusst bleibt. *In-vivo*-Experimente demonstrierten, dass der MRTF-A-*Knockdown* das Xenograft-Wachstum von CRC reduzierte. Damit konnte diese Arbeit eine entscheidende Rolle von MRTF-A bei der funktionellen Differenzierung von MSC zu CAF und deren Unterstützung des CRC-Tumorwachstums *in vivo* belegen. Allerdings wurde durch den MRTF-A *Knockdown* das Xenograft-Wachstum nicht gänzlich aufgehoben. Dies deutet darauf hin, dass neben MRTF-A auch andere Mechanismen zur Differenzierung von MSC zu CAF und zum Tumorwachstum beitragen könnten. Zukünftige Studien sollten sich demnach auf die Untersuchung zusätzlicher Signalwege konzentrieren, insbesondere die COL1A1 regulierenden, um die Rolle von MSC bei der frühen Tumorentwicklung vollständig zu verstehen.

# 1 INTRODUCTION

*"To eventually win the war on cancer, and meanwhile to win more battles against particular forms of cancer, we need to better understand the enemy."*

Douglas Hanahan, Presentation at Technion Integrated Cancer Centre, Israel, 2016

## 1.1 Cancer and carcinogenesis

### 1.1.1 General characteristics

Cancer is a disease where normal cells begin to divide abnormally without any control and can invade nearby tissues in any organ. In 2018 9.6 million people worldwide are estimated to have died from cancer, whereby colorectal, lung and liver cancer are most common among men and women (WHO 2021).

The transformation from normal to malignant cells can be triggered by outside noxa e.g. pollutant burden, radiation, inappropriate diet and physical activity or even by genetic predisposition. Those factors lead to genetic mutations that occasionally cause growth advantages compared to normal cells. Taking advantage of mutations, tumour development follows a process, formally analogous to Darwinian rules (Foulds 1954, Nowell 1976). Hanahan and Weinberg became famous describing the *hallmarks of cancer* as "rules that govern the transformation of normal human cells into malignant cancer" (Hanahan and Weinberg 2000). The six common traits shared by all types of cancer are (1) self-sufficiency in growth signals, (2) insensitivity to anti-growth signals, (3) tissue invasion and metastasis, (4) limitless replicative potential, (5) sustained angiogenesis (6) evading apoptosis (see Figure 1).

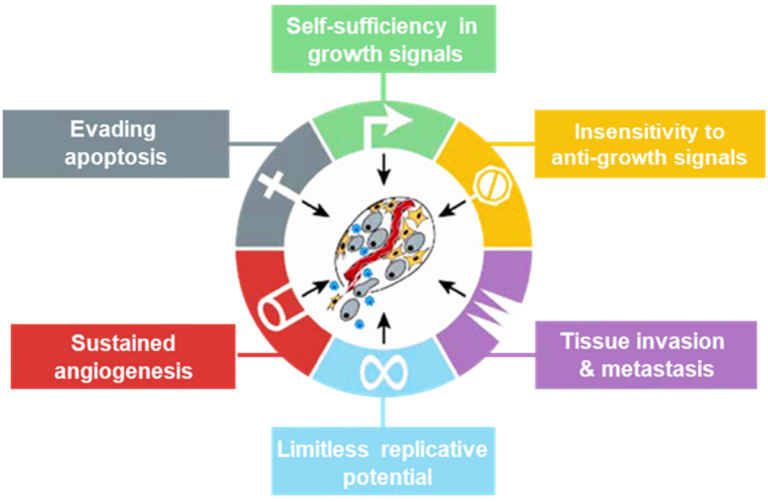


**Figure 1: The hallmarks of cancer**
The illustration shows the six hallmarks of cancer.
Modified according to (Hanahan and Weinberg 2000).

### 1.1.2 The tumour microenvironment – cell types, cytokines and micro-RNA

Over the years cancer research changed massively from focussing on cancer cells themselves to including surrounding tissue, considering the cancerous condition as a bigger entity. David W. Smithers, a British pioneer in cancer radiotherapy, already outlined in 1962 that *"Cancer is a disease of organisation, not a disease of cells […]. The main task of this science is to analyse the reactions between one cell or tissue and another and of both to the outside world, and to learn to foresee their repercussions as far as possible, even though some of them may well be unforseeable.*" (Smithers 1962). Consequently, Hanahan and Weinberg decided in 2011 to extend the *hallmarks of cancer* by the tumour microenvironment (TME) (Hanahan and Weinberg 2011). The tumour is like a "*rogue organ*" consisting of malignant cells and other cells recruited to its periphery (Balkwill *et al.* 2012). The interaction of cancer cells and non-malignant host tissue cells creates the TME. The communication of cancer and surrounding cells implements secreted factors like cytokines and other regulatory factors like micro-RNA (Taylor *et al.* 2011, Pan *et al.* 2020b). An overview of typical cells found in TME is shown in Figure 2.

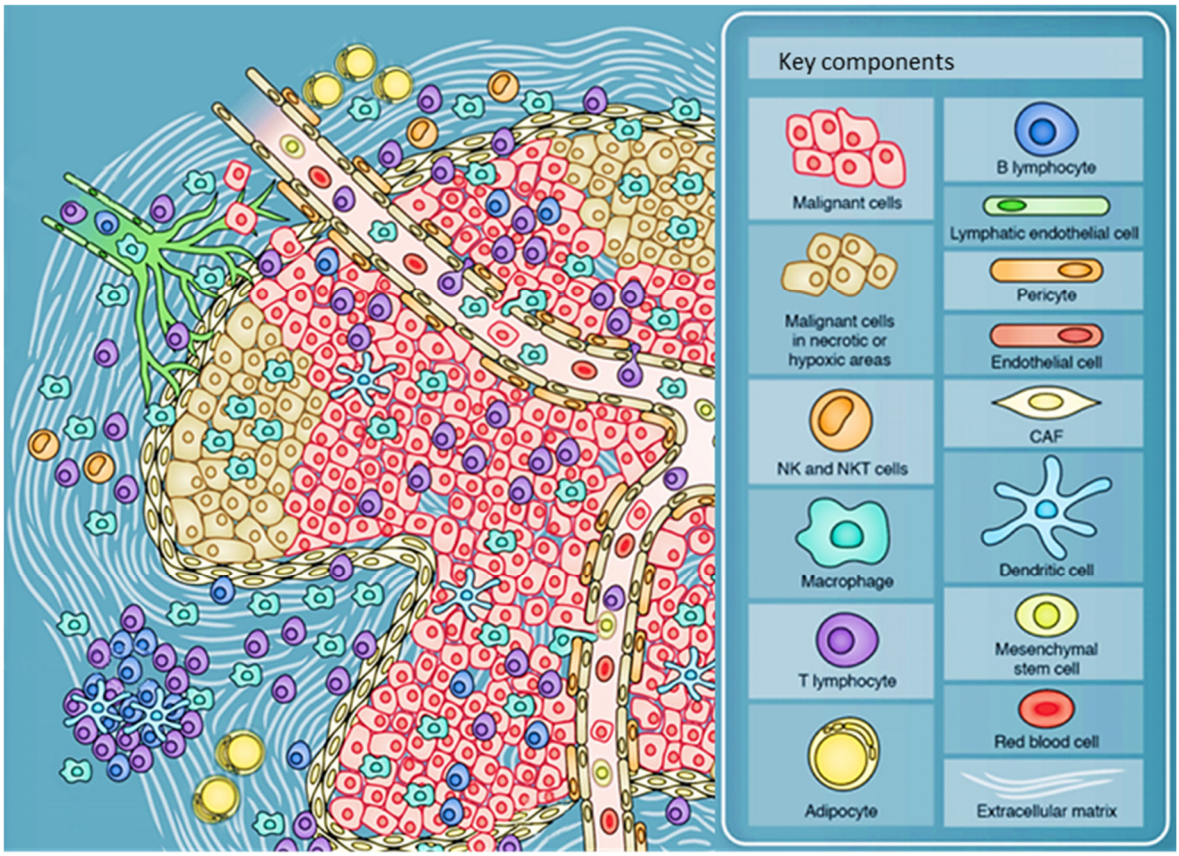


**Figure 2: The tumour microenvironment at a glance**
The figure shows the key cell types found in the tumour microenvironment including malignant cells, pericytes, endothelial cells, carcinoma-associated fibroblasts (CAF), dendritic cells, mesenchymal stem cells, red blood cells, extracellular matrix, adipocytes, cells of the immune system (macrophages, T lymphocytes, B lymphocytes), lymphatic cells (NK- and NKT-cells, lymphatic endothelial cells)
Modified according to (Balkwill *et al.* 2012)

It involves, next to the malignant cells, a framework of extracellular matrix (ECM) and all non-malignant cellular and non-cellular components e.g., fat cells, lymphatic cells, blood cells, endothelial cells, stromal cells, and immune cells (Pienta *et al.* 2008, Beltrao *et al.* 2010, Mareel and Constantino 2011, Ziogas *et al.* 2011, Valkenburg *et al.* 2018). In short, tumours are more like a separate ecosystem where the cancer cells interact and communicate with host cells (Camacho and Pienta 2012). As different as the components of the TME are as multifaceted their impact is on the TME. Accordingly, the following sections will focus on ECM, Cytokines, immune cells, and microRNA.

#### 1.1.2.1 The extracellular matrix (ECM)

The diverse cell types within the TME are embedded in the ECM. A bidirectional communication between the **ECM** macromolecules and the cells determines tumour progression and metastasis (Brassart-Pasco *et al.* 2020). One main cell type, the CAF, secretes the majority of ECM. It is composed of collagens, polysaccharides, proteoglycans, and glycoproteins (Santi *et al.* 2018, Socovich and Naba 2019). During cancer progression the tumour cells aim to cross the ECM, for example, to invade nearby tissue. By secreting several proteolytic enzymes like MMPs (Matrix metalloproteinases) the cancer cells can break down and modify the ECM barrier to pierce through it. This process is part of the tumourigenic ECM remodelling and results in the release of soluble active ECM fragments, called matrikines (Winkler *et al.* 2020). They act either pro- or anti-tumourigenic in several cancer models [reviewed in (Brassart-Pasco *et al.* 2020)] and can be used to measure tumour invasiveness and activity, thereby they are proposed as biomarkers (Kehlet *et al.* 2016). Furthermore, the ECM binds soluble factors like cytokines [interleukin 6 (IL-6), transforming growth factor-β (TGF-β) etc.] and growth factors [e.g. epidermal growth factor (EGF)]. During ECM degradation, these factors are released and receptors on the cell surface interact with them, regulating processes like apoptosis, differentiation, migration or proliferation (Hastings *et al.* 2019).

#### 1.1.2.2 Cytokines – Focus TGF-β1

**Cytokines** per se are signal molecule proteins that affect nearly every biological process: specific and non-specific responses to infections and antigens, embryonic development, ageing, disease pathogenesis and cancer. Furthermore, cytokines are included in vaccine efficacy, allograft rejection and stem cell differentiation (Dranoff 2004, Dinarello 2007). There is no standardised classification system for cytokines. Therefore, cytokines are sorted by functional activity, primary cell origin (lymphokine, monokine etc.), and numeric order of discovery (interleukins). The **TGF-β superfamily** consists of pleiotropic proteins, including the TGF-subfamily, the bone morphogenetic proteins (BMPs), the glial cell line-derived neurotrophic factor (GDNF) family, and the activin/inhibin family (Kubiczkova *et al.* 2012). Further statements will focus on the TGF-β-subfamily, consisting of TGF-β1, TGF-β2, and

TGF-β3, whereby all of them share highly conserved regions. TGF-β1 is the most abundant member of the TGF-β-subfamily in mammalian tissue. Independent of the isoform, the signalling pathway works by the same receptor (Cheifetz *et al.* 1987, Mittl *et al.* 1996).
Newly synthesised TGF-β is secreted as a latent and biologically inactive form, which cannot bind its receptor (Khalil 1999a). This form is inactive since the mature TGF-β peptide is bound to the latency-associated peptide (LAP), forming the small latent complex (SLC) (Gentry and Nash 1990). Additionally, there is the large latent complex (LLC), composed of the latent TGF-β binding protein (LTBP) bound to the SLC via disulfide bonds (Hayashi and Sakai 2012). After secretion, the LTBP is crucial for ECM anchoring, as its C-terminal and N-terminal regions bind to the ECM components fibrillin or fibronectin, respectively. Most cell types secrete the LLC, whereas the SLC is secreted in exceptional, but its secretion is described as ineffective cases (Miyazono *et al.* 1991, Olofsson *et al.* 1992, Dallas *et al.* 1994). By tissue injury or tumourigenic ECM remodelling active TGF-β is released by several mechanisms mediated via integrins, thrombospondin, proteases, and reactive oxygen species (Barcellos-Hoff and Dix 1996, Crawford *et al.* 1998, Yu and Stamenkovic 2000, Yang *et al.* 2007). In detail, the TGF-β precursor undergoes several processing steps before it can bind to its receptor. Most crucial, after the LLC was divided into SLC and LTBP the SLC is digested by the endopeptidase furin into (LAP) and the mature TGF-β peptide (Dubois *et al.* 1995).
In general, TGF-β cytokines are a group of versatile and powerful cytokines with anti-inflammatory, immune-suppressing, tumour-suppressing and tumour-promoting effects and well-documented roles in adhesion, differentiation, proliferation, and invasion (Santibanez *et al.* 2011, Taylor *et al.* 2011). TGF-β1 is one of the most abundant and important cytokines within the TME along with interleukins and tumour necrosis factor alpha. Especially, TGF-β1 plays a special role in tumour progression. Normally, TGF-β1 has an anti-cancerous effect preventing uncontrolled proliferation in hematopoietic, endothelial, and epithelial cells. During tumourigenesis, defects in TGF-β1 signalling develop and cause cell resistance to its cytostatic activity. TGF-β1 converts from a tumour suppressor to a supporter of growth, metastasis and invasion. This is called the TGF paradox (Tian and Schiemann 2009). For example, in a low dose, TGF-β1 supports tumour growth by activating angiogenic factors like VGEF (vascular endothelial growth factor). In contrast, higher TGF-β1 levels impair angiogenesis, since the growth of endothelial cells is inhibited in the tumour niche (Sakurai and Kudo 2011, Roy *et al.* 2015). Additionally, TGF-β1 is proposed to influence **immune cells** in the TME by affecting inflammatory response via T-cells.

#### 1.1.2.3 Immune cells

In general, immune cells in the TME can be divided into two categories: Tumour-suppressing and tumour-supporting immune cells. **Tumour-suppressing immune cells** include natural

killer (NK) cells, M1-macrophages, effector T cells (e.g. $CD8^+$ cytotoxic and $CD4^+$ effector T cells), dendritic cells and N1-neutrophiles (Lei *et al.* 2020).

**NK cells** are guided to the cancer tissue by dendritic cell-secreted chemokines (Habif *et al.* 2019). Their tumour-killing response is mainly performed by the release of cytolytic proteins and proteases inducing the target cell apoptosis (Voskoboinik *et al.* 2006). In addition, NK cells are described to secrete chemokines and cytokines with pro-inflammatory properties like tumour necrosis factor (TNF), IL-6 and many others (Guillerey *et al.* 2016).

**Macrophages** belong to the white blood cells of the immune system and digest and engulf every type of foreign cells and substances that do not belong to a healthy body like microbes, cell debris and cancer cells (Mills *et al.* 2000, Wynn *et al.* 2013). They originate from circulating monocytes or embryonic precursors that create self-sustaining peripheral areas surviving the host lifetime (Ginhoux *et al.* 2016, Perdiguero and Geissmann 2016). Macrophages are typically sectioned in M1-polarized (proinflammatory) and M2-polarized (anti-inflammatory, pro-tumourigenic, tumour-associated macrophages [TAM]). M1-polarized macrophages, also known as classically activated macrophages, produce cytokines and reactive oxygen or nitrogen species pivotal for killing tumour cells and host defence. Thus, M1 macrophages are classified as ‘good’ macrophages (Aras and Zaidi 2017).

**Effector T cells**, especially cytotoxic $CD8^+$ and $CD4^+$ cells represent essential groups of T-lymphocytes within tumour suppression. $CD8^+$ T cells, formerly known as killer cells, interact with major histocompatibility complex class I molecules (MHC I). As soon as MHC I present viral or cancerous antigens, $CD8^+$ cells interact with them via its T cell receptor and get activated to annihilate the harmful foreign cells (Maimela *et al.* 2018). Additionally, there are costimulatory signals by dendritic cells that trigger the maturation of $CD8^+$ cells, whereby they mainly act as professional antigen-presenting cells. Moreover, the help signals from $CD4^+$ cells were described to be essential for $CD8^+$ activation. $CD4^+$ cells either interact directly with $CD8^+$ cells to promote proliferation, empower dendritic cells by cross-presenting antigens or embark on producing cytokines (e.g. IL-2) and costimulatory molecules (Bennett *et al.* 1997, Ahrends and Borst 2018).

As specified above, **dendritic cells** act as professional antigen-presenting cells related to T-cell activation. Furthermore, they interact with NK cells and B cells [details in (Batista and Harwood 2009, Guillerey *et al.* 2016). Once mature, active dendritic cells infiltrate tumours, they enhance the recruitment and activation of immune effector cells. On the other hand, tumour cells can suppress dendritic cell function. An exemplary colorectal tumour explant tissue set-up revealed that dendritic cells pre-treated with tumour-conditioned medium (TCM) exhibited maturation inhibition. This effect is mediated by high levels of cytokines like Vascular Endothelial Growth Factor (VEGF) and other angiogenic cytokines like CXCL1 and CXCL5 (Michielsen *et al.* 2011)

**N1-polarized neutrophils** are found to invade several tumour types. Classically, neutrophils defend the human body from infections mainly by phagocytosis and secretion of chemokines and cytokines to induce the inflammatory response (Kolaczkowska and Kubes 2013). Neutrophils are described as potent anti-tumour effector cells that can destroy malignant cells which can also recruit other cells with anti-tumourigenic activity by cytokine and chemokine secretion (Uribe-Querol and Rosales 2015). Nevertheless, evidence is accumulating for the existence of tumour-associated neutrophils (TAN) which support tumour progression. In greater detail, similar to the macrophage phenotypes, neutrophils are divided into N1- and N2-polarized neutrophils, whereby the latter seem to represent TAN (Coffelt *et al.* 2016).

**Tumour-supporting immune cells** will be described in the next paragraphs, whereby the focus is set on regulatory T cells (Tregs) and myeloid-derived suppressor cells (MDSCs).

**Tregs** are a specialized subgroup of T cells, which are essential for immune tolerance. Normally they deactivate $CD4^+$ and $CD8^+$ T cells after a viral or microbial infection has been overcome. But in a cancerous context, this ability of Tregs leads to impaired immune reaction towards the tumour. In detail, Tregs inhibit dendritic cells, NK cells and effector T-cells in targeting tumour cells (van der Veeken *et al.* 2016). Five main mechanisms of Tregs affect the immune response to tumour cells: (1) Secretion of inhibitory cytokines like TGF-β and IL-10, (2) Termination of effector T cells, NK cells and others by granzymes and perforin, (3) Affection of effector cell function by interference with their metabolism, (4) Regulatory impact on dendritic cells and (5) Crosstalk with MDSCs to expand the suppressive environment for other immune cells [reviewed in (Li *et al.* 2020)].

**MDSCs** can be subdivided into polymorphonuclear (PMN-MDSCs) and monocytic MDSCs (M-MDSCs), whereby PMN-MDSCs share morphologic characteristics with N2 neutrophils and M-MDSCs with M2 Macrophages (Veglia *et al.* 2018). The interaction between the tumour and MDSC is described to be crucial for tumour progression: cytokines and chemokines within the TME stimulate MDSC proliferation which themselves trigger angiogenesis via e.g. VEGF (Talmadge and Gabrilovich 2013). Immunosuppressive cytokines like TGF-β and IL-10 produced by MDSC inhibit T cell function (Gabrilovich *et al.* 2012). Additionally, MDSCs promote metastasis, since they induce cancer cells to migrate towards endothelial cells (Zhou *et al.* 2018).

#### 1.1.2.4 microRNA

MicroRNA (miR) are small non-coding RNA molecules of 22 nucleotide length which are known to regulate post-transcriptional gene expression (Pan *et al.* 2020a). MiR are involved in a tremendous amount of pathological and physiological processes. The biogenesis and maturation pathway of miR starts with the primary miR which is transcribed from DNA (deoxyribonucleic acid) sequences followed by a stepwise procession from precursor to mature miR (Figure 3, [reviewed in (Winter *et al.* 2009)]). In most cases, there is a functional

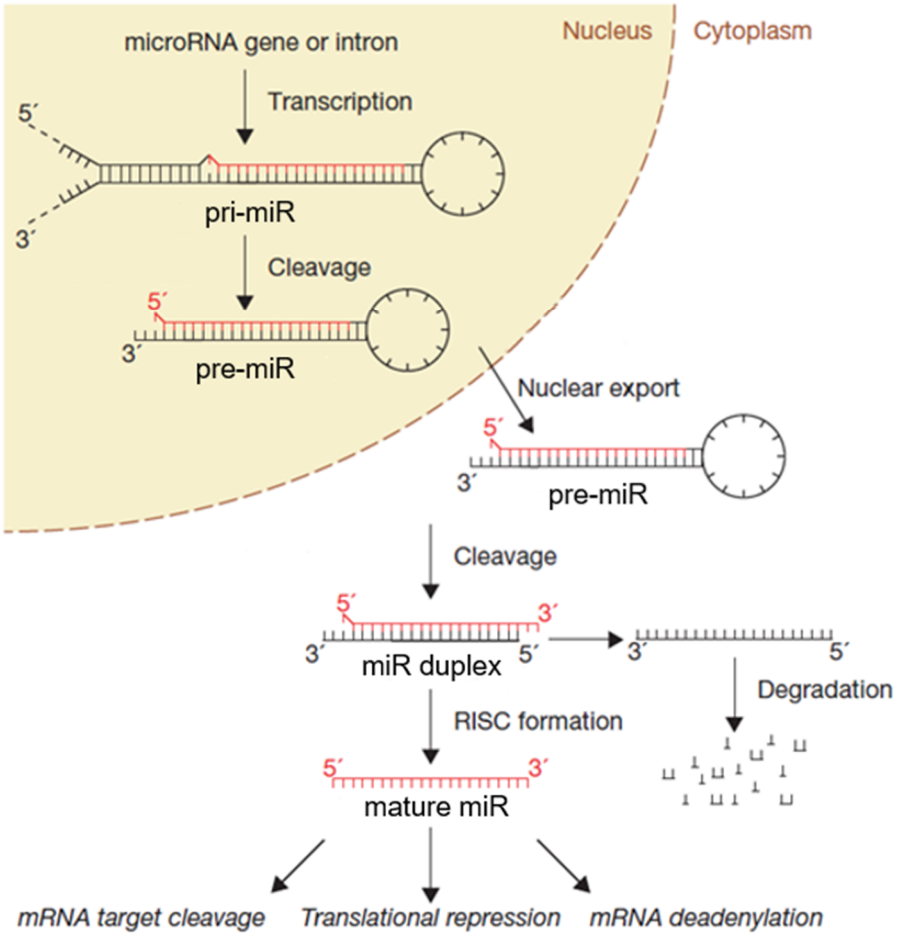


**Figure 3: MiR Processing**
In general, the primary miR (pri-miR) is generated by transcription of a miRNA gene or an intron in the nucleus and is processed into the precursor hairpin (pre-miR). The pre-miR is exported to the cytoplasm where the hairpin is cleaved and the miR duplex with its mature length remains. The functional strand of the miR (red) is guided by different proteins to silence its target mRNA by deadenylation, translational repression or mRNA cleavage. Simultaneously, the passenger strand (black) is degraded.
Modified according to (Winter *et al.* 2009)

miR leading strand and a passenger strand which is degraded. It depends on the miR if the 5'-3' (5p) or the 3'-5' (3p) arm is the biologically active miR species, the leading strand. Moreover, the co-expression of both miR species in parallel has been reported in colon cancer cells (Choo *et al.* 2014). In detail, miR bind the target mRNA within the 3' untranslated region (3'UTR) causing translational inhibition or mRNA degradation (O'Brien *et al.* 2018). Additionally, miR interaction has also been shown with 5' untranslated region (5'UTR), promoters and coding sequence (Broughton *et al.* 2016). Under certain conditions, gene activation by miR has been proven, too (Vasudevan 2012).

Within the last decades, increasing evidence implies a key role of miR in the function and biology of cancer cells in almost every part of cancer initiation and progression (Iorio and Croce 2012, Chou *et al.* 2013b). Tumour suppressors and classic oncogenes are predicted targets of miR. The miR-21 family was one of the first oncogenic miR to be discovered in 2006 with a high expression level in colon and breast cancer. Overexpression of miR-21 was associated with higher patient mortality (Volinia *et al.* 2006). MiR-21 was shown to support tumour growth

by targeting an apoptosis-inducing protein (Asangani *et al.* 2008, Frankel *et al.* 2008, Becker Buscaglia and Li 2011). Additionally, miR-21 is involved in TGF-β1-induced CAF formation by targeting SMAD7 (Mothers against decapentaplegic homolog 7), an inhibitory SMAD protein (Yao *et al.* 2011, Li *et al.* 2013). Since its linkage to cancer progression, CAF formation and TGF-β1 signalling, miR-21 was one of the chosen miR to be researched in this project.
The second miR of interest is miR-29 family. miR-29 targets proteins linked to fibrosis including fibrillins, elastin and collagens. Hence, the downregulation of miR-29 is anticipated to enhance fibrotic processes (van Rooij *et al.* 2008). Independent research attempts have shown a connection of miR-29, TGF-β1 and collagens in cardiac fibrosis. In detail, high levels of miR-29 were accompanied by low levels of collagen and TGF-β1. In contrast, high levels of TGF-β1 cause decreased miR-29 levels and increased collagen amounts (Bi *et al.* 2017). MiR-29 is considered a promising biomarker to predict e.g., the pathogenesis of cancer, since it is meant to be related to prognosis and aggressive progression of malignant neoplasms (Jiang *et al.* 2014, Peng *et al.* 2019). For instance, the increased amount of miR-29 is described to promote colorectal cancer (CRC) cell invasion targeting the transcription factor Kruppel-like factor 4 (KLF4) (Tang *et al.* 2014).
In conclusion, the influence of miRs is implicated in processes within the TME e.g., the activation of stromal cells to their CAF-like state. Furthermore, miRs are key players in regulatory mechanisms of the cancer cells by facilitating metastasis and progression and can be shuttled by exosomes between tumour cells and the TME (Tan *et al.* 2020).

### 1.1.3 Key player: The Cancer-associated fibroblast

The most abundant cell type in the TME is the CAF, supporting tumour growth and metastasis (Orimo *et al.* 2005, Karnoub *et al.* 2007). But what is the difference between a ‘normal’ fibroblast and a CAF? Fibroblasts in healthy tissue are described as non-immune non-epithelial cells having a likely mesenchymal lineage origin and being part of the diverse connective tissue components (Tarin and Croft 1969). Fibroblasts are quiescent cells present in the interstitial space or occasionally near a capillary as single cells. They have no association with the basement membrane even so they are embedded within the interstitial fibrillar ECM (Kalluri 2016). Kalluri divides the activation process of fibroblasts into reversible and irreversible profiles (Kalluri 2016) whereby the latter is partly affected by epigenetic regulation (Zeisberg and Zeisberg 2013, Tampe and Zeisberg 2014). The activation of resting fibroblasts to normally activated fibroblasts (NAF), such as during wound healing is a reversible process. Once the wound is closed, NAF revert to a resting state or undergo apoptosis (Desmouliere *et al.* 1995). Due to their increased alpha-smooth muscle actin (α-SMA) expression activated fibroblasts are also called myofibroblasts (Micallef *et al.* 2012). Myofibroblasts exhibit a temporary increased abundance in wounds but are also present in areas of chronic inflammation. Despite their beneficial influence on tissue repair, myofibroblasts are problematic in contributing to

pathological fibrosis in tissues like lung, kidney, and liver (Hanahan and Weinberg 2011). Even though wound healing is the most noted process activating quiescent fibroblasts, the leading principles still need to be unravelled.

In contrast, the differentiation of fibroblasts into CAF is described as an irreversible process partly influenced by epigenetic regulation (Mrazek *et al.* 2014). CAF are phenotypically as well as functionally different from normal fibroblasts which are in the same tissue but not in the tumour environment. The difference between general fibroblasts to CAF is that the latter are perpetually activated, neither revise to a normal phenotype nor undergo apoptosis and elimination. CAF share characteristics with activated fibroblasts in wounds as they appear as spindled cells expressing α-SMA in the TME (Li *et al.* 2007). In this accordance already Dvorak proposed tumours to be “wound[s] that never heal” (Dvorak 1986).

CAF are shown to be associated with a bunch of pro-tumourigenic mechanisms like supporting initiation, proliferation/progression of cancer cells as well as angiogenesis and metastasis of the tumour (Figure 3) as further described in detail.

Tumour growth is subjected to cancer cells with rogue proliferation beyond control (Tao *et al.* 2017). Increasing evidence has revealed that CAF are initiating tumour growth by supplementing tumourigenic activation signals (Bhowmick *et al.* 2004, Gonda *et al.* 2010). CAF produce paracrine and/or autocrine cytokines for example monocyte chemotactic protein 1, interleukin 1, vascular endothelial growth factor and TGF-β1 (De Boeck *et al.* 2013).

The increased proliferation and progression of cancer cells are also highly connected to the CAF secretome since they contribute diverse growth factors, hormones and cytokines. Classical mitogens such as epidermal growth factor (EGF) and hepatocyte growth factor (HGF), as well as cytokines like stromal cell-derived factor 1 (SDF-1) and interleukin 6 (IL-6), are all considerably expressed by CAF (Cirri and Chiarugi 2011). Furthermore, ECM remodelling by CAF was described to contribute to cancer proliferation by expressing members of the matrix metalloproteinase (MMP) family (Knauper *et al.* 1997, Vong and Kalluri 2011). Besides, reconstitution experiments, whereby CAF and tumour cells are injected as mixed xenografts, demonstrate that in the presence of CAF, tumour progression is enhanced (Orimo *et al.* 2005, Mishra *et al.* 2008, Widder *et al.* 2016)

Tumour growth and progression depend on an adequate supply of nutrients and oxygen as well as the removal of waste products (Nishida *et al.* 2006). For that, angiogenesis (new growth of vasculature) is crucial. CAF are described to support angiogenesis by enhanced promotor activity of the Vascular Endothelial Growth Factor (VEGF) in spontaneous mammary tumours (Fukumura *et al.* 1998). Also increased SDF-1 production in CAF causes enhanced recruitment of endothelial progenitor cells promoting angiogenesis in MCF-7-ras human breast carcinoma xenograft tumours (Orimo *et al.* 2005).

Aside from the processes already mentioned, CAF support metastasis of primary tumours. Secreting HGF and TGF-β1 epithelial-to-mesenchymal transition (EMT) is promoted, a process directly connected to metastasis (Bhowmick *et al.* 2004). During EMT cells acquire mesenchymal properties and loose cell-cell contact (Hay 1995). While metastatic cancer cells physically enter the blood vessels whereby proteolytic degradation by stromal cell-derived proteases like MMP or plasminogen activator is needed (Joyce and Pollard 2009). Tommelein *et. al* demonstrate that CAF incubated with CRC cell supernatants expressed an increased amount of various MMPs and urokinase-type plasminogen activators adopting a proteolytic phenotype (Tommelein *et al.* 2015). As a result of the associated ECM degradation cell-cell contacts and adhesion to the ECM are disrupted facilitating cancer cell migration to blood vessels and other tissues (Pietras and Ostman 2010)

### 1.1.4 Origins of CAF

The sources of CAF are versatile and continuously researched. They develop from different mesodermal cell types (De Wever *et al.* 2014), are locally present at the place of tumour growth (Arina *et al.* 2016) or invade from the bone marrow (Quante *et al.* 2011). Based on different theories of where CAF come from, they were roughly classified depending on their line of origin (Cirri and Chiarugi 2011):

1) resident cells
2) mutational
3) mesenchymal stromal cell (MSC)-derived.

According to the first theory, CAF originate from resident stromal cells including adipocytes, pericytes, smooth muscle cells, inflammatory cells and resting fibroblasts by activation through tumour-secreted factors like TGF-β (Cirri and Chiarugi 2011). It was shown that α-SMA (typical CAF marker) production is induced associated with the activation process (Rønnov-Jessen and Petersen 1993). This first model of CAF origin was confirmed *in vivo* demonstrating that human mammary fibroblasts convert to CAF in the course of tumour progression in a breast cancer xenograft model. This effect is mediated by TGF- β and SDF-1 causing autocrine activating signalling loops (Kojima *et al.* 2010). Moreover, SDF-1 was reported as a key factor in resident fibroblast activation in human adenocarcinoma (Toullec *et al.* 2010).

The second proposed CAF origin are normal epithelial cells that transdifferentiate by EMT achieving mesenchymal characteristics by becoming fibroblasts (Petersen *et al.* 2001, Kalluri and Neilson 2003, Kalluri and Zeisberg 2006b, Radisky *et al.* 2007). EMT was demonstrated to respond to stimuli from the TME in fibrosis (Zeisberg *et al.* 2003, Zeisberg and Kalluri 2004). In kidney fibrosis, 30 % of activated fibroblasts were shown to originate from tubular epithelial cells by EMT (Iwano *et al.* 2002). Therefore, EMT of resident epithelial cells could contribute to the pool of CAF in cancer.

Furthermore, a connection between genetic alteration and EMT of epithelial cells to CAF was established. In detail, MMP-driven oxidative stress caused DNA oxidation and mutations in epithelial cells causing a specialized EMT into activated myofibroblasts (Radisky *et al.* 2005). Also, genetic studies reported somatic mutations in p53 and PTEN [Phosphatase and Tensin homolog (mainly carried out in breast cancers)] together with copy number alterations in the tumour stroma (Moinfar *et al.* 2000, Kurose *et al.* 2002, Tuhkanen *et al.* 2004). Taken together these studies foster the idea that the tumour promoting CAF activity may be mainly based on somatic mutations in key tumour suppressor genes.

Besides normal epithelial cells, CAF are hypothesised to directly emerge from cancer cells by EMT (Kalluri and Zeisberg 2006a, Radisky *et al.* 2007). Thereby cancer cells become more migrative and invasive adopting a mesenchymal phenotype. Analyses in mammary carcinoma confirmed this hypothesis. An X-chromosome-inactivation pattern was found in fibroblasts as well as in cancer cells, suggesting a shared origin of both cell types (Petersen *et al.* 2003). In contrast, other studies have expounded that genetic alterations were only detected in cancer epithelial cells and not in CAF with the result that a mutual origin of CAF and cancer cells remains doubtful (Allinen *et al.* 2004)

Addressing the third and most relevant source of CAF for the current thesis, several studies suggest that CAF are derived from infiltrating or resident MSC (Melzer *et al.* 2018). It was shown that bone marrow-derived MSC can engraft into injured tissues like lung or kidney to contribute to the myofibroblast population in these organs (Direkze *et al.* 2003). Further studies indicate that the bone marrow can contribute to the tumour microenvironment (Direkze *et al.* 2004, Ishii *et al.* 2005). Since MSC reside as pericytes in many tissues throughout life (Crisan *et al.* 2008) they are suggested to play an initial role in cell-to-cell contacts with circulating tumour cells providing a pre-metastatic niche. MSC actively migrate towards tumours (Khakoo *et al.* 2006) and tumour-integrated MSC with myofibroblast characteristics are demonstrated to enhance tumour growth in CRC xenografts (Shinagawa *et al.* 2010, Widder *et al.* 2016).

## 1.2 Mesenchymal stromal cells: Characteristics and potential role in tumour biology

### 1.2.1 General characteristics of mesenchymal stromal cells

In the 1970s Friedenstein *et al.* first described non-hematopoietic mesenchymal precursor cells isolated from human bone marrow. The cells were cultivated *in vitro* using plastic cell culture flasks in a humified atmosphere. Small colonies of spindle-shaped cells, described as CFU-F (colony-forming unit fibroblasts), appeared within the first days of cultivation (Friedenstein *et al.* 1970, Friedenstein *et al.* 1976). Further studies revealed a multipotent character of the cells identified by Friedenstein, differentiating into multiple mesodermal cell lineages e.g. osteoblasts, chondrocytes and adipocytes (Prockop 1997). Thereby the term ‘mesenchymal

stem cells' was introduced (Caplan 1991). Resident cells with mesenchymal stem cell characteristics have been also isolated from other sources than bone marrow: salivary glands (Rotter *et al.* 2008), umbilical cord blood (Lee *et al.* 2004a), the human gut (Lanzoni *et al.* 2009) and adipose tissue (Kern *et al.* 2006). MSC isolated from bone marrow have been used for the current thesis. The amount of MSC in the bone marrow among all nucleated cells accounts notably below 1 % (Pittenger *et al.* 1999). However, mesenchymal stem cells derived from bone marrow and other sources are not functionally identical. Consequently, studies using bone marrow-derived mesenchymal stem cells may not be replicated with cells isolated from other sources (Lee *et al.* 2004b, Wagner *et al.* 2005).

However, the term 'mesenchymal stem cells' is controversially discussed in the literature, since convincing data supporting the 'stemness' of unfractionated plastic-adherent cells from bone marrow are lacking (Horwitz and Keating 2000). For this reason, using the label 'mesenchymal stromal cells' was recommended (Horwitz *et al.* 2005). To minimise confusion among researchers and due to the lack of one unique marker for MSC, Dominici and colleagues defined the following consensus criteria for MSC (Dominici *et al.* 2006):

- adherence to plastic
- specific surface antigen (Ag) expression: ≥95 % of the cells must express CD73, CD90 and CD105 and these cells must lack (≤2 %) expression of CD11b or CD14, CD19 or CD79α, CD34, CD45 and HLA-DR
- multipotent *in vitro* differentiation potential to osteoblasts, adipocytes, chondroblasts (demonstrated by staining of *in vitro* cell culture)

In the bone marrow, MSC are described to take part in the establishment of the haematopoietic niche (Muguruma *et al.* 2006). Furthermore, MSC seem to be involved in the maintenance of the haematopoietic homeostasis by influencing the proliferation and differentiation of haematopoietic stem cells (Valtieri and Sorrentino 2008). Another beneficial role of MSC has been found in wound healing and tissue regeneration. Thereby murine MSC, tagged with the green fluorescent protein (GFP), have been injected intravenously in wounded mice, resulting in the detection of GFP-positive cells around the wounded sites. MSC reside throughout life as pericytes in many tissues (Crisan *et al.* 2008). In this regard, it has been shown that these cells detach from local capillaries and migrate to the site of injury supporting wound healing by secreting soluble factors and differentiating into myofibroblasts [reviewed by (Wong *et al.* 2015)].

Furthermore, MSC are described as 'hypoimmunogenic' escaping alloreactive cells showing immunomodulatory and immunosuppressing properties (Rasmusson 2006). The immunomodulatory competence of MSC is determined by the concentration and types of inflammatory mediators in the MSC microenvironment. Besides, there are distinctly various

responses to MSC treatment dependent on the state of inflammation indicating immunomodulatory plasticity of MSC (Wang *et al.* 2014). For instance, there is a major role of MSC immunomodulatory ability in the graft-versus-host disease (GvHD), a cytotoxic reaction that can occur as a result of allogeneic bone marrow or stem cell transplantation, whereby mainly T-lymphocytes from the donor react against the recipient organism (Jacobsohn and Vogelsang 2007). It has been reported that in GvHD severely progressing inflammation can be treated by MSC, but infusing MSC on the same day as the bone marrow transfusion is less effective (Sudres *et al.* 2006, Ren *et al.* 2008). This demonstrates that MSC do not constitutively exhibit their immunosuppressive function it's rather activated by inflammation (Wang *et al.* 2014). Next to their application in GvHD, MSC are implicated in a wide variety of clinical trials and experimental settings for numerous diseases according to the US National Institute of Health, including skeletal muscle (most targeted), haematological malignancies, autoimmune diseases, kidney disease, diabetes, cardiovascular conditions, neurological diseases and bones and cartilage defects (Jo *et al.* 2014, Squillaro *et al.* 2016, Moreira *et al.* 2017, Ayala-Cuellar *et al.* 2019, Bochon *et al.* 2019, Pittenger *et al.* 2019). At *Clinical Trials.gov* there is a detailed overview of about 270 clinical trials with MSC, for example, their implications in Type-1 diabetes, heart failure and of course COVID-19 (National Library of Medicine 2021, April 4th).

### 1.2.2 MSC as part of the tumour stroma

Next to all the beneficial roles of MSC in wound healing and curing diseases, there exists a contrasting perspective. MSC own tumour-homing characteristics. In detail, MSC were found to actively migrate to wounded structures (Fox *et al.* 2007, Ponte *et al.* 2007). They are capable of homing to sites of inflammation, including several kinds of tissue e.g. injured skin (Cihova *et al.* 2011). Concerning the hypothesis of Dvorak, about the likeness between tumours and "wounds that do not heal", it immediately suggests itself that there is an important role of MSC in tumour biology (Dvorak 1986). Indeed, it was found that MSC actively migrate towards tumour sites. Thereby MSC are attracted by chemokines, growth factors and great numbers of further signals (Spaeth *et al.* 2008). It was shown by experimental tumour research, that MSC have both suppressive and promotive effects on tumour cells. Those bidirectional effects could be shown for breast cancer, lung cancer, melanoma, bladder cancer, gastric cancer, colorectal cancer and much more [reviewed in (Wang *et al.* 2020)].

But how do MSC affect tumour growth? At first, it depends on the source of MSC. For example, studies on glioblastoma have shown that umbilical cord blood-derived MSC inhibit cancer proliferation whereas adipose tissue-derived MSC promoted cancer growth (Akimoto *et al.* 2013). Also, several studies have shown promotive effects of bone marrow-derived MSC on breast cancer (Karnoub *et al.* 2007, Mishra *et al.* 2008, Shangguan *et al.* 2012a, Lacerda *et al.* 2015) whereby Sun and colleagues have shown suppressive effects of umbilical cord blood-

and adipose tissue-derived MSC on the same tumour entity (Sun *et al.* 2009). Those findings are potentially based on findings that MSC isolated from different sources (bone marrow, adipose tissue, umbilical cord blood) show significant differences in their transcriptome and functionality (Lee *et al.* 2004b, Wagner *et al.* 2005).

Secondly, MSC play an essential special role in the TME. As described in 1.1.2, the TME itself holds a key role in tumour growth consisting of several cell types. Thereby CAF are supposed to play an essential role in tumour growth, invasion and metastasis (Galie *et al.* 2005, Powell *et al.* 2005). CAF secrete several extracellular matrix proteins and signalling molecules generating a beneficial surrounding for cancer cells to grow and develop. Boriello and colleagues demonstrated CAF sharing protumourigenic activity with MSC, supporting the hypothesis of CAF originating from MSC (Borriello *et al.* 2017). This process was proven by several independent research groups. In detail, MSC differentiate into CAF induced by several tumour-secreted factors thereby contributing to the tumour stroma (Jeon *et al.* 2008, Bagley *et al.* 2009, Quante *et al.* 2011). The MSC to CAF differentiation is described as myofibroblastic differentiation characterised by elevated amounts of marker proteins like α-smooth muscle actin (α-SMA), Calponin 1 (CNN1) and collagen 1 A1 (COL1A1) (Mishra *et al.* 2008, Martinez-Outschoorn *et al.* 2010, Cirri and Chiarugi 2011). Whether MSC are already present in the tissue as a part of the premetastatic niche (Psaila and Lyden 2009) or migrate towards the tumour site (Khakoo *et al.* 2006) is not fully understood.

Since colorectal cancer cells were used in several experimental settings in the current thesis, the following paragraph sums up the ambivalent effects of MSC on colorectal cancer. On the one hand it was shown that human bone marrow-derived MSC reduced colorectal cancer progression and initiation resulting in a decreased tumour size in an immunocompetent rat model. The MSC affected CRC by polarizing resident immune cells resulting in attenuated tumour development (Francois *et al.* 2019). In contrast, human bone marrow-derived stem cells were shown to support CRC in mice as well. In greater detail, MSC led to increased proliferation and metastasis (Zhu *et al.* 2006). Additively, Mele and colleagues demonstrated that epithelial-mesenchymal transition in CRC cells is induced in MSC coculture triggered by TGF-β1 resulting in increased tumour size and invasiveness *in vitro* (Mele *et al.* 2014).

Most importantly, cooperating local researchers (Lutz Müller, Jana Lützkendorf, Miriam Widder) demonstrated human bone marrow-derived MSC promoting CRC tumour growth in a β1-integrin-dependent manner in mice (Widder *et al.* 2016).

### 1.2.3 Myofibroblastic differentiation

Myofibroblasts are defined as an intermediate cell type between normal fibroblasts and smooth-muscle cells (SMC). They can develop from e.g. fibroblasts, MSC or several other cell types and are described as contractile, ECM-depositing cells with ruffled membranes expressing typical marker proteins like α-SMA (Gabbiani 1992, Baum and Duffy 2011).

Myofibroblasts were first detected in granulation tissue; formed in the initial phase of wound healing containing fibroblasts and several numbers of inflammatory cells. The differentiation of fibroblasts, MSC or several other cell types into myofibroblasts starts with the transformation of quiescent cells into activated, migratory and proliferative proto-myofibroblasts, but those cells are mainly devoid of contractile proteins like α-SMA (Tomasek *et al.* 2002, Hinz 2007). This process is mainly triggered by mechanical stress (stiffened ECM), pro-fibrotic cytokines or inflammatory signals. In the further course of differentiation proto-myofibroblasts transform into myofibroblasts by growing ECM stiffness and activated cytokine signalling e.g. TGF-β1, resulting in a α-SMA positive, highly ECM depositing cell type which is known as myofibroblast (Otranto *et al.* 2012). In the case of MSC, the myofibroblastic differentiation into CAF can be simply detected under the microscope. Since MSC typically exhibit a small and triangular shape, myofibroblastic differentiation leads to cell flattening (Haasters *et al.* 2009, Barcellos-de-Souza *et al.* 2016). On the molecular level, Crider and colleagues demonstrated in 2011 that the α-SMA gene expression is regulated by the activity of the serum response factor (SRF) and its co-factor myocardin-related transcription factor A (MRTF-A) binding a special promotor region named CArG box (Crider *et al.* 2011). Besides α-SMA other myofibroblastic marker genes like collagen 1 A1 (COL1A1) and CNN1 are regulated by MRTF-A as well (Descot *et al.* 2009, Esnault *et al.* 2014). The MRTF-SRF signalling pathway is crucially connected to actin treadmilling and thereby to actin cytoskeleton reorganization, inevitable for the myofibroblastic differentiation (Miralles *et al.* 2003, Olson and Nordheim 2010).

## 1.3 The actin-MRTF-SRF-signal pathway

### 1.3.1 The serum response factor (SRF)

SRF was discovered in 1986 by Richard Treisman and is a ubiquitously expressed 67 kDa MADS-box (MCM1, Agamous, Deficiens, SRF) transcription factor conserved from fly to human (Treisman 1986). It is characterized as a nuclear protein that binds to specific promotor elements, regulating 'immediate early genes' like e.g., c-fos or cytoskeletal actin (Treisman 1985, Treisman 1986, Miralles *et al.* 2003). Furthermore, SRF target genes include transcription factors, signalling molecules and plenty of cytoskeletal components (Philippar *et al.* 2004, Sun *et al.* 2006). The 57 amino acid MADS-box in SRF mediates protein-protein-interactions, homodimerization and most importantly DNA binding at its target genes (Shore and Sharrocks 1995). The SRF binding site on c-fos was described as serum response element (SRE) which is a conserved 23 bp DNA sequence with a special consensus sequence of 10 base pairs $CC(A/T)_6GG$ called CArG-box nowadays (Treisman 1986, Boxer *et al.* 1989, Taylor *et al.* 1989). SRF was found to coordinate entirely different sets of gene expression associated with cellular growth, migration and differentiation in a tremendous diversity of tissues and cell types (Philippar *et al.* 2004, Selvaraj and Prywes 2004, Posern and Treisman

2006, Miano *et al.* 2007). The vast complexity of regulated genes and processes led to the assumption that cooperating transcriptional factors specify spatial and temporal gene expression. A huge number of studies has been made to identify and specify two major families of transcriptional co-activators for SRF: ternary complex factors (TCF) and myocardin-related transcription factors (MRTF) [review by (Gualdrini *et al.* 2016)]. Since the present thesis is focussing on the MRTFs, TCFs are skipped and MRTFs are discussed below.

### 1.3.2 Myocardin and Myocardin-Related Transcription Factors

In mammals, there are three myocardin family members: Myocardin (MYOCD), MRTF-A and MRTF-B [reviewed in (Pipes *et al.* 2006)]. Structurally, the myocardin family members share several functional domains: At the N-terminus MRTFs comprise up to 3 RPEL motives (core sequence RPxxxEL; Pfam accession number: PF02755) mediating G-acting binding, whereby responsiveness to cytoskeletal signalling is provided (Miralles *et al.* 2003, Mouilleron *et al.* 2008). C-terminally from the RPEL motives, there is a basic box (B-box/B1) and a glutamine-rich Q-domain (Q), necessary for nuclear translocation and SRF interaction (Wang *et al.* 2001, Wang *et al.* 2002, Miralles *et al.* 2003, Posern and Treisman 2006). Furthermore, the myocardin family harbours an SAP domain, named after SAF-A/B, Acinus and PIAS proteins, adjacent to the B1 and Q areas. The function of SAP domains is not finally resolved yet. In general, SAP domains are described to be involved in DNA binding and -repair, RNA processing and chromosomal dynamics (Aravind and Koonin 2000). It is known that SAP-domain deletion leads to abrogation of the ability of MYOCD to activate the cardiac-specific *ANF* gene *in vitro* (Wang *et al.* 2001). For MRTF-A things are even more complicated, since its target genes can be either be transcribed SRF-dependent + SAP-independent, SRF-dependent + SAP-dependent or SRF-independent + SAP-dependent (Gurbuz *et al.* 2014). The leucine zipper (LZ) followed on the SAP domain is described to mediate homodimerization and to be required for the efficient activation of smooth muscle genes (Wang *et al.* 2003). The transcriptional activation domain (TAD) at the C-terminus mediates transcriptional activity.

Overall MYOCD, MRTF-A and MRTF-B share 35 % amino acid identity, whereby the identity is 60 % within the important functional domains (B1, Q, SAP). Beyond those regions, further amino acid consensuses are found in the TAD ()region. Additionally, the amino acid identity between MRTF-A and -B is 42 %. Nevertheless, MYOCD and MRTF-A/-B display important differences.

MYOCD was discovered in 2001 by Wang and colleagues using a bioinformatics-based screen to discover unknown cardiac-specific genes (Wang *et al.* 2001). Initially, MYOCD was thought to be mainly found in heart and smooth-muscle cells in different isoforms, but its mRNA was also detected in multipotent stem cells stimulated by TGF-β1 to undergo SMC differentiation (Yoshida *et al.* 2003, Yoshida *et al.* 2004, Kurpinski *et al.* 2010). Compared to MRTF-A and -B,

MYOCD has a much weaker affinity for G-actin and is exclusively localized in the nucleus caused by the sequence aberrations within the RPEL domains (Wang *et al.* 2001, Miralles *et al.* 2003, Kuwahara *et al.* 2005). Myocardin forms a ternary complex with SRF, in detail binds it as a dimer and is described as extraordinarily potent transcriptional co-activator of SRF pushing the expression of cardiac and smooth muscle genes, including alpha-smooth muscle actin, transgelin, smooth muscle myosin light and heavy chain and many more (Wang *et al.* 2003, Gurbuz *et al.* 2014).

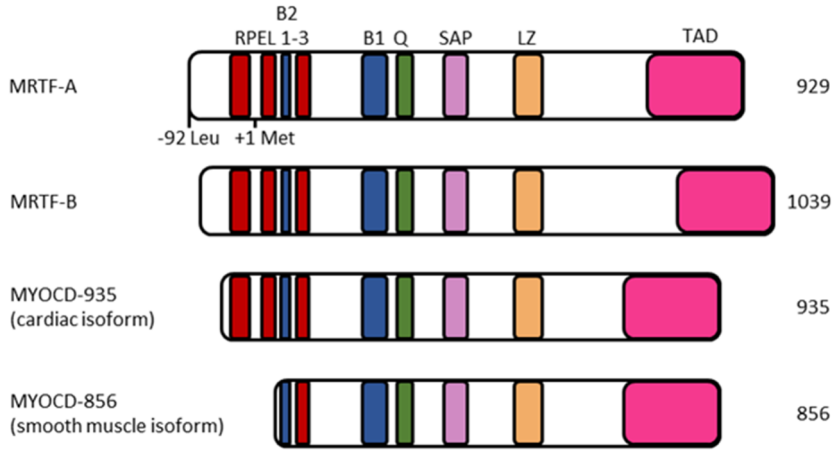


**Figure 4: Schematic structure of MRTF-A, MRTFB and MYOCD isoforms**
Functional domains are displayed in coloured stripes. RPEL: RPxxxEL actin-binding motif core consensus, B1/B2: basic boxes, Q: glutamine-rich domain, SAP: 35-residue motif, homology domain found in SAF-A/B, acinus and PIAS, LZ: leucine zipper, TAD: transcriptional activation domain.
Modified according to (Posern and Treisman 2006)

Even though several commercial antibodies are available to detect MYOCD, there is evidence that they do not reliably detect endogenous but exogenous proteins. Thus, MYOCD research is mainly restricted to RNA (Miano 2015). To circumvent the trouble of unreliable MYOCD antibodies, in 2018 Lyu and colleagues created a new mouse model by targeting the endogenous MYOCD locus with two independent epitope tags (3x FLAG or 3x HA). The molecular weight of MYCOD isoforms is predicted to 97-106 kDa, resulting in the expectation to detect protein signals at around 100 kDa. Interestingly, Lyu et al. detected a specific 150 kDa band, using the mouse model they created, which was verified as MYOCD by mass spectrometry, whereby the 100 kDa band revealed no evidence of MYOCD protein (Lyu *et al.* 2018).

MRTF-A and MRTF-B are expressed in an extensive range of tissues, including epithelial cells of various organs (Wang *et al.* 2002) as well as embryonic stem cells (Du *et al.* 2004). MRTF-A, also known as megakaryoblastic leukaemia 1 (MKL1), was first described in 2001 by two independent publications in connection with a genetic defect of children causing acute megakaryoblastic leukaemia (Ma *et al.* 2001, Mercher *et al.* 2001). In 2002 MRTF-A and

MRTF-B were found to be effective SRF co-activators (Wang *et al.* 2002). Comparing MYOCD, MRTF-A and MRTF-B, the latter is a relatively weak SRF co-activator, even though it contains a powerful TAD domain like MRTF-A and MYOCD (Wang *et al.* 2002). In general, the activity of MRTF-A and MRTF-B is regulated by Rho family GTPases (RhoA, Rac1, CDC42 etc.) and depends on actin treadmilling (Hill *et al.* 1995, Sotiropoulos *et al.* 1999, Gineitis and Treisman 2001, Miralles *et al.* 2003, Ge *et al.* 2018). Remarkably, combined RNAi knockdown (KD) of MRTF-A and MRTF-B is necessary to efficiently compromise RhoA-dependent SRF-mediated gene expression, suggesting redundant functions of MRTF-A and MRTF-B (Cen *et al.* 2003). Knockout studies in mice demonstrated that MRTF's and MYOCD are not able to assume respective functions in total. The MYOCD knockout (KO) resulted in a lack of vascular SMC causing lethal mouse embryos at E 10.5. As opposed to this cardiac development seemed to be unaffected. Thereby the authors postulated a functional takeover of MRTF's in MYOCD knockout mice possibly lacking in the SMC lineage (Li *et al.* 2003). MRTF-A KO mice show a surprising defect in lactation: The myoepithelial cells in the mammary glands of MRTF-A KO mice fail to differentiate resulting in abolished contractility needed to secrete milk (Li *et al.* 2006, Sun *et al.* 2006). In detail, Seifert and Posern demonstrated the necessity of concise temporal MRTF expression control in MCF10A mammary acini to ensure normal morphogenesis. MRTF-A KD (knockdown) led to obviously smaller acini size and impaired lumen formation, whereby those effects were rescuable by MRTF-A and partially by MRTF-B re-expression. In contrast, MRTF-A and -B overexpression caused increased acini size without lumen and affected apicobasal polarity. Additionally, high expression of MRTF-A was associated with decreased survival in two breast cancer cohorts (Seifert and Posern 2017). MRTF-B KO mice are not viable. Two independent studies show defective cardiovascular development as well as affected differentiation of SMC (Li *et al.* 2005, Oh *et al.* 2005). Furthermore, MRTF-B -/- embryonic stem cells show an altered cytoskeleton and reduced cell adhesion based on a TGF-β2 signal cascade malfunction (Li *et al.* 2012). Since the focus of the present thesis was set to MRTF-A, the following paragraphs will omit MRTF-B.

### 1.3.3 The actin-MRTF-A-SRF signalling pathway

In general, MRTF-SRF-regulated genes include a plethora of cytoskeletal, cell motility, transcriptional and cell adhesion components, including α-SMA, Calponin 1 and collagen (Descot *et al.* 2009, Esnault *et al.* 2014). The regulatory pathway activated by MRTF-A is strongly connected to actin treadmilling as displayed in Figure 5:. Actin was first shown to regulate the MRTF-A activity in 2003 (Miralles *et al.* 2003). MRTF-A is sequestered in the cytoplasm in resting cells and unstimulated fibroblasts (Olson and Nordheim 2010, Gualdrini *et al.* 2016). Confined to the cytoplasm, MRTF-A it is bound to G-Actin via its N-terminal RPEL motives. In this MRTF-A/G-actin complex, the nuclear translocation signal for the importin α/β

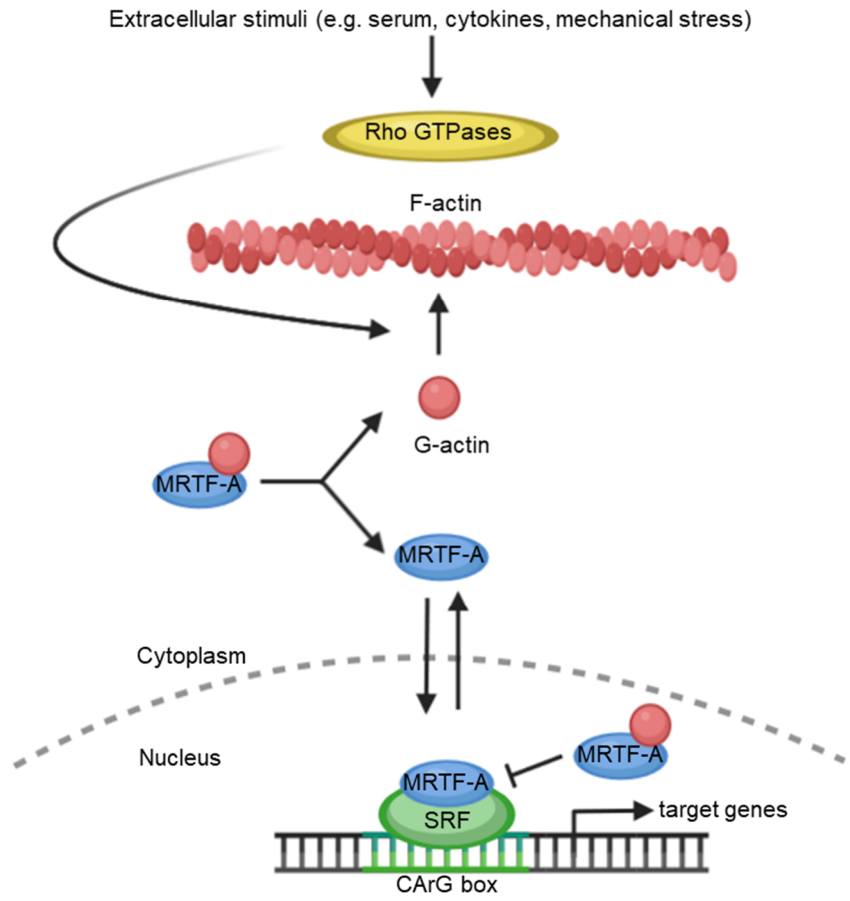


**Figure 5: General regulatory pathway of SRF target gene expression through actin-MRTF interaction.**
Altered actin dynamics, aroused by Rho GTPase signalling induced by extracellular stimuli, are regulating MRTF-A activity. MRTF-A is prevented from nuclear translocation being bound to G-actin. MRTF-A:G-actin dissociation appears in result to forced F-actin formation, associated with extracellular stimuli or differentiation processes.

Modified according to (Olson and Nordheim 2010)

transport receptor is blocked, preventing MRTF-A from nuclear translocation (Pawlowski *et al.* 2010). By extracellular stimuli (serum, cytokines, mechanical stress) the activation of RhoGTPases is triggered, leading to the activation of several cytoskeletal regulators increasing F-actin polymerisation (Sotiropoulos *et al.* 1999, Copeland and Treisman 2002, Gau and Roy 2018). The enhanced F-actin assembly leads to decreased G-actin amounts in the cytoplasm. Thereby MRTF-A/G-actin complexes dissociate and MRTF-A is capable of translocating into the nucleus. Once in the nucleus, MRTF-A binds to SRF as a homo – or heterodimer to stimulate MRTF-SRF-dependent gene expression, including α-SMA, Calponin 1 and collagen (Descot *et al.* 2009, Esnault *et al.* 2014). The regulatory capabilities of actin on MRTF-A within the nucleus are also employable on nuclear MRTF-A. As G-actin prevents cytoplasmic MRTF-A from nuclear import it also unleashes nuclear export and prevents SRF activation (Vartiainen *et al.* 2007)

Alongside the classical regulatory pathway, it was also shown that there are cell lines with predominant nuclear expression of MRTF-A. In breast cancer epithelial cells and primary neurons MRTF-A was shown to be constitutively located in the nucleus, prompting the presence of unknown additional regulatory pathways (Kalita *et al.* 2006, Medjkane *et al.* 2009). As mentioned above, extracellular stimuli can be versatile: from serum to mechanical stress through to cytokines. For example, MRTF-A is a key regulator of TGF-β1-induced fibroblast to myofibroblast differentiation (Crider *et al.* 2011).

As recently shown, MRTF-A was found to be regulated by miRs. A novel mechanism was described whereby endogenous MRTF-A protein abundance and activity were inhibited by several miRs in C2C12 myoblasts during myogenic differentiation (Holstein *et al.* 2020). Moreover, MRTF-A is capable of regulating the expression of miR-21. The promotor of miR-21 contains a highly conserved CArG box where SRF in conjunction with MRTF-A binds to regulate its expression.

## 1.4 Aim of the thesis

Colorectal cancer (CRC) is a severe disease that represents approximately 10 % of cancer-related mortality in western countries (Kuipers *et al.* 2015). Hence, it is necessary to understand the molecular mechanisms of tumour initiation and progression of CRC in detail. Tumour growth and metastasis are heavily influenced by the surrounding tumour microenvironment, especially by the tumour stroma including cancer-associated fibroblasts (CAF). Even though multipotent mesenchymal stromal cells (MSC) are mainly known to possess beneficial traits within the human body they are also known precursors of CAF. On the one hand, MSC are attributed to hold protective and regenerative potential since their well-known trilineage differentiation ability to osteoblasts, chondrocytes and adipocytes (Prockop 1997, Dominici *et al.* 2006). As opposed to this, upon tumour interaction or cytokine stimulation by TGF-β1, it was shown that MSC undergo myofibroblastic differentiation into CAF-like cells (Mishra *et al.* 2008), connected to distinct morphological changes which are most likely connected to cytoskeletal changes and reorganisation. Myocardin-related transcription factor A (MRTF-A) is a key transcriptional regulator of smooth muscle cell differentiation, targeting specific genes like α-smooth muscle actin, Calponin-1 and collagen 1A1 (Miralles *et al.* 2003, Descot *et al.* 2009, Esnault *et al.* 2014). Moreover, MRTF-A, CAF differentiation and TGF-β1 signalling are connected to microRNA (miR).

This thesis intends to examine the regulation of MRTF-A during the myofibroblastic MSC to CAF differentiation. Additionally, the role of MRTF-A on the tumour-propagating function of MSC in CRC was assessed. Therefore, this thesis aims to investigate the following topics in detail:

1) Primary MSC, isolated from the iliac crest of human donors, should be analysed if they own the ability to differentiate into CAF upon stimulation by tumour-conditioned medium from HCT8 colorectal cancer cells or recombinant TGF-β1 cells *in vitro.*
2) The role of MRTF-A during MSC to CAF differentiation was investigated through transient siRNA transfection and stable shRNA knockdown via lentiviral transduction.
3) The expression of miR-21 and miR-29 in MSC upon TGF-β1 stimulation and the effects of their overexpression and knockdown was investigated.
4) The role of MRTF-A should be resolved for MSC-mediated support of CRC tumour formation via HCT8 xenograft experiments in nude mice *in vivo*.

# 2 MATERIALS AND METHODS

## 2.1 Materials

### 2.1.1 Equipment

**Table 1: List of technical supplies**

| UTILIZATION | DESCRIPTION | MANUFACTURER |
|---|---|---|
| Agarose gel equipment | Horizontal Elpho | Workshop of MPI of Biochemistry (Martinsried) |
| Agarose gel documentation | Gel Stick | Intas Science Imaging |
| Balances | Kern ABS<br>Kern 752 | Kern & Sohn GmbH |
| BD Accuri Flow Cytometer | Flow Cytometer | BD Biosciences |
| Cell counter | Neubauer Improved<br>Casy Cell Counter | Marienfeld GmbH & Co. KG<br>OMNI Life Science |
| Cell culture incubator | HERAcell 150i | Thermo Scientific |
| Cell culture safety cabinet | HERAsafe | Thermo Scientific |
| Centrifuges | Allegra X-15R<br>Centrifuge 5417C<br>Centrifuge 5417R<br>Sprout Mini-Centrifuge<br>Perfect Spin 24R | Beckmann Coulter<br>Eppendorf<br>Eppendorf<br>Biozym<br>PEQLAB |
| Incubation | Duomax 1030 (orbital shaker)<br>Mixing Block MB-102<br>RM5 (Roller mixer)<br>Thermomixer comfort<br>WB 120 K (37°C incubator)<br>New Brunswick Scientific I26 | Heidolph<br>BIOER<br>CAT<br>Eppendorf<br>Mytron<br>Eppendorf |
| Microplate readers | Clariostar<br>GloMax 96 Microplate Luminometer w/Dual Injectors | BMG Labtech<br>Promega |
| Microscopes | Axio Observer7<br>Evos Core AMG<br>Evos fl AMG | Zeiss Jena<br>Thermo Fischer<br>Thermo Fischer |
| Mixing | Lab Dancer<br>Magnetic Stirrer R 1000<br>MR Hei-Standard<br>Vortex Genius 3 | IKA<br>Carl Roth gmbH<br>Heidolph<br>IKA |
| Page equipment | Mini-PROTEAN Tetra System | BIO-RAD |

**Continued table 1**

| UTILIZATION | DESCRIPTION | MANUFACTURER |
|---|---|---|
| PCR equipment | LightCycler 480 Instrument II<br>T3000 Thermocycler | Roche Life Science<br>Biometra |
| pH meter | LE409 | Mettler Toledo |
| Power supplies | Consort EV261<br>peqPOWER | Peqlab<br>Peqlab |
| Sonicator | UTR2000 | Hielscher Ultrasonic |
| Spectrophotometer | Nanodrop 2000c | Thermo Scientific |
| Ultracentrifuge | Optima L-100 XP | Beckman Coulter |
| Western Blot imaging | Odyssey CLx | LI-COR |

### 2.1.2 Chemicals and Reagents

**Table 2: General Laboratory Chemicals**

| CHEMICAL / REAGENT | MANUFACTURER |
|---|---|
| Acrylamide/Bis solution | Carl Roth GmbH |
| Agar-Agar, bacteriological grade | Carl Roth GmbH |
| Agarose Standard | Carl Roth GmbH |
| Albumin fraction from bovine serum (BSA) | Carl Roth GmbH |
| Ammonium persulfate (APS) | Merck |
| Boric acid ($BH_3O_3$) | Merck |
| Bromophenol blue | Carl Roth GmbH |
| Citric acid monohydrate ($C_6H_8O_7$ x $H_2O$) | Carl Roth GmbH |
| Coomassie Brilliant Blue R-250 | Carl Roth GmbH |
| Deoxynucleotides, solution mix | New England Biolabs |
| N,N-dimethylformamide (DMF) | Merck |
| Dimethyl sulfoxide (DMSO) | Merck |
| Ethylene-diamine-tetra-acetic acid (EDTA) | Carl Roth GmbH |
| Ethidium bromide, 1 % solution | Promega |
| Ethyl alcohol, absolute | Merck |
| Glutaraldehyde, 50 % | Carl Roth GmbH |
| Glycerol, 87 % | Carl Roth GmbH |
| Glycine | Carl Roth GmbH |
| 4-(2-hydroxyethyl)-1-piperazineethanesulfonic acid (HEPES) | Merck |
| Hydrochloric acid (HCl), 37 % | Merck |
| Hydrogenperoxide ($H_2O_2$), 30 %, ROTIPURAN®, p.a., ISO, stabilised | Carl Roth GmbH |
| Magnesium chloride hexahydrate ($MgCl_2$ x 6 $H_2O$) | Merck |
| 2-Mercaptoethanol | Merck |
| Methyl alcohol, absolute | Merck |
| Monopotassium phosphate ($KH_2PO_4$) | Merck |
| Mowiol 4–88 | Carl Roth GmbH |
| Non-fat milk powder | Carl Roth GmbH |
| Paraformaldehyde | Merck |

**Continued table 2**

| CHEMICAL / REAGENT | MANUFACTURER |
|---|---|
| Potassium chloride (KCl) | Merck |
| Potassium hexacyano-ferrate (II) trihydrate ($K_4[Fe(CN)_6]$ x 3 $H_2O$) | Merck |
| Potassium hexacyano-ferrate (III) ($K_3[Fe(CN)_6]$) | Merck |
| Potassium dihydrogen phosphate ($KH_2PO_4$) | Merck |
| Di-potassium hydrogen phosphate trihydrate ($K_2HPO_4$ x 3 $H_2O$) | Merck |
| Polybrene (hexadimethrine bromide) | Merck |
| Prolong Gold Antifade | Life Technologies |
| 2-Popanol | Merck |
| Sodium acetate ($C_2H_3NaO_2$) | Merck |
| Sodium chloride (NaCl) | Carl Roth GmbH |
| Sodium hydroxide (NaOH) | Merck |
| Sodium phosphate dibasic ($Na_2HPO_4$) | Merck |
| Sodium dihydrogen phosphate monohydrate ($NaH_2PO_4$ x $H_2O$) | Merck |
| Di-sodium hydrogen phosphate dihydrate ($Na2HPO_4$ x 2 $H_2O$) | Merck |
| N,N,N,N-Tetra-methyl-ethylene-diamine (TEMED) | SERVA |
| 2-amino-2-(hydroxymethyl) propane-1,3-diol (Tris) | Carl Roth GmbH |
| Triton-X 100 | Carl Roth GmbH |
| Tween20 | Carl Roth GmbH |
| 5-bromo-4-chloro-3-indolyl-β-D-galactopyranoside (X-Gal) | |

**Table 3: Cell Culture Reagents, antibiotics, transfection reagents**

| CHEMICAL / REAGENT | MANUFACTURER |
|---|---|
| Ampicillin | Carl Roth GmbH |
| Antibiotic-Antimycotic (Penicillin/Streptomycin) | Life Technologies |
| DMEM, Glutamax, low glucose, pyruvate | Gibco |
| Fetal bovine serum (FBS) | Life Technologies |
| Heparin | Ratiopharm GmbH |
| Human platelet lysate (hPL) | Transfusion Medicine, University Hospital Halle (Saale) |
| L-Glutamin (100x, 200 mM) | Life Technologies |
| Opti-MEM reduced serum medium (Gibco) | Life Technologies |
| Polyethylenimine (PEI) | Sigma Aldrich |
| Puromycin | Gibco |
| TGF-β1, recombinant human (C-63499) | Promocell |
| 0,5 % Trypsin-EDTA (10x) | Life Technologies |
| Viromer Blue | Lipocalyx |

**Table 4: Standards**

| DESCRIPTION | MANUFACTURER |
|---|---|
| GeneRuler 100 bp DNA ladder | Thermo Scientific |
| GeneRuler 100 bp Plus DNA ladder | Thermo Scientific |
| GeneRuler 1 kb DNA ladder | Thermo Scientific |
| Precision Plus Protein Standard (10-250 kDa) | BIO-RAD |

### 2.1.3 Kits, enzymes, inhibitors

**Table 5: Kits and miscellaneous materials**

| DESCRIPTION | MANUFACTURER |
|---|---|
| Dual-Glo Luciferase Assay Kit | Promega |
| Fast SYBR Green Master Mix | Thermo Scientific |
| Human TGF-β1 DuoSet ELISA | R&D Systems |
| Immobilon-FL PVDF membrane | Merck Millipore |
| Micro BCA Protein Assay Kit | Thermo Scientific |
| miRCURY RNA Isolation Kit - Cell and Plant | Exicon |
| miScript II RT Kit | Qiagen |
| miScript SYBR Green PCR Kit | Qiagen |
| NucleoSpin RNA XS | Macherey-Nagel |
| QIAGEN Plasmid Maxi Kit | Qiagen |
| QIAGEN Plasmid Mini Kit | Qiagen |
| QIAquick MinElute Gel Extraction Kit | Qiagen |
| QIAquick MinElute PCR Purification Kit | Qiagen |
| Substrate Reagent Pack | R&D Systems |
| Verso cDNA Kit | Thermo Scientific |

**Table 6: Enzymes and Buffers**

| DESCRIPTION | MANUFACTURER |
|---|---|
| BstBI restriction enzyme | New England Biolabs |
| ClaI restriction enzyme | New England Biolabs |
| CutSmart Buffer | New England Biolabs |
| MluI restriction enzyme | New England Biolabs |
| Q5 High-Fidelity DNA Polymerase | New England Biolabs |
| Q5 High-Fidelity Reaction Buffer (10x) | New England Biolabs |
| Q5 High GC Enhancer (10x) | New England Biolabs |
| Shrimp Alkaline Phosphatase | Thermo Scientific |
| T4 DNA Ligase | New England Biolabs |
| T4 DNA Ligase buffer | New England Biolabs |
| Taq DNA Polymerase | New England Biolabs |
| Thermo Pol Reaction Buffer (10x) | New England Biolabs |

**Table 7: Inhibitors**

| DESCRIPTION | MANUFACTURER |
|---|---|
| Aprotinin | Merck |
| Phenylmethylsulfonyl fluoride (PMSF) | Merck |
| RepSox (kindly provided by AG Hüttelmaier) | Selleckchem, S7223 |
| Sodium orthovanadate ($Na_3VO_4$) | Merck |

### 2.1.4 Plasmids, oligonucleotides and antibodies

**Table 8: Plasmids**

| NAME | DESCRIPTION | REFERENCE |
|---|---|---|
| p3D.A-Luc | Firefly luciferase expression is controlled by triple cfos-derived SRF binding sites, in front of a TATA-box of cytoskeletal actin in pGL3 (Sotiropoulos *et al.* 1999, Geneste *et al.* 2002) | Guido Posern |
| TRC2 pLKO.5-puro Non-Mammalian shRNA Control (MISSION® Control Vector) | lentiviral plasmid, harbouring control shRNA and puromycin resistance cassette | Merck, SHC202 |
| MKL1 MISSION shRNA Plasmid (#41) | lentiviral plasmid, harbouring shRNA against MRTF-A (CCGGTTGTGGGCCAGGTGAACTATCCTCGAGGATAGTTCACCTGGCCCACAATTTTTG) and puromycin resistance cassette | Merck, TRCN0000303841 |
| MKL1 MISSION shRNA Plasmid (#42) | lentiviral plasmid, harbouring shRNA against MRTF-A (CCGGCTGTCTGTCTGGCTACAATTTCTCGAGAAATTGTAGCCAGACAGACAGTTTTTG) and puromycin resistance cassette | Merck, TRCN0000303842 |
| MKL1 MISSION shRNA Plasmid (#77) | lentiviral plasmid, harbouring shRNA against MRTF-A (CCGGGACTATCTCAAACGGAAGATTCTCGAGAATCTTCCGTTTGAGATAGTCTTTTTG) and puromycin resistance cassette | Merck, TRCN0000299977 |
| MKL1 MISSION shRNA Plasmid (#78) | lentiviral plasmid, harbouring shRNA against MRTF-A (CCGGGCTCAAGTACCACCAGTACATCTCGAGATGTACTGGTGGTACTTGAGCTTTTTG) and puromycin resistance cassette | Merck, TRCN0000299978 |
| pLVX_shRNA2_Crimson_ Puro | pLVX_shRNA2 (Clonetech) was modified exchanging ZsGreen with E2-Crimson and inserting an IRES site connected to a puromycin resistance cassette | Kindly provided by AG Hüttelmaier |

**Continued table 8**

| NAME | DESCRIPTION | REFERENCE |
|---|---|---|
| pLVX_shRNA2_3D.A-Luc | Originated from pLVX-shRNA2-Crimson-Puro by exchanging the U6 promoter with the 3D.A-Luc firefly luciferase reporter (amplified from p3D.A-Luc plasmid) via *ClaI/BstBI* | This study |
| psPAX2 | 2nd generation lentiviral packaging plasmid, Addgene #12260 | Kindly provided by Didier Trono |
| pMD2.G | VSV-G envelope expressing plasmid, Addgene #12259 | Kindly provided by Didier Trono |

**Table 9: Oligonucleotides for qPCR**

| AMPLICON | NAME | SEQUENCE (5'-3') | SOURCE |
|---|---|---|---|
| ACTA2 | SMA_fwd<br>SMA_rev | CGGTGCTGTCTCTCTATGCC<br>AGCAGTAGTAACGAAGGAATAGCCA | A. Descot |
| ALAS | ALAS_fwd<br>ALAS _rev | CTGCAAAGATCTGACCCCTC<br>CCTCATCCACGAAGGTGATT | This study |
| CNN1 | CNN1_fwd<br>CNN1_rev | CTGTCAGCCGAGGTTAAGAAC<br>GAGGCCGTCCATGAAGTTGTT | This study |
| COL1A1 | COL1A1_fwd<br>COL1A1_rev | CGATGGATTCCAGTTCGAGTAT<br>GACAGTGACGCTGTAGGTGAAG | This study |
| GAPDH | GAPDH_fwd<br>GAPDH_rev | ACCCAGAAGACTGTGGATGG<br>TTCTAGACGGCAGGTCAGGT | A. Kehlen |
| MRTF-A | MRTF-A_fwd<br>MRTF-A_rev | GAGCCAGACTAGCCGATGAC<br>CACAGAACCCTGGGACTCAT | This study |
| MYOCD | Myocd_fwd<br>Myocd_rev | ACCAGTCAGATGCGGGGAA<br>CCAAGGATTTGGACTTTACAGCA | This study |
| TGF-β1 | TGF_fwd<br>TGF_rev | CTAATGGTGGAAACCCACAACG<br>TATCGCCAGGAATTGTTGCTG | This study |
| miR-21-5p | miR-21<br>primer assay | TAGCTTATCAGACTGATGTTGA | Qiagen,<br>MS00009079 |
| miR-29-3p | miR-29<br>primer assay | TAGCACCATTTGAAATCAGTGTT | Qiagen,<br>MS00006566 |
| SNORD61 | SNORD61<br>primer assay | Not given by the company | Qiagen,<br>MS00033705 |
| SNORD72 | SNORD72<br>primer assay | Not given by the company | Qiagen,<br>MS00033719 |
| SNORD95 | SNORD95<br>primer assay | Not given by the company | Qiagen,<br>MS00033726 |

**Table 10: Oligonucleotides for cloning and sequencing**

| AMPLICON/ PURPOSE | NAME | SEQUENCE (5'-3') |
|---|---|---|
| 3DA_Luc | 3DA_fwd_ClaI<br>3DA_rev_BstBI | CTGAATCGATCATTTCACACAGGAAACAGCT<br>GATCTTCGAAAACTTGTTTATTGCAGCTTATAATGG |
| Sequencing | 3DA_Seq_fwd<br>3DA_Seq_rev | GGGTACAGTGCAGGGGAAA<br>CGTTACTATGGGAACATACGTC |

**Table 11: Small interfering RNA (siRNA)**

| TARGET | NAME | MANUFACTURER |
|---|---|---|
| Non target control | siCtrl. | siTOOLs Biotech |
| MRTF-A | siMRTF-A | siTOOLs Biotech, 30 siRNA species against GeneID: 57591 |

**Table 12: Antagomirs and miR mimics**

| TARGET | NAME | MANUFACTURER |
|---|---|---|
| miR-21-5p | *mir*Vana miRNA inhibitor (antagomir) | Thermo Fischer Scientific, AssayID: MH10206, Catalog # 4464084 |
| miR-29b-3p | *mir*Vana miRNA inhibitor (antagomir) | Thermo Fischer Scientific, AssayID: MH10103, Catalog # 4464084 |
| miR-21-5p | *mir*Vana miRNA mimic | Thermo Fischer Scientific, AssayID: MC10206, Catalog # 4464066 |
| miR-29b-3p | *mir*Vana miRNA mimic | Thermo Fischer Scientific, AssayID: MC10103 , Catalog # 4464066 |

**Table 13: Primary antibodies and reagents used for Western Blot and immunofluorescence**

| ANTIBODY/REAGENT | DESCRIPTION | SOURCE | USED IN |
|---|---|---|---|
| anti-Calponin 1 | Mouse monoclonal IgG1 | Santa Cruz, sc-58707 | WB 1:250 |
| anti-MRTF-A | Rabbit polyclonal | Cell Signaling, #14760 | WB 1:500<br>IF 1:100 |
| anti-α-SMA | Mouse monoclonal IgG2a, clone 1A4 | Merck, A5228 | WB 1:500<br>IF 1:500 |
| anti-SMAD2 | Rabbit monoclonal | Cell Signaling, #3122 | WB 1:1000 |
| Anti-pSMAD2 | Rabbit polyclonal | Cell Signaling, #3104 | WB 1:1000 |
| anti-α-tubulin | Mouse monoclonal IgG1, clone DM1A | Merck, T9026 | WB 1:2000 |
| DAPI | 4′,6-Diamidino-2-phenylindole dihydrochloride | Merck, D9542 | IF 1:50000 |
| Phalloidin-Alexa 647 | F-actin marker | Invitrogen, A22287 | IF 1:200 |

All antibodies used for Western Blot (WB) were diluted in 5 % milk/TBS-T, despite Anti-pSMAD2 which is diluted in 5 % BSA/TBS-T. Reagents and antibodies used for immunofluorescence (IF) are diluted in a special antibody diluent (2.1.5.1).

**Table 14: Secondary antibodies used for Western Blot and immunofluorescence**

| REAGENT | SOURCE | USED IN |
|---|---|---|
| Alexa 488-goat anti-mouse IgG | Molecular Probes, A11001 | IF 1:200 |
| Alexa 546-goat anti-rabbit IgG | Invitrogen, 11010 | IF 1:200 |
| Anti-rabbit-HRP | Cell Signaling, #7076 | WB 1:1000 |
| IRDye680RD-goat anti-mouse IgG | LI-COR, 926-68070 | WB 1:15000 |
| IRDye680RD-goat anti-rabbit IgG | LI-COR, 926-68071 | WB 1:15000 |
| IRDye800CW-goat anti-mouse IgG | LI-COR, 926-32210 | WB 1:15000 |

All antibodies used for Western Blot (WB) were diluted in 5 % milk in TBS-T. Reagents and antibodies used for immunofluorescence (IF) are diluted in a special antibody diluent (2.1.5.1).

### 2.1.5 Buffers, solutions and media

#### 2.1.5.1 Common buffers and solution

**ANTIBODY DILUENT (IF)**

| | |
|---|---|
| 0.05 % (v/v) | Tween20 |
| | In PBS |

**BLOCKING SOLUTION (IF)**

| | |
|---|---|
| 10 % (v/v) | Horse Serum |
| 1 % (w/v) | BSA |
| | In PBS |

**BLOCKING SOLUTION (WESTERN BLOT)**

| | |
|---|---|
| 5 % (w/v) | Milk Powder |
| | In TBS-T |

**FIXATION (IF)**

| | |
|---|---|
| 3.7 % (v/v) | Formaldehyde (pH 7) |
| | In PBS |

**6X LOADING BUFFER (DNA) PH 8**

| | |
|---|---|
| 85 % (v/v) | Glycerol |
| 0.5 M | EDTA |
| 0.03 % (w/v) | Bromophenol blue |
| 1x | TE-Buffer |

**LOW SALT LYSIS BUFFER (PROTEIN)**

| | |
|---|---|
| 50 mM | HEPES (pH 7.5) |
| 150 mM | NaCl |
| 1 mM | EGTA |
| 10 % | Glycerol |
| 1 % | Triton X-100 |
| 100 mM | NaF |
| 10 mM | $Na_4P_2O_7$ x 10 $H_2O$ |
| 1 mM | $Na_3VO_4$ |
| 1 mM | PMSF |
| 10 mg/ml | Aprotinin |

**PBS (PH 7.4)**

| | |
|---|---|
| 2.7 mM | KCl |
| 137 mM | NaCl |
| 10 mM | $Na_2HPO_4$ |
| 1.8 mM | $KH_2HPO_4$ |

**PERMEABILIZATION SOLUTION (IF)**

| | |
|---|---|
| 0.2 % (v/v) | Triton-X 100 |

**RUNNING BUFFER (SDS PAGE)**

| | |
|---|---|
| 25 mM | TRIS |
| 192 mM | Glycine |
| 0.1 % (v/v) | SDS |

**RUNNING GEL (PAGE) PH 8.8**

| | |
|---|---|
| 9 % | Acrylamide/Bis |
| 375 mM | TRIS HCl |
| 0,1 % (v/v) | SDS |
| 0,1 % (v/v) | APS |
| 0,1 % (v/v) | TEMED |

**6X SDS PROTEIN LOADING BUFFER**

| | |
|---|---|
| 375 mM | TRIS HCl |
| 9 % | SDS |
| 50 % | Glycerol |
| 0.03 % (w/v) | Bromophenol blue |

**STACKING GEL (PAGE) PH 6.8**

| | |
|---|---|
| 5 % | Acrylamide/Bis |
| 127 mM | TRIS HCl |
| 4,5 % | Glycerol |
| 0,1 % (v/v) | SDS |
| 0,1 % (v/v) | APS |
| 0,1 % (v/v) | TEMED |

**TAE BUFFER (1X) PH 8.0**

| | |
|---|---|
| 400 mM | TRIS |
| 50 mM | $C_2H_3NaO_2$ |
| 10 mM | EDTA |

**TBS BUFFER (1X) PH 7.5**

| | |
|---|---|
| 20 mM | TRIS |
| 150 mM | NaCl |

**TBS-T BUFFER (1X) PH 7.5**

| | |
|---|---|
| 20 mM | TRIS |
| 150 mM | NaCl |
| 0.1 % (v/v) | Tween 20 |

**TE Buffer (1x) pH 8.0**

| | |
|---|---|
| 10 mM | Tris-HCl |
| 1 mM | EDTA |

**TRANSFER BUFFER (WESTERN BLOT)**

| | |
|---|---|
| 25 mM | TRIS |
| 192 mM | Glycine |
| 20 % (v/v) | Methanol |
| 0.05 % (v/v) | SDS |

### 2.1.5.2 Cell culture media

**FREEZING MEDIUM**

| | |
|---|---|
| 90 % | FBS |
| 10 % | DMSO |

**HCT8 MEDIUM**

| | |
|---|---|
| 10 % | FBS |
| 1 % | Antibiotic-antimycotic |
| | In RPMI 1640 (Gibco, 21875091) |

**HEK293T MEDIUM**

| | |
|---|---|
| 10 % | FBS |
| 1 % | Antibiotic-antimycotic |
| 1 % | L-glutamine |
| | In DMEM (Gibco, 11965084) |

**MSC CULTIVATION MEDIUM**

| | |
|---|---|
| 10 % | hPL |
| 1 % | Antibiotic-antimycotic |
| 1 IE | Heparin |
| | In DMEM GlutaMAX (Gibco, 21885025 |

**MSC STARVATION MEDIUM**

| | |
|---|---|
| 0.5 % | BSA |
| 1 % | Antibiotic-antimycotic |
| | In DMEM GlutaMAX |

**MSC TRANSFECTION/TRANSDUCTION MEDIUM**

| | |
|---|---|
| 10 % | FBS |
| 1 % | Antibiotic-antimycotic |
| | In DMEM GlutaMAX |

#### 2.1.5.3 Bacterial growth media

**FLUID LB CULTURE MEDIUM**

| | |
|---|---|
| | Lysogen broth powder (LB, Carl Roth) |
| 100 µg/ml | Ampicillin |
| | In $H_2O$ |

**SOLID LB CULTURE MEDIUM**

| | |
|---|---|
| | LB-agar powder (Carl Roth) |
| 100 µg/ml | Ampicillin |
| | In $H_2O$ |

### 2.1.6 Cells

**Table 15: Used bacterial strains**

| BACTERIAL STRAIN | GENOTYPE | SOURCE |
|---|---|---|
| *E. coli* DH5α | F– Φ80*lac*ZΔM15 Δ(*lac*ZYA-*arg*F) U169 *rec*A1 *end*A1 *hsd*R17 (rK–, mK+) *pho*A *sup*E44 λ– *thi*-1 *gyr*A96 *rel*A1 | Thermo Scientific |
| *E. coli* JM110 | rpsL thr leu thi lacY galK galT ara tonA tsx dam dcm glnV44 Δ(lac-proAB) e14- [F' traD36 proAB+ lacIq lacZΔM15] hsdR17(rK-mK+) | Addgene (#49763) |

**Table 16: Used cell lines**

| CELL LINE/CELL TYPE | DESCRIPTION | SOURCE |
|---|---|---|
| Human bone marrow-derived stromal cells (MSC) | Primary cells, fibroblastic morphology, isolated from bone-marrow samples taken from the iliac crest | Kindly provided by Dr. Jana Lützkendorf (University Hospital Halle, Polyclinic of Internal Medicine) (Mueller *et al.* 2006) |
| HEK293T | human embryonic kidney cells with epithelial morphology, genetically modified to express the Sv40 T antigen | Kindly provided by Dr. Robert Torka |
| HCT8 | Human colorectal cancer cell line | ATCC Nr. CCL-244 |

### 2.1.7 Software

**Table 17: Used software**

| SOFTWARE | SOURCE |
|---|---|
| Adobe Photoshop CS6 *Extended*, Version 13.0.1 | Adobe Systems GmbH (München) |
| AxioVision Rel. 4.8.1 | Carl Zeiss Jena GmbH (Jena) |
| Clariostar Reader Control and MARS Data Analysis Software | BMG Labtech |
| GloMax Software, Version 1.9.2 | Promega GmbH (Mannheim) |
| Image Studio Software für Odyssey CLx, Version 3.1 | LI-COR Biosciences GmbH (Bad Homburg) |
| ImageJ/Fiji | (Schindelin *et al.* 2012) |
| Light Cycler 480 Software, Version 1.5.0 SP4 | Roche (Mannheim) |
| Microsoft Office 2010 | Microsoft Deutschland GmbH (München) |
| NanoDrop 2000c, Version 1.6.198 | Thermo Fisher Scientific (Schwerte) |
| SnapGene, Version 2.8.3 | GSL Biotech LLC (Chicago, IL, USA) |
| SPSS 24.0 | IBM Corp., Armonk, NY, USA) |

## 2.2 Methods

### 2.2.1 Microbiological techniques

#### 2.2.1.1 Cultivation and maintenance of bacterial strains

*E. coli* strains DH5α and JM110 were grown at 37 °C overnight in LB culture medium or on LB agar plates supplemented with 100 µg/ml ampicillin for selection. For short-term storage, *E. coli* cultures were kept on LB agar plates at 4 °C. For long-term storage, 1 ml glycerol stocks were generated containing 500 µl of the overnight culture and 500 µl of 50 % sterile glycerol. Glycerol stocks were stored at -80 °C.

#### 2.2.1.2 Transformation of competent bacteria

Chemically competent *E. coli* strains DH5α and JM110 were used for transformation. One hundred ng plasmid DNA or 5 µl of a ligation reaction was used for transformation for 100 µl cells. The DNA was mixed with competent cells by snapping the Eppendorf tube and incubated on ice for 30 minutes. Afterwards, a thermal shock (45 seconds at 42 °C) was done followed by re-incubation for 5 minutes on ice. Next, cells were mixed with 500 µl pre-warmed LB-medium without antibiotics and incubated for 1 hour under constant shaking (550 rpm) at 37 °C. One hundred µl of transformed cells were plated on LB-agar plates containing 100 µg/ml ampicillin and incubated overnight at 37 °C to cultivate positively transformed DH5α cells.

### 2.2.2 Cell culture techniques

#### 2.2.2.1 General procedures and cell cultivation

Cell culture work was performed in sterile laminar flow cabinets under biosafety level S1 conditions. All cell types were cultured at 37 °C and 5 % $CO_2$. Cell passaging was done every 2-3 days depending on cell density and type. For passaging, cells were washed with warmed PBS followed by detaching cell-cell- and cell-surface-contacts using warmed 1 x trypsin solution (10 x trypsin-EDTA in PBS). The trypsin reaction was stopped by adding fresh medium. The mixture was resuspended to obtain a single-cell suspension. New passages were seeded diluting cells in fresh medium depending on cell type: 1:10-1:20 for HCT8 and HEK293T and 1:3 to 1:5 regarding MSC. Cell number and size were determined using the CASY cell counter according to the manufacturer's instructions. Cryo stocks were maintained at -150 °C for long-term storage. Per tube, 1 x $10^6$ cells (HCT8 & HEK293T) or 2.5-5 x $10^5$ cells (MSC) were resuspended in 1 ml freezing medium (2.1.5.2). For gentle freezing conditions, stocks were stored at -80 °C for 48 hours in CryoTube™ vials in an isopropanol-filled container and afterwards transferred to a -150 °C freezer. For re-use, cells stocks were thawed at 37 °C in the water bath for 1-2 minutes, mixed with culture medium and transferred into sterile culture dishes.

#### 2.2.2.2 Cultivation of human primary bone marrow-derived MSC

Primary bone marrow-derived MSC were recovered from patients at the University Clinic Halle. All donors gave written consent to the additional bone marrow aspiration according to a protocol approved by the institutional review board (Ethics Committee of the Medical Faculty of Martin-Luther-University Halle-Wittenberg; Prüfplan Vers. 2, Amendment 1, Ethikvotum 20.04.2010). Isolation and initial cultivation of MSC were done in the University Clinic in the Department of Internal Medicine IV by Dr. Jana Lützkendorf and colleagues and performed as described previously (Mueller *et al.* 2006, Werner *et al.* 2019). MSC with passage number 1 or 2 were kindly provided by Dr. Jana Lützkendorf. All experiments were performed with MSC from at least three different donors and passage numbers between 3 and 6.

#### 2.2.2.3 Generation of tumour-conditioned medium from HCT8 cells

Tumour cell-conditioned medium (TCM) was generated by seeding 2.5 x $10^6$ HCT8 cells in 25 ml MSC starvation medium in 150 mm cell culture dishes. After 72 h TCM was separated from the cells by centrifugation (5200 g, 10 min. The control medium was processed in parallel. TCM has been activated directly before use by acidification to release mature TGF-β from its latent complex, as described by Mazzieri (Mazzieri *et al.* 2000).

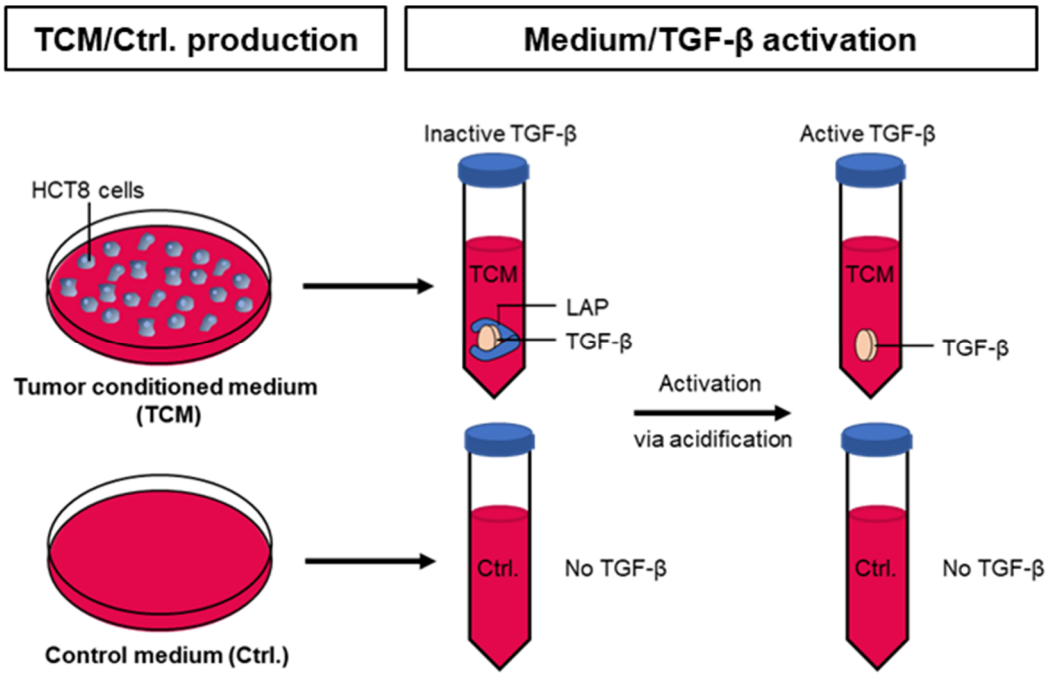


**Figure 6: Schematic representation of the generation of TCM from HCT8 cells**
TCM and control medium were incubated for 72 h. After harvesting the medium acidification to pH 2 by HCl was performed followed by neutralization to pH 7,4 using NaOH. Acidification led to the release of TGF-β from LAP. LAP= latency associated protein

TGF-β is known to be secreted in its inactive form bound to the latency-associated protein (LAP) by cultured cells (Lawrence *et al.* 1984). The interaction can be easily disrupted by enzymatic or physical treatments (Gleizes *et al.* 1997). Here, acidification (1 M HCl to pH 2, for 1 h, room temperature) followed by neutralisation (1 M NaOH to pH 7.4) was used to disrupt TGF-β:LAP interaction and to release mature active TGF-β1.

#### 2.2.2.4 MSC treatment (TGF-β1, TCM, RepSox)

5000 cells/cm$^2$ MSC were seeded into a 100 mm dish and cultivated 24 h under standard conditions. Afterwards, medium was removed, MSC were washed with PBS and 6 ml starvation medium (2.1.5.2) containing 10 ng/ml TGF-β1 or 6 ml TCM medium (2.2.2.3) was added per dish. As control either 6 ml starvation medium or control TCM were added. Cells were cultivated for a further 24 h or 48 h for RNA or protein harvest, respectively. For continuous TGF-β1 stimulation over 10 days, media were replaced every 48 h. Combined TGF-β1/RepSox or TCM/RepSox treatment was performed by supplementing the media with 200 nM RepSox. Cells were additionally incubated 1 h with 200 nM RepSox in 6 ml starvation medium 24 h medium post-seeding.

#### 2.2.2.5 siRNA transfection of MSC

Transient transfection of siRNA (see Table 11) was performed using Viromer Blue (Lipocalyx) according to the manufacturer's instructions. Five thousand cells/cm$^2$ were seeded and cultured overnight in cultivation medium (2.1.5.2) in 60 mm dishes. The next day cells were washed with PBS, following transfection medium (2.1.5.2) and 2 nM siRNA were added. Cells were harvested after 24h for gene expression analysis.

In case siRNA transfection and TGF-β1 stimulation were conducted in parallel, 10 nM siRNA were transfected overnight (approximately 16 h) followed by a medium change to starvation medium (2.1.5.2) supplemented with 10 ng/ml human recombinant TGF-β1. Cells were harvested as described in 2.2.4.1 after 24 h.

#### 2.2.2.6 microRNA mimic/antagomir transfection of MSC

Transient transfection of miR mimics and antagomirs (listed in Table 12) was performed using Viromer Blue (Lipocalyx) according to the manufacturer's instructions. Five thousand cells/cm$^2$ were seeded and cultured overnight in cultivation medium (2.1.5.2) in 60 mm dishes. The next day cells were washed with PBS once and the medium was changed to transfection medium (2.1.5.2) followed by transfection of 30 nM miR mimic/antagomir in total. Cells were harvested for miR and gene expression analysis after 48 h.

#### 2.2.2.7 Generation and preparation of lentiviral particles, titer determination

For virus production, HEK293T were transfected using Polyethylenimine (PEI) as transfection reagent using the guidelines by Longo *et al.* (Longo *et al.* 2013). For each transfer plasmid,

3 x $10^6$ cells were seeded in a 100 mm dish. The following day, cells were transferred to the S2 laboratory and transfection was performed using a DNA:PEI ratio of 1:1.5. Fourteen µg of DNA, including the transfer vector (Merck shRNA plasmids and pLVX_shRNA2_3DA-Luc; listed in Table 8) and the packaging plasmids psPAX2 and pMD2.G (ratio 4:2:1) were mixed with Opti-MEM to a final volume of 500 µl. PEI were diluted in 500 µl Opti-MEM as well. DNA and PEI solution were mixed in equal volumes and incubated for 20 min at room temperature. Meanwhile, HEK293T cells received 9 ml fresh medium. The transfection mix was added dropwise to the cells. The medium was harvested 48 h after transfection and filtered through a 0.45 µl PVDF (polyvinylidene fluoride)syringe to remove living cells. Viral particles were harvested by ultracentrifugation (80000 rcf, 4 °C, 2 h). The translucent pellet was air-dried (5-10 min) at room temperature, resuspended in 50 µl of ice-cold PBS and stored at 4 °C overnight. The next day aliquots were transferred to the -80 °C freezer or used for infection.

#### 2.2.2.8 Lentiviral transduction and generation of stable cell batches of MSC

For the infection, 5000 MSC cells/$cm^2$ were seeded in 100 mm dishes in cultivation medium (2.1.5.2). After 24 h, MSC were transferred to the S2 laboratory, washed with PBS and supplemented with 6 ml transfection/transduction medium (2.1.5.2) containing 8 µl/ml Polybrene and 7.5 µl concentrated virus particle suspension. Medium was removed 24 h after infection. Cells were washed with PBS and cultivation medium (2.1.5.2) containing 0.5 mg/ml Puromycin for selection was applied. Transduced MSC pools were kept under selection pressure for 2 days and afterwards constantly cultivated with 0.1 mg/ml puromycin as multi-clonal population.

### 2.2.3 Molecular cloning, DNA Manipulation and techniques

#### 2.2.3.1 Plasmid isolation

Preparation and purification of plasmid DNA from bacterial cultures were performed using QIAGEN Plasmid Mini (4 ml *E. coli* overnight culture) or Maxi Kit (100 ml *E. coli* overnight culture) according to the manufacturer's instructions. Plasmid DNA was eluted in 40 µl and 200 µl $H_2O$, respectively. DNA purity and concentration were determined using the Nanodrop 2000c system.

#### 2.2.3.2 High fidelity PCR

DNA fragments of interest for molecular cloning were amplified via polymerase chain reaction (PCR) (Mullis *et al.* 1986) using Q5 High-Fidelity DNA polymerase and primers depicted in Table 10. In detail, the following reagents were mixed:

| | |
|---|---|
| x µl | Plasmid DNA (0.3-1 µg) |
| 10 µl | 5 x Q5 High-Fidelity Reaction Buffer (final concentration 1 x) |
| 10 µl | 1 x Q5 High GC Enhancer (final concentration 1 x) |
| 1 µl | 10 mM dNTPs (final concentration 200 µM) |
| 2.5 µl | 10 µM primers each (final concentration 0.5 µM) |
| 0.5 µl | Q5 High-Fidelity DNA Polymerase (0.02 U/µl) |
| add x µl | $H_2O$ to a final volume of 50 µl |

The Amplification reaction was performed in the T 3000 Thermocycler utilising the PCR program described in Table 18.

**Table 18: PCR program Q5 High-Fidelity DNA Polymerase**

| STEP | TEMPERATURE | TIME | CYCLES |
|---|---|---|---|
| Initial denaturation | 98 °C | 30 seconds | 1 |
| Denaturation | 98 °C | 10 seconds | 30 |
| Primer annealing | 3 °C lower than primer melting temperature | 30 seconds | |
| Synthesis | 72 °C | 30 seconds/kb | |
| End synthesis | 72 °C | 2 minutes | 1 |
| Hold | 4 °C | ∞ | - |

After synthesis PCR products were analysed in an agarose gel and afterwards purified using QIAquick MinElute Gel Extraction Kit or directly cleaned up by QIAquick MinElute PCR Purification Kit.

#### 2.2.3.3 Restriction digestion and 5'-end dephosphorylation

For restriction digestion (plasmid DNA or amplified DNA fragment from PCR) approximately 0.5 - 2 µg of DNA were digested using NEB restriction endonucleases. According to the manufacturer's instructions, the reaction mixture contained:

| | |
|---|---|
| x µl | DNA (0.5 – 2 µg) |
| 0.5 µl | Restriction enzyme 1 (5 units) |
| 0.5 µl | Restriction enzyme 2 (5 units) |
| 2.5 µl | CutSmart Buffer |
| add x µl | $H_2O$ to a final volume of 25 µl |

Incubation temperature and time were adapted to the corresponding restriction enzyme. To prevent recircularization of digested DNA de-phosphorylation of the 5'-end using 1 µl shrimp alkaline phosphatase (NEB) for 30 minutes at 37 °C was conducted. DNA was analysed by agarose gel electrophoresis and purified using the QIAquick MinElute Gel Extraction Kit.

#### 2.2.3.4 Ligation

DNA ligation was performed in a molar ratio of 1:5 (vector:insert) using T4 DNA ligase (NEB). Molar ratios were calculated using the following formula:

$$V_i = 5 * (M_i/M_v) * (C_v/C_i) * V_v$$

$C_i$ Concentration of solution with the insert

$C_v$ Concentration of solution with the vector

$M_i$ Mass in base pairs of the insert

$M_v$ Mass in base pairs of the vector

$V_i$ Volume in µl of insert solution

$V_v$ Volume in µl of vector solution (corresponding to 100 ng)

The ligation reaction mixture was set up according to NEB standard protocol and contained:

| | |
|---|---|
| x µl | Vector DNA (~100 ng) |
| y µl | Insert DNA |
| 1 µl | 10x T4 DNA ligase buffer |
| 0.5 µl | T4 DNA ligase |
| add z µl | $H_2O$ to a final volume of 10 µl |

Ligation was carried out overnight at 16 °C or 2 hours at room temperature. As a control, the ligation was performed without insert DNA. After ligation, 5 µl of the reaction were transformed into chemically competent *E. coli* DH5α.

#### 2.2.3.5 Agarose gel electrophoresis

Agarose gel electrophoresis was performed using 1 % agarose gels (1 g of agarose powder in 100 ml 1x TAE buffer) containing 0.01 % (v/v) ethidium bromide. DNA samples were mixed with 5x DNA loading dye, loaded into the wells and separated at 100-120 V for approximately 40 min. Utilising the Gel Stick imaging system (Intas Science Imaging) DNA separation was visualized using UV light (312 nm). The fragment sizes were determined using a suitable GeneRuler DNA ladder (Thermo Scientific) which was loaded as size control.

#### 2.2.3.6 DNA extraction

DNA fragments cut out from agarose gels were purified using QIAquick MinElute Gel Extraction Kit. For PCR products QIAquick MinElute PCR Purification Kit was used according to the manufacturer's instructions. Elution was performed using 10 µl $H_2O$. DNA amounts were measured with the Nanodrop 2000c (Thermo Scientific).

#### 2.2.3.7 Determination of DNA and RNA concentrations

For spectrophotometric analysis of DNA fragments and plasmids, purity and concentration were determined using Nanodrop 2000c measuring absorption at 260 nm and 280 nm.

#### 2.2.3.8 DNA Sequencing

Sequencing of plasmids and DNA fragments was performed by Microsynth Seqlab according to the Sangers chain-terminating technique (Sanger *et al.* 1977). Sequencing results were analysed using the SnapGene software.

#### 2.2.3.9 Cloning of the lentiviral MRTF-A reporter construct pLVX_shRNA2_3D.A-Luc

The reporter plasmid pLVX_shRNA2_3D.A-Luc (Supplementary figure 1) originated from a lentiviral shRNA plasmid (pLVX-shRNA2-Crimson-Puro) and was modified to create a lentiviral transducable reporter construct for MSC. The U6 promoter of the original plasmid (pLVX-shRNA2-Crimson-Puro) was exchanged with the 3D.A-Luc firefly luciferase reporter, amplified from p3D.A-Luc plasmid, via ClaI/BstBI restriction sites. The luciferase reporter expression is regulated by a special MRTF-SRF dependent promoter called 3D.A, consisting of triple cfos-derived SRF binding sites, in front of a TATA-box of cytoskeletal actin (Sotiropoulos et al. 1999, Geneste et al. 2002). Additionally, a constitutively expressed E2-Crimson was inserted being used as an internal control for the firefly luciferase. The construct shown in Supplementary figure 4 was inserted in the MSC genome randomly by long terminal repeats (LTR) at the 3' and 5' end. By external stimuli, like TGF-β1 or TCM, MRTF-A is triggered to translocate to the nucleus binding SRF inducing MRTF/SRF dependent gene expression by binding the 3D.A promoter. Afterwards MRTF-A activity was monitored as described in 2.2.5.5.

### 2.2.4 RNA techniques

#### 2.2.4.1 RNA isolation

Total RNA was isolated from cell cultures using the NucleoSpin RNA XS Kit (Macherey-Nagel). 1.4 x $10^5$ MSC were seeded in 6 cm cell culture dishes, grown overnight and harvested after 24 h (TGF-β1/TCM treatment), 48 h (siRNA transfection) or 72 h (siRNA transfection combined with TGF treatment). Harvesting was performed as follows: cell culture medium was removed, cells were gently washed with PBS, complete PBS was removed, and the kit's lysis buffer was directly added to the cells. Cell lysates were harvested using a cell scraper and immediately stored on ice. Further purification steps were performed according to the manufacturer's instructions. RNA purity and concentration were determined using the Nanodrop 2000c. Isolated RNA was directly used for cDNA synthesis or stored at -20 °C.

#### 2.2.4.2 microRNA (miR) isolation in parallel with total RNA

The miRCURY RNA Isolation Kit - Cell and Plant (Exicon) allows the isolation of miR and total RNA in the same attempt. 1.4 x $10^5$ MSC were seeded in 6 cm cell culture dishes, grown overnight and harvested after 48 h (miR mimic or antagomir transfection; TGF-β1 treatment) or 10 days (TGF-β1 treatment). Cells were washed with PBS, subsequently PBS was completely removed, and lysis solution (kit included) was added to the culture plate. By using

a cell scraper, the lysis buffer was evenly distributed, and cells were detached. Further steps were performed according to the manufacturer's instructions. RNA purity and concentration were determined using the Nanodrop 2000c. Isolated RNA was directly used for cDNA synthesis or stored at -20 °C.

#### 2.2.4.3 cDNA synthesis from total RNA

Single-stranded complementary DNA (cDNA) was synthesized from total RNA via reverse transcription. First-strand cDNA synthesis was performed in a 10 µl reaction using Verso cDNA Synthesis Kit (Thermo Scientific), 500 ng RNA and oligo dT primer according to the manufacturer's instructions. The reaction mix was filled up with $H_2O$ to a total volume of 100 µl after synthesis.

#### 2.2.4.4 cDNA synthesis from miR in parallel with total RNA

Using the miScript II RT Kit (Qiagen) and the included HiFlex buffer mature miRNA, precursor miRNA, ncRNA and mRNA were reversely transcribed. The synthesis mix was prepared in 10 µl reaction volume with 500 ng of template according to the manufacturer's instructions. The final solutions were diluted 1:10 with $H_2O$ for further analysis.

#### 2.2.4.5 Quantitative real-time PCR (qPCR) from total RNA

The qPCR reactions were performed using the DyNAmo ColorFlash SYBR Green qPCR Kit (Promega). Gene-specific primer (Table 9) mixes were prepared by mixing 10 µl forward primer solution (100 µM), 10 µl reverse primer solution (100 µM) and 80 µl $H_2O$. According to the manufacturer's instructions the reaction mixture for the qPCR contained:

| | |
|---|---|
| 1.5 µl | Diluted cDNA (~5 ng/µl) |
| 5 µl | SYBR Green |
| 0.25 µl | gene-specific primer mix |
| Add 3.25 µl | $H_2O$ to a final volume of 10 µl |

The qPCR was performed using LightCycler 480 II and the PCR programme in Table 19.

**Table 19: qPCR program DyNAmo ColorFlash SYBR Green**

| STEP | TEMPERATURE | TIME | CYCLES |
|---|---|---|---|
| Initial denaturation | 95 °C | 7 minutes | 1 |
| Denaturation | 95 °C | 10 seconds | 40 |
| Primer annealing and extension | 60 °C | 30 seconds | |
| Melting curve | 65-95 °C | 0.11 °C/s | - |
| Hold | 40 °C | ∞ | - |

ALAS and GAPDH expression levels were analysed as references (housekeeping genes) and $H_2O$ was included as negative control for each primer pair. To access the specificity of PCR,

melting curves were routinely generated from every reaction. Relative gene expression levels were calculated according to the Pfaffl method (Pfaffl 2001). Thereby the differences of target gene $C_t$ value to housekeeping gene $C_t$ value were calculated and compared as fold inductions between samples.

#### 2.2.4.6 Quantitative real-time PCR (qPCR) from miRNA

The qPCR reaction was performed using the miScript SYBR Green PCR Kit (Qiagen). According to the manufacturer's instructions. The reaction mixture contained:

| | |
|---|---|
| 1µl | Diluted cDNA (~5 ng/µl) |
| 5 µl | SYBR Green |
| 1 µl | 10x miScript universal primer |
| 1 µl | 10x miScript primer assay |
| Add 3.25 µl | $H_2O$ to a final volume of 10 µl |

The qPCR was performed using the LightCycler 480 II and the program in Table 20.

**Table 20: qPCR program miScript SYBR Green**

| STEP | TEMPERATURE | TIME | CYCLES |
|---|---|---|---|
| Initial denaturation | 95 °C | 15 minutes | 1 |
| Denaturation | 94 °C | 15 seconds | 40 |
| Primer annealing | 55 °C | 30 seconds | |
| Extension | 70 °C | 30 seconds | |
| Melting curve | 65-95 °C | 0.11 °C/s | - |
| Hold | 40 °C | ∞ | - |

SNORD61, SNORD72 and SNORD95 expression levels were analysed as references (housekeeping genes) and $H_2O$ was included as negative control for each primer pair. Melting curve analysis and calculation were performed as described in 2.2.4.5.

### 2.2.5 Protein analysis

#### 2.2.5.1 Cell lysis for immunoblotting

For protein analysis, 5000 cells/cm$^2$ MSC were cultured in 60 mm dishes and harvested after 48 h of TCM or TGF treatment. For this, cells were directly placed on ice and washed with pre-chilled PBS. Afterwards, 70 µl pre-chilled low salt lysis buffer (2.1.5.1) were applied to the cells which were harvested using cell scrapers. Lysates were transferred into Eppendorf tubes and sonicated for 30 seconds (Sonicator UTR2000, Hielscher Ultrasonic, 100 W, cycle 0.5, amplitude 70 %, duration 30 s) and centrifuged at 4 °C and 20000 rcf 10 minutes. Supernatants were transferred into fresh Eppendorf tubes. There was no quantitative measurement of protein concentration done since MSC starvation medium and TCM contain 0.5 % BSA. Due

to this, protein quantification would give distorted results. Hence, equal volumes of protein lysate were supplemented with 6 x SDS protein loading buffer (2.1.5.1), denatured (5 minutes at 95 °C) and loaded on SDS gel or stored at -20 °C.

#### 2.2.5.2 SDS-polyacrylamide gel electrophoresis (SDS-PAGE)

Proteins were analysed using SDS-polyacrylamide gel electrophoresis for electrophoretic size separation according to Laemmli (Laemmli 1970). Running- and stacking-gels were prepared as listed above (2.1.5.1). Equal volumes of protein lysate (20-50 µl) were loaded. Separation on SDS gel was performed at 130V for 1-1.5 h, depending on the protein size to be analysed. Protein size was determined using the Precision Plus Protein Standards (BIO-RAD). SDS gels with size-separated proteins were used for immunoblotting.

#### 2.2.5.3 Immunoblotting (Western Blot)

Size-separated proteins in the SDS gel (2.2.5.2) were transferred via wet blotting onto PVDF membranes using the Mini-PROTEAN Tetra System (BIO-RAD) according to the manufacturer's instructions. Initially, the PVDF membranes were activated in 100 % methanol for 5 min and afterwards equilibrated in transfer buffer. The blotting was performed in cold transfer buffer at 100 V for 75 min at room temperature under constant cooling by ice packs. Following blotting, the membranes were washed in TBS-T and blocked in 5 % milk/TBS-T for 60 min to avoid unspecific antibody binding. Next, the membranes were incubated with primary antibodies diluted in 5 % milk or BSA (depending on antibody) dissolved in TBS-T at 4 °C over night. Subsequently, membranes were washed in TBS-T (3 x 5 min) and incubated with fluorophore- or HRP-conjugated secondary antibody in 5 % milk/TBS-T for 1 h. Applied antibody concentrations are listed in Table 13 and Table 14. Afterwards, the membrane was washed 3 x 5 min in TBS-T. In case of HRP-substrate use, the membrane was washed once with 1x TBS prior to substrate addition, since tween could disturb the HRP to properly convert the substrate. Substrate incubation was performed using transparent film. Fluorescence signals were detected and quantified using ODYSSEY CLx (LI-COR) and quantified using the associated LI-COR Image Studio software according to the manufacturer's recommendations. Signals are given as fluorescence intensity per area and were calculated relative to the loading control.

#### 2.2.5.4 Immunofluorescence staining, microscopy and quantification

For fluorescence microscopy analysis of cytoskeletal structures and protein localisation, cells underwent immunostaining using fluorophore-labelled antibodies and staining reagents. In 12-well plates 5000 cells/cm$^2$ cells were seeded on glass coverslips and cultured overnight. Cells underwent TCM or TGF treatment for 48 h and were fixed (3.7 % formaldehyde in PBS for 10 minutes), permeabilized (0.2 % (v/v) Triton X-100 in PBS for 10 minutes) and unspecific

binding sites were blocked in blocking solution (2.1.5.1) for 60 minutes. Incubation with primary antibodies (in antibody diluent, dilutions listed in Table 13 and Table 14, 1 h at room temperature) was followed by washing (3 x with PBS) and incubation with Alexa-conjugated secondary antibodies and DAPI (in antibody diluent, dilutions listed in Table 14, 1 hour at room temperature). Stained cells were washed 3 x with PBS and embedded in Mowiol. For imaging, the Zeiss Axio Observer7 (20 x objective) equipped with a monochrome Axiocam MRm camera was used. For image adaption, Adobe Photoshop CS6 software was used.

#### 2.2.5.5 Luciferase reporter assay

A luciferase-based reporter system (Supplementary figure 4) was used to analyse the MRTF-SRF transcription factor activity. Seven x $10^4$ reporter-MSC (harbouring pLVX_shRNA2_3DA-Luc plasmid) were grown in a 12-well plate overnight. The next day, cells were washed once with PBS and medium changed to starvation medium (0) for 24 h. Following starvation, stimuli were set for 7 h, 24 h and 48 h. The luciferase assay was done using the Dual-Glo Luciferase Assay Kit (Promega) according to the manufacturer's instruction. In brief, cells were washed 1 x with PBS, 100 µl pre-chilled 1 x passive lysis buffer (Promega) was applied and the 12-well plate was placed on an orbital shaker for 15 min at room temperature until cells were lysed and detached. Next, the lysates were transferred to Eppendorf tubes and centrifuged (15 minutes at 20817 x g and 4 °C). 20 µl of cell extract were transferred in a white 96-well plate. Using the GloMax 96 Microplate Luminometer, injectors automatically dispensed 50 µl of the luciferase substrate in the wells and measured the bioluminescence signal. For normalisation purposes the constitutively expressed E2-Crimson [far-red noncytotoxic tetrameric variant of DsRed fluorescent protein (Strack *et al.* 2009), stably expressed from 3D.A reporter MSC] was measured separately. 50 µl of the cell extract were transferred in a black 96-well plate and measurements were performed using the Clariostar (BMG Labtech) at 600-25/650-25 nm. Firefly luciferase signals were normalised to E2-Crimson and are displayed as fold induction.

#### 2.2.5.6 TGF-β1 ELISA (Enzyme-linked Immunosorbent Assay)

Human TGF-β1 DuoSet ELISA was performed according to the manufacturer's instructions to determine amounts of active TGF-β1 in TCM. Buffer compositions are listed in 2.1.5.1. Samples of three independent TCM productions were analysed.

#### 2.2.5.7 Senescence assay detecting senescence-associated β-galactosidase

The senescence-associated β-galactosidase (SA-βgal) is a biomarker to detect senescence. Five thousand MSC cells/$cm^2$ were seeded per well in a 6 well plate and grown under standard conditions overnight. The next day, the growth medium in one well was supplemented with 5000 µM $H_2O_2$ to serve as positive control. In case effects of TCM or TGF stimulation were analysed the medium was exchanged as described in section 2.2.2.4. One untreated well

served as negative control. After 48 h of treatment the cell staining procedure was performed as described by Debacq-Chainiaux and colleagues (Debacq-Chainiaux *et al.* 2009). In brief, 2 ml of staining solution (containing 1 mg/ml X-gal) were applied per well. The plate was sealed with parafilm to prevent evaporation and to omit crystal formation. The plate was incubated at 37 °C at least overnight in a dry incubator (no $CO_2$, bacterial growth incubator was used). Finally, the staining solution was removed, cells embedded in Mowiol and stored at 4 °C for long term storage. Morphology of at least 50 cells per condition were analysed using the Evos Core AMG (Thermo Fischer). Experiments were performed in three biologically independent replicates.

### 2.2.6 Calculation and Statistics

Data represent means with corresponding standard deviation (SD) including experimental results of at least three independent biological replicates. Statistical analysis was performed using SPSS 24.0 software applying an unpaired two-sample Student's t-test, a one-way ANOVA with Dunnett's multi comparison test (post-hoc) or a one-way ANOVA with Tukey's multiple comparison test (post-hoc) as indicated. Significance is indicated by * $p \leq 0.05$.

# 3 RESULTS

The myofibroblastic differentiation from mesenchymal stem cell (MSC) to cancer-associated fibroblast (CAF) is likely to be connected to myocardin-related transcription factor (MRTF-A) dependent gene regulation. Furthermore, we hypothesised that MRTF-A influences the tumour-supporting role of MSC in mixed colorectal cancer (CRC) xenografts. To examine these issues, primary human bone marrow-derived MSC were differentiated with recombinant transforming growth factor beta 1 (TGF-β1) or tumour-conditioned medium (TCM) and monitored for myofibroblastic markers. The influence of microRNA (miR) on differentiation initiation and progression was additionally analysed. Furthermore, MRTF-A was knocked down by RNA interference (RNAi) in a transient or stable approach, respectively. In mixed xenograft experiments, MSC partially depleted for MRTF-A were used to investigate their effect towards HCT8 CRC cells *in vivo*.

## 3.1 Primary human MSC undergo myofibroblastic differentiation

Even though MSC are known to differentiate into myofibroblasts (Mishra *et al.* 2008) the primary human MSC used in the present thesis needed to be analysed for their myofibroblastic differentiation potential. Initial experiments aimed at the characterisation of the myofibroblastic differentiation process per se. For this purpose, differentiation was stimulated by TGF-β1 and protein markers indicating differentiation and CAF formation were analysed. In particular, alpha-smooth muscle actin (α-SMA) is one of the most reliable markers for myofibroblastic differentiation (Cherng *et al.* 2008). Calponin 1 and collagen 1A1 (COL1A1) were investigated since they are described as myofibroblast markers too (Martinez-Outschoorn *et al.* 2010, Cirri and Chiarugi 2011). Thus, an upregulation of α-SMA, Calponin 1 and COL1A1 should indicate the transition of MSC.

To analyse the MSC myofibroblastic differentiation, cells were seeded under standard culture conditions and treated with human recombinant TGF-β1 serving as differentiation initiator for 24 h (mRNA) or 48 h (protein) in starved medium. The experiment was performed with MSC from 3 different donors to include inter-individual differences and increase the robustness of the results (n=3). The MSC donors were chosen independently of age, sex, or disease but on the following characteristics: similar endogenous expression of myofibroblastic markers and availability of enough cell material for the whole study. Changes in mRNA or protein amount after TGF-β1 treatment were monitored (Figure 7) as fold changes compared to the unstimulated starved control (Ctrl.$^{TGF}$).

TGF-β1 treatment resulted in significantly upregulated mRNA amounts of all considered myofibroblastic markers (Figure 7 a). In detail, the RNA level of α-SMA was increased 4.9-fold, Calponin 1 RNA showed 6.5-fold upregulation and the RNA encoding the ECM component

COL1A1 exhibited a 2-fold rise. Furthermore, a similar increase of α-SMA (2-fold) and Calponin 1 (3.4-fold) protein expression was detected following TGF-β stimulation (Figure 7 b). COL1A1 was not analysed by western blot, as no reliable primary antibody was available. Referring to the results displayed in Figure 7, myofibroblastic differentiation of MSC is triggered by TGF-β1 and results in a CAF-like mRNA and protein expression pattern. Next, it was aimed to establish conditions mimicking the pathophysiological differentiation of MSC into CAF-like myofibroblasts, reminiscent of the influence of colorectal cancer cells on MSC in xenografts. The HCT8 cell line was selected because those cells have been shown to be growth-promoted by MSC when co-transplanted in subcutaneous xenografts of male athymic Nude-Foxn1nu mice (Widder *et al.* 2016). By using cell culture-conditioned medium, cytokines like TGF-β1 and other soluble mediators that can affect MSC are included. It is hypothesised that extracellular signals, especially TGF-β1 from HCT8 tumour cells are required to trigger MSC differentiation. Therefore, it was tested if tumour cell conditioned medium (TCM) obtained from the HCT8 CRC line may trigger the same effects as recombinant TGF-β1. Thus, TCM was obtained by growing HCT8 cells in MSC starvation medium (see 2.1.5.2) for 72 h as described in 2.2.2.3 in detail.

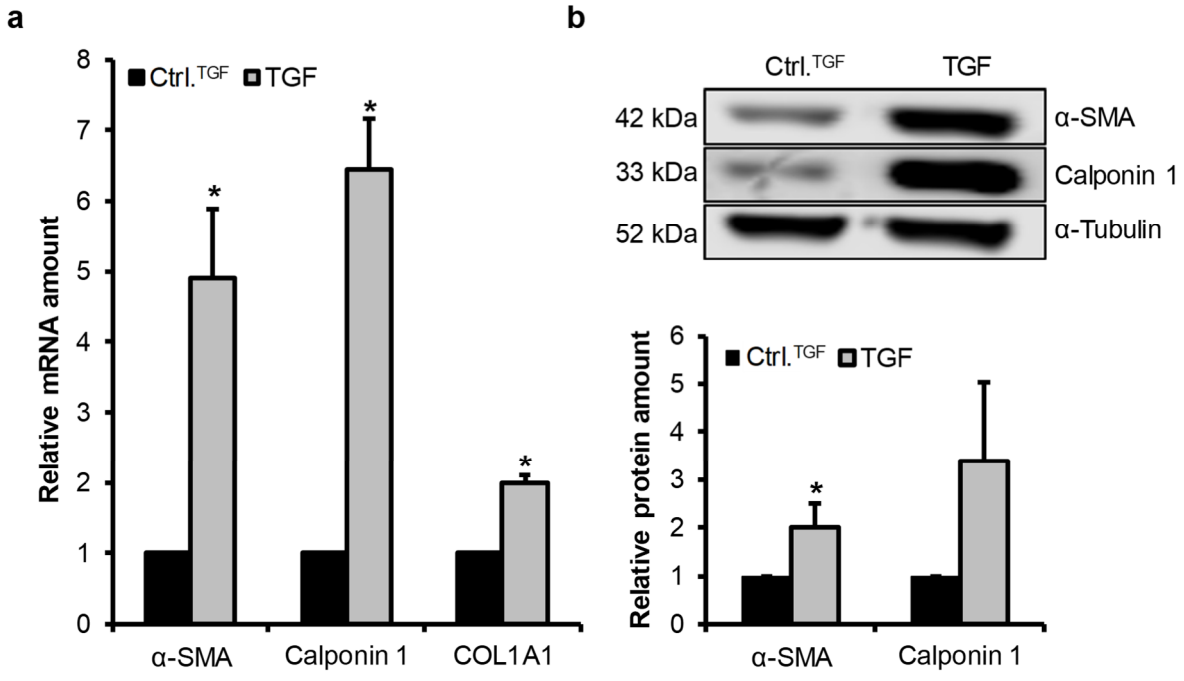


**Figure 7: TGF-β induces expression of myofibroblastic markers in MSC.**
MSC were treated with TGF-β1 (TGF) and analysed for myofibroblastic markers on mRNA and protein levels. **(a)** Endogenous expression of Calponin 1, α-smooth muscle actin (α-SMA) and collagen 1A1 (COL1A1) was increased after TGF-β1 treatment for 24 h. mRNA amounts were quantified by qPCR and normalised to the mean of ALAS and GAPDH. **(b)** Western blots of α-SMA and Calponin 1 show increased protein amounts after 48 h of TGF-β1 (TGF) treatment. Relative protein amounts were normalised to the α-tubulin signal. All data were normalised to the value of the starved control (Ctrl.) which was set to 1. Equal loading was controlled by α-tubulin. Error bars correspond to SD (n=3). Asterisks indicate significant differences *p≤0.05 according to an unpaired Student's t-test.

MSC were treated with TCM or control medium (Ctrl.$^{TCM}$) for 24 h to analyse mRNA expression changes and for 48 h to validate effects on protein level. In line with the results obtained with TGF-β1 treatment; α-SMA, Calponin 1 and COL1A1 mRNA levels were significantly induced in MSC by TCM treatment by 4.6-, 5- and 2-fold; respectively (Figure 8 a). Furthermore, α-SMA and Calponin 1 protein amounts were substantially increased to 3.4- and 2.7-fold 48 h after TCM stimulation compared to control treatment (Figure 8 b).

MSC change their cellular shape significantly during differentiation (Han *et al.* 2017). To monitor the stretching and enlargement of differentiating MSC, phase contrast pictures were taken of MSC growing under standard conditions (medium supplemented with 10 % hPL, cycling MSC), starved MSC and MSC after TGF-β1 and TCM treatment with 20 x magnification. Cycling MSC are of relatively small size and display a triangular shape with lamellipodia-like protrusions at the cell edges. In comparison, starved cells can be characterised by spindle-shaped slender cell bodies. Most importantly, it was observed that MSC spread-out exhibiting a flattened cell shape after TGF-β1 or TCM stimulus (Figure 9 a) suggesting a CAF phenotype according to literature (Mishra *et al.* 2008).

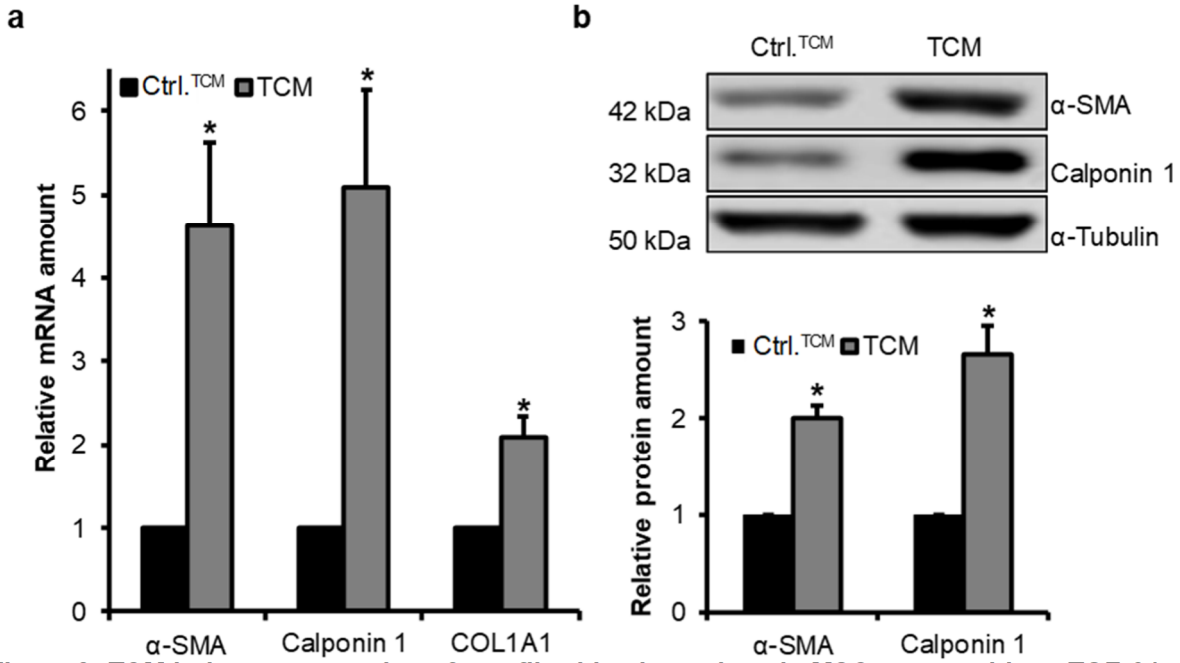


**Figure 8: TCM induces expression of myofibroblastic markers in MSC comparable to TGF-β1.** MSC were treated with freshly activated TCM and analysed for myofibroblastic markers on mRNA and protein levels. **(a)** Endogenous expression of Calponin 1, α-SMA and COL1A1 were increased after TCM treatment for 24 h. mRNA amounts were quantified by qPCR and normalised to the mean of ALAS and GAPDH. **(b)** Western blots of α-SMA and Calponin 1 show increased protein amounts after 48 h of TCM treatment. Relative protein amounts were normalised to the α-tubulin signal. All data were normalised to the value for the starved control (Ctrl.) which was set to 1. Equal loading was controlled by α-tubulin. Error bars correspond to SD (n=3). Asterisks indicate significant differences *p≤0.05 according to an unpaired Student's t-test.

Additionally, MSC were immunostained for α-SMA to analyse their expression pattern during the myofibroblastic MSC to CAF differentiation. Next to α-SMA (Figure 9 b, green) the nucleus of MSC was counterstained with DAPI (Figure 9 b, blue). Fluorescence signals were captured with the Axio Observer7 epifluorescence microscope at 20 x magnification. In conjunction with the ascertained morphological changes (Figure 9 a), the expression pattern of α-SMA was significantly altered (Figure 9 b), comparing cycling, starved and differentiated cells (TGF, TCM). Cycling and starved MSC showed a diffusely distributed and unorganized α-SMA signal localised across the whole cell. However, the α-SMA signal changed to distinct fibres in TGF-β1 or TCM differentiated MSC samples, typical for myofibroblasts and accompanied by cytoskeletal changes (Hinz *et al.* 2007).

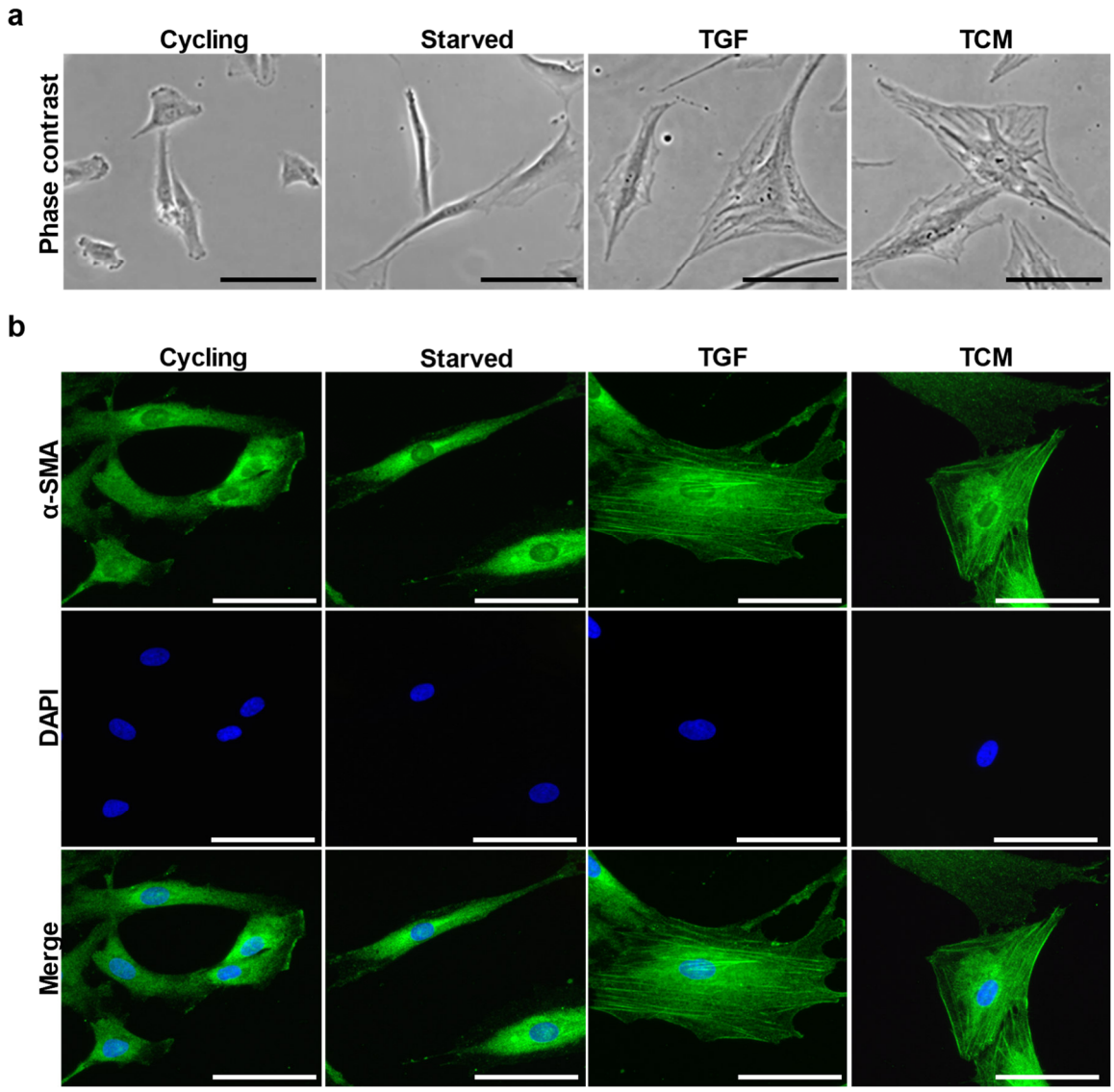


**Figure 9: TGF-β1 and TCM cause morphological and cytoskeletal changes in MSC.**
MSC have been treated with TGF-β1 or TCM for 48 h. **(a)** Phase contrast images displaying the morphology of untreated proliferating MSC (cycling), quiescent MSC (starved) and MSC differentiated by TGF-β1 or TCM. Treated cells display a flattened cell shape compared to cycling and starved cells **(b)** Immunofluorescence images of α-SMA in MSC. Cells were seeded on glass coverslips, treated with TGF-β1 or TCM for 48 h, fixed, immunostained for α-SMA (green) and counterstained with DAPI (blue). 20 x magnification, scale bars 20 µm.

## 3.2 TCM contains active amounts of TGF-β1 activating SMAD2

The above data hint at the presence of secreted factors like TGF-β1 by HCT8 cells, triggering MSC myofibroblastic differentiation in the same way as recombinant human TGF-β1. In this context, TCM from HCT8 was checked for active amounts of TGF-β1 by ELISA. As already mentioned, TGF-β1 is known to be secreted in its inactive form complexed with the LAP (Khalil 1999b). In this context, the harvested TCM was activated by acidification before it was used for MSC differentiation, to gain stable and reproducible amounts of activated TGF-β1 as described in 2.2.2.3.

To investigate an approximate amount of active TGF-β1 in TCM, an ELISA was performed which enables to exclusively quantify active TGF-β1. There was one set of non-acidified samples, harvested by centrifugation without further processing. The acidified set of samples was harvested by centrifugation and acidified according to the protocol in 2.2.2.3. Additionally, non-acidified and acidified samples underwent ELISA included sample activation, which is similar to the acidification process. In non-acidified samples, active amounts of human TGF-β1 could be only detected in the ELISA-activated TCM sample. Ctrl. Medium as well as TCM without activation lack the presence of measurable active TGF-β1 amounts.

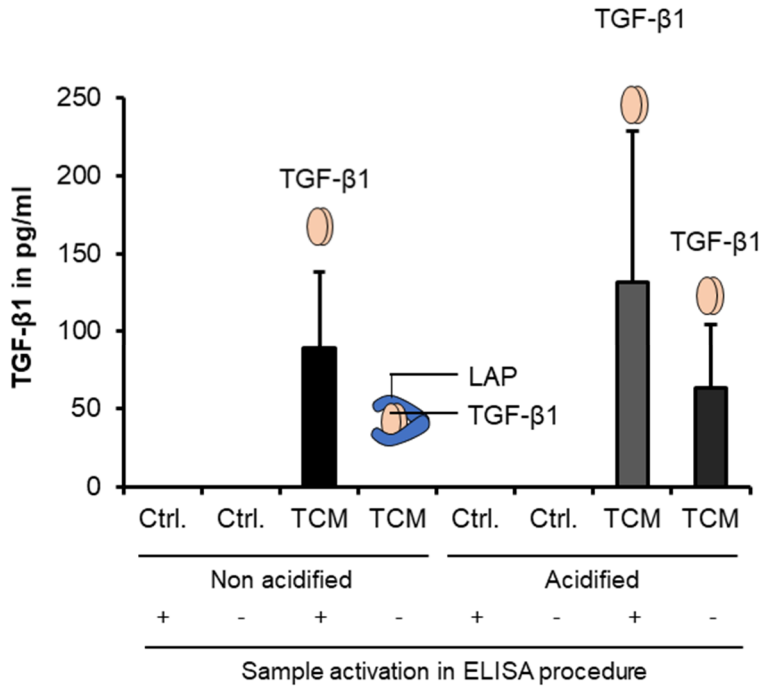


**Figure 10: Physiological amounts of TGF-β1 detected in TCM**
HCT8 tumour-conditioned medium (72 h) and corresponding control medium (Ctrl.) were analysed via ELISA for active amounts of TGF-β1. Non-acidified samples on the left side were harvested by centrifugation and directly used for the Elisa. Acidified samples were acidified after centrifugation to release biologically active TGF-β1 from the LAP. The + and – signs below the bar chart indicate whether samples underwent additional ELISA-included acid treatment. Human recombinant TGF-β1 was used for calibration. *n.d.*, not detectable. Error bars correspond to SD (n=3). LAP, latency-associated protein

In acidified samples, active amounts of TGF-β1 were detected in ELISA-activated and non-activated samples. These data suggest that acidification releases the mature TGF from its latent non-active complex. Compared to the amount of recombinant human TGF-β1 (10 ng/ml) the concentration of TGF-β1 in the HCT8 TCM is relatively low but obviously not less effective as demonstrated in Figure 8.

Since the ELISA data prove the presence of TGF-β1 in TCM it was the next step to monitor TGF-β1 specific signalling events. SMAD2 phosphorylation was analysed after TCM treatment. An increase of phosphorylated SMAD2 (pSMAD2) with unaltered total SMAD2 (tSMAD2) signal points towards activated TGF-β1 signalling. Attempts using recombinant TGF-β1 to trigger differentiation served as positive control. Furthermore, two negative controls were included (Ctrl.$^{TCM}$, Ctrl.$^{TGF}$). While Ctrl.$^{TGF}$ consists of MSC starvation medium (see 2.1.5.2) without any supplements, Ctrl.$^{TCM}$ was treated as TCM without having contact with HCT8 cells (see 2.2.2.3). TGF-β1 specific signalling events were monitored by pSMAD2 after TGF-β1 and TCM treatment (Figure 11). Both stimuli significantly induced SMAD2 phosphorylation by 6.5-fold (TGF-β1) or 7.7-fold (TCM) in MSC within 1 h, whilst tSMAD2 protein levels remained unaffected. Control media (Ctrl.$^{TCM}$, Ctrl.$^{TGF}$) showed no effect on pSMAD2, as expected. Therefore only Ctrl.$^{TCM}$ was used as negative control for future experiments, named Ctrl.

Together, these results demonstrate that TGF-β1 is secreted by HCT8 tumour cells and elicits SMAD signalling responses upon differentiation of MSC.

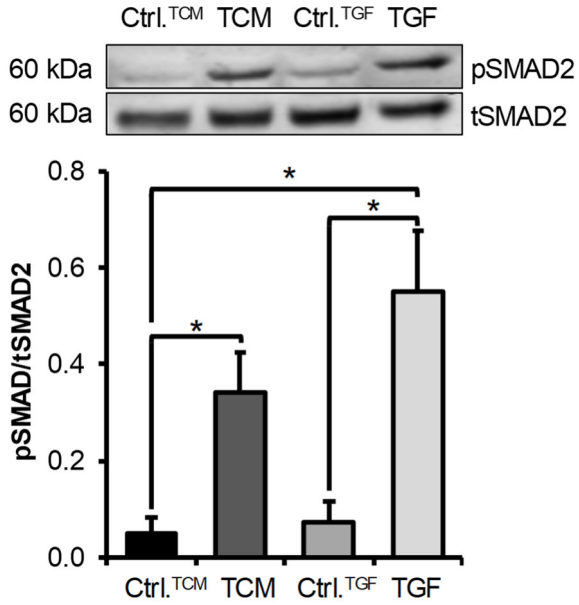


**Figure 11: TGF-β-like signalling via SMAD 2 triggered in MSC during CAF differentiation**
Western Blot showing the ratio between phosphorylated SMAD2 (pSMAD2) and total SMAD2. Cells were treated with TCM or TGF-β1 (TGF) for 1 h, respectively. For quantification, pSMAD2 was normalised to the total SMAD2 signal. Error bars correspond to SEM (n=3). Asterisks indicate significant differences (*p≤0.05) compared to the control sample (Ctrl.) according to an unpaired Student's t-test.

## 3.3 Blocking TGF-β1 signalling interferes with MSC differentiation

To further investigate the role of TGF-β1 signalling, combinatory experiments were done using the Alk5 kinase inhibitor RepSox together with TGF-β1 and TCM treatment. RepSox is inhibiting ATP (adenosine triphosphate) binding to ALK5 and its autophosphorylation (Gellibert *et al.* 2004). By using RepSox along with TGF-β1 or TCM impaired phosphorylation of SMAD2 was shown.

The MSC were treated with 200 nM RepSox for 1 h prior to TGF-β1 and TCM stimulus blocking the Alk5 receptor. During stimulation, RepSox was also present in TGF-containing medium and TCM to ensure constant blocking of Alk5 (western blot Figure 12 a). Protein expression changes of pSMAD2 were quantified and normalised to tSMAD2. Without RepSox TGF-β1 and TCM induced SMAD2 phosphorylation 2.6- to 3.3-fold, respectively. tSMAD2 levels were not affected. RepSox did not change the pSMAD2 protein amount (Figure 12 a) under control conditions (Ctrl. +) but prevented pSMAD2 increase triggered by TGF-β1 (TGF +) and TCM (TCM +). pSMAD2 levels upon RepSox treatment during differentiation (TGF +, TCM +) dropped to endogenous protein levels, as there are no significant differences compared to the unstimulated control sample (Ctrl. -) as well as to the RepSox treated control (Ctrl. +). The corresponding Western Blot quantification is shown in Figure 12 b.

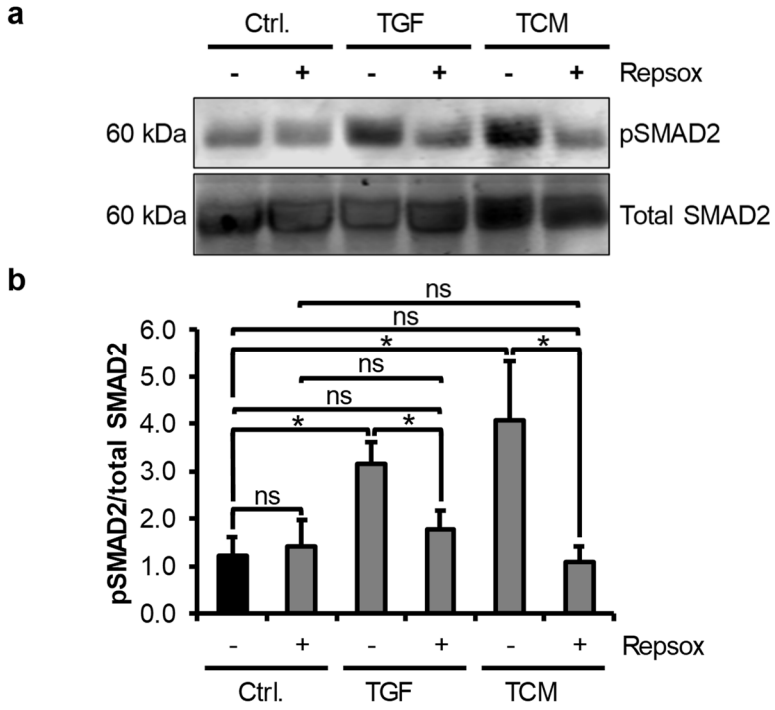


**Figure 12: Increased SMAD2 signalling during MSC differentiation is impaired by RepSox.** MSC were pre-treated with 200 nM RepSox for 1h, afterwards differentiated with recombinant TGF-β1 or freshly activated TCM under the presence of RepSox. Samples were analysed for phosphorylated (pSMAD2) and total SMAD2 protein levels. **(a)** Representative Western blots of pSMAD2 and total SMAD2 show increased protein amounts after 1 h of TGF-β1 and TCM treatment. RepSox prevents the induction caused during differentiation. The + and – signs indicate whether samples have been treated with DMSO as negative control (-) or RepSox (+). **(b)** For quantification, pSMAD2 was normalised to the total SMAD2 signal. Error bars correspond to SEM (n=3). Asterisks indicate significant differences (*p≤0.05) compared as specified by brackets according to an unpaired Student's t-test.

Moreover, changes in myofibroblastic marker expression were analysed via western blot during the differentiation of MSC into CAF (Figure 13 a). MSC were pre-treated for 1 h with RepSox, whereat TGF-β1 and TCM medium were supplemented with RepSox as well during 48 h of stimulation. Stimulating MSC with TGF-β1 and TCM without RepSox (TGF -, TCM -) increased Calponin 1 (2.7-fold) and α-SMA (1.3-fold) protein levels compared to Ctrl. - which was set to 1. α-SMA and Calponin 1 induction by either TGF-β1 or TCM was effectively blocked by RepSox (TGF +, TCM+, Figure 13 b). Both markers seemed to be expressed below endogenous protein levels comparing TGF + (α-SMA $p \leq 0.05$, Calponin 1 $p \geq 0.05$) and TCM + (α-SMA $p \geq 0.05$, Calponin 1 $p \leq 0.05$) samples with Ctrl. -. The inhibitor itself slightly downregulates α-SMA and Calponin 1 protein amounts (Ctrl. +), independent of differentiation (TGF +, TCM +). Together, these results demonstrate, that HCT8 colorectal cancer cells are likely to produce secreted factors such as TGF-β1 inducing SMAD2 signalling, stimulating Calponin 1 and α-SMA in an Alk5 S/T kinase activity dependent way.

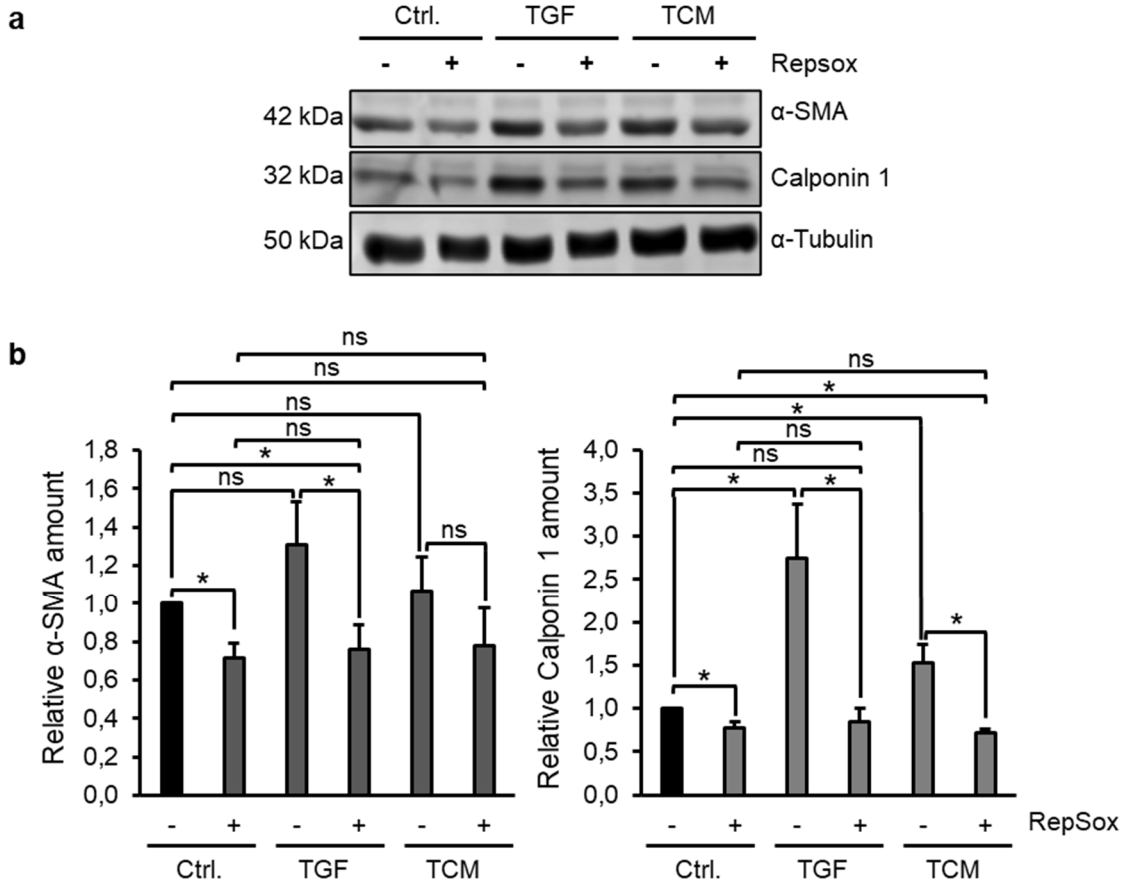


**Figure 13: Impaired MSC differentiation by RepSox treatment disturbing TGF-β1 signalling.** MSC were pre-treated with 200 nM RepSox for 1h, afterwards differentiated with recombinant TGF-β1 or freshly activated TCM under the presence of RepSox. Samples were analysed for myofibroblastic markers protein level. **(a)** Representative Western blots of α-SMA and Calponin 1 show increased protein amounts after 48 h of TGF-β1 and TCM treatment. The + and – signs indicate whether samples have been treated with DMSO as negative control (-) or RepSox (+). **(b)** Relative protein amounts of α-SMA and Calponin 1 were normalised to the α-tubulin signal. Quantification data were normalised to the value for the starved control without RepSox (Ctrl. -) which was set to 1. Equal loading was controlled by α-tubulin. Error bars correspond to SEM (n=3). Asterisks indicate significant differences *$p \leq 0.05$ according to an unpaired Student's t-test.

## 3.4 MSC to CAF differentiation does not lead to altered senescence

Several publications associate senescence with CAF-dependent tumour support (Alspach *et al.* 2013, Schosserer *et al.* 2017, Wang *et al.* 2017). CAF are a very heterogeneous cell population that can be divided into several sub-populations. Mellone *et. al* described two prominent sub-populations: senescent fibroblasts and myofibroblasts, whereby both express α-SMA and promote tumour malignancy (Mellone *et al.* 2016). The differentiation of MSC into CAF, induced by either recombinant TGF-β1 or TCM, was characterized as a myofibroblastic process, marked by an increase in α-SMA expression, as described in this thesis. By analysing the senescence status of CAF differentiated MSC it was aimed to gain additional information on their role within the tumour stroma and tumour support.

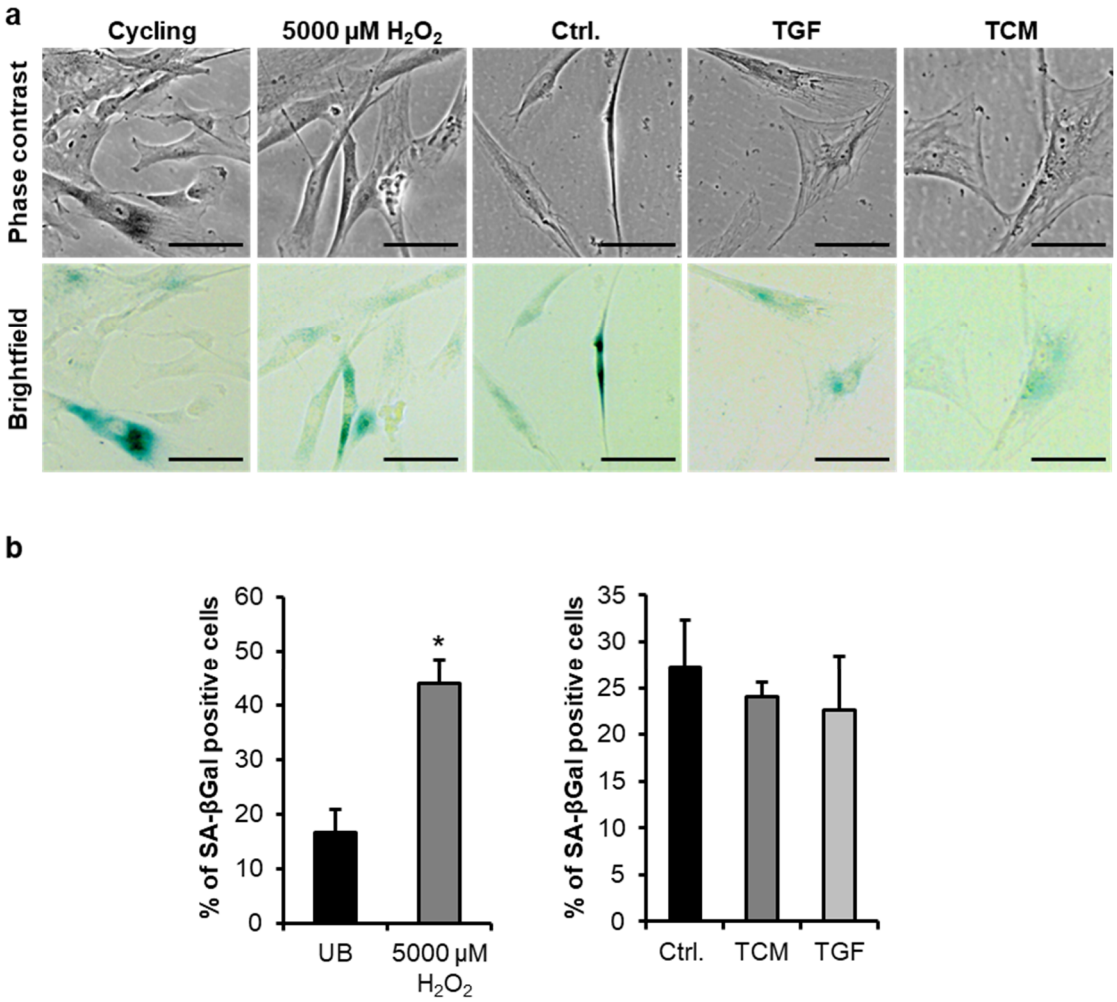


**Figure 14: Senescence assay to detect SA-βgal positive cells.**
MSC have been treated with TGF-β1 or TCM for 48 h. **(a)** Phase contrast images (upper panel) of untreated proliferating MSC (cycling), $H_2O_2$ treated, quiescent MSC (starved) and MSC differentiated by TGF-β1 or TCM. $H_2O_2$-treated cells serve as positive control. Starved cells show an elongated cell shape whereas treated cells (TGF/TCM) display a flattened cell shape. The lower panel shows the same cells using a brightfield ocular which enables visualising the bluish stained SA-βGal-positive cells (20 x magnification, scale bars 20 µm). **(b)** Quantification of SA-βGal positive cells. Fifty cells have been counted whereby blue and non-coloured cells were noted. The left panel shows an increased number of blue cells upon $H_2O_2$ treatment (positive control). The right panel shows a comparison between starved cells (Ctrl.) and differentiated MSC. Error bars correspond to SD (n=3). Asterisks indicate significant differences *p≤0.05 according to an unpaired Student's t-test.

MSC were analysed for increased senescence by senescence-associated β-galactosidase (SA-βGal) staining. For control purposes, MSC have been treated with 5000 µM $H_2O_2$ (in standard hPL containing cell culture medium) serving as senescence inducer. After 48 h of TGF-β1 and TCM stimulated differentiation, MSC were stained for SA-βGal-activity as described in 2.2.5.7. Morphological changes were documented by phase contrast and brightfield microscopy. Figure 14 a shows phase contrast images of cycling, $H_2O_2$ treated, starved as well as TGF-β1 and TCM stimulated cells in the upper panel. The lower panel displays brightfield images of the same samples in an identical area, whereby the blue colour in the lower panel tags SA-βGal-positive cells. Moreover, cells were counted (50 cells each in 3 independent MSC populations) and the percentage of positively stained cells was calculated (Figure 14 b). The results of $H_2O_2$-treated and differentiated MSC (TGF, TCM) were displayed in two independent graphs since basic culture conditions are different. Cycling cells and $H_2O_2$-treated cells were cultivated in standard culture medium whereby Ctrl., TGF and TCM medium underlies starving medium (see 2.1.5.2). For this reason, the senescence of differentiated MSC is not directly comparable with cycling cells or the $H_2O_2$ positive control. Supplementing the starving medium with $H_2O_2$ quickly caused cell death, making it an unsuitable control.

Cycling cells contain only a small number of SA-βGal-positive cells (18 %) which significantly increased upon $H_2O_2$ treatment (50 % SA-βGal-positive). In comparison, no significant changes were measured comparing starved cells (Ctrl.) with TGF-β1 and TCM-treated cells, concluding MSC undergoing CAF differentiation are not altered in cellular senescence.

## 3.5 Investigation of miR-21 and miR-29 during MSC differentiation

The differentiation of MSC to CAF is a complex process and might be influenced by microRNA. Human miR-21 is described to play a role in TGF-β1-induced CAF-formation in human primary foreskin fibroblasts (Li *et al.* 2013). In addition, miR-29 was shown to be one of the most down-regulated miR in CAF (Liu *et al.* 2017) and miR-29 is targeting COL1A1 (van Rooij *et al.* 2008), which I found to be increased during MSC to CAF differentiation. Accordingly, the next part of the project aimed at analysing the influence of hsa-miR-21-5p (miR-21) and hsa-miR-29-3p (miR-29) on MSC differentiation.

First, miR-21 and miR-29 expression during MSC to CAF differentiation was quantified by qPCR (Figure 15). Therefore, cells were stimulated with recombinant TGF-β1 for 2 and 10 days, respectively. MiR-21 showed a slight upregulation after 2 days of differentiation which further increased to a significant 1.6-fold up-regulation after 10 days of TGF-β1. In contrast, miR-29 significantly decreased by 20 % after 2 days of MSC to CAF differentiation. The effect became even more prominent (-40 %) after 10 days.

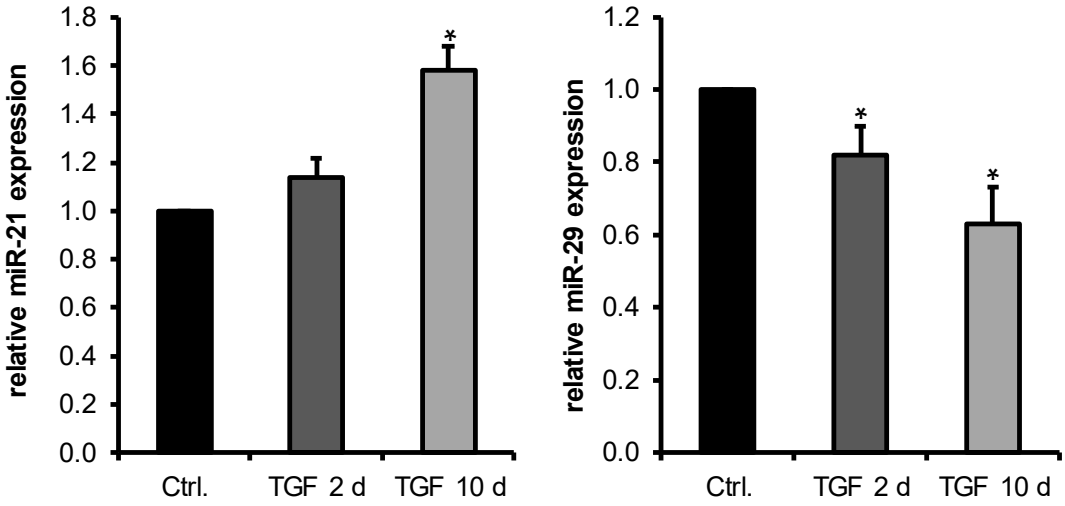


**Figure 15: miR-21 and -29 expression upon TGF-β1 stimulation and CAF differentiation.** MSC have been treated with TGF-β1 for 2 days (2 d) or 10 days (10 d) to analyse changes in miR-21 and miR-29 expression during MSC differentiation. The left panel shows relative miR-21 expression changes, while the right panel displays results for miR-29. The relative miR amounts were determined by qPCR, normalised to the mean of SNORD61, SNORD72 and SNORD 95. For quantification, the untreated control (Ctrl.) was set to 1. Error bars correspond to SD (n=3). Asterisks indicate significant differences (*p≤0.05) according to an unpaired Student's t-test.

To further investigate the role of microRNA, transient miR knockdowns using antagomir and overexpression studies via miR mimic transfection were performed for miR-21 and miR-29. Antagomirs are synthetic single-stranded RNA oligonucleotides perfectly complementary to the mature miR of interest. After transfection, an antagomir binds the target resulting in the degradation of the miR/antagomir duplex (Krützfeldt *et al.* 2007). In contrast, miR mimics are synthetic double-stranded RNA oligonucleotides mimicking endogenous pre-mature miR.

30 nM antagomir or miR mimics were transfected into MSC and the cells were harvested after 48 h. Figure 16 a shows that the transfection of miR-21 and -29 antagomirs resulted in significantly decreased miR amounts of 97 % and 54 %, respectively. Corresponding overexpression by miR mimics (Figure 16 b) resulted in a moderate 4.7-fold increase for miR-21 and a significant 397-fold increase for miR-29 expression. Subsequently, the effect of miR-21 and miR-29 on the expression of differentiation marker proteins (α-SMA, Calponin 1, COL1A1) was analysed (Figure 16c-f). The miR-21 knockdown decreased α-SMA, Calponin 1 and COL1A1 expression (Figure 16 c) by 26-43 % whereas its overexpression resulted in increased mRNA amounts of 1.7-fold for α-SMA and 2.3-fold for Calponin 1. COL1A1 remained unaffected by the mimic transfection. (Figure 16 d). In comparison, miR-29 antagomir transfection caused a mild α-SMA and Calponin 1 mRNA decrease whereby COL1A1 is upregulated significantly by 1.3-fold (Figure 16 e).

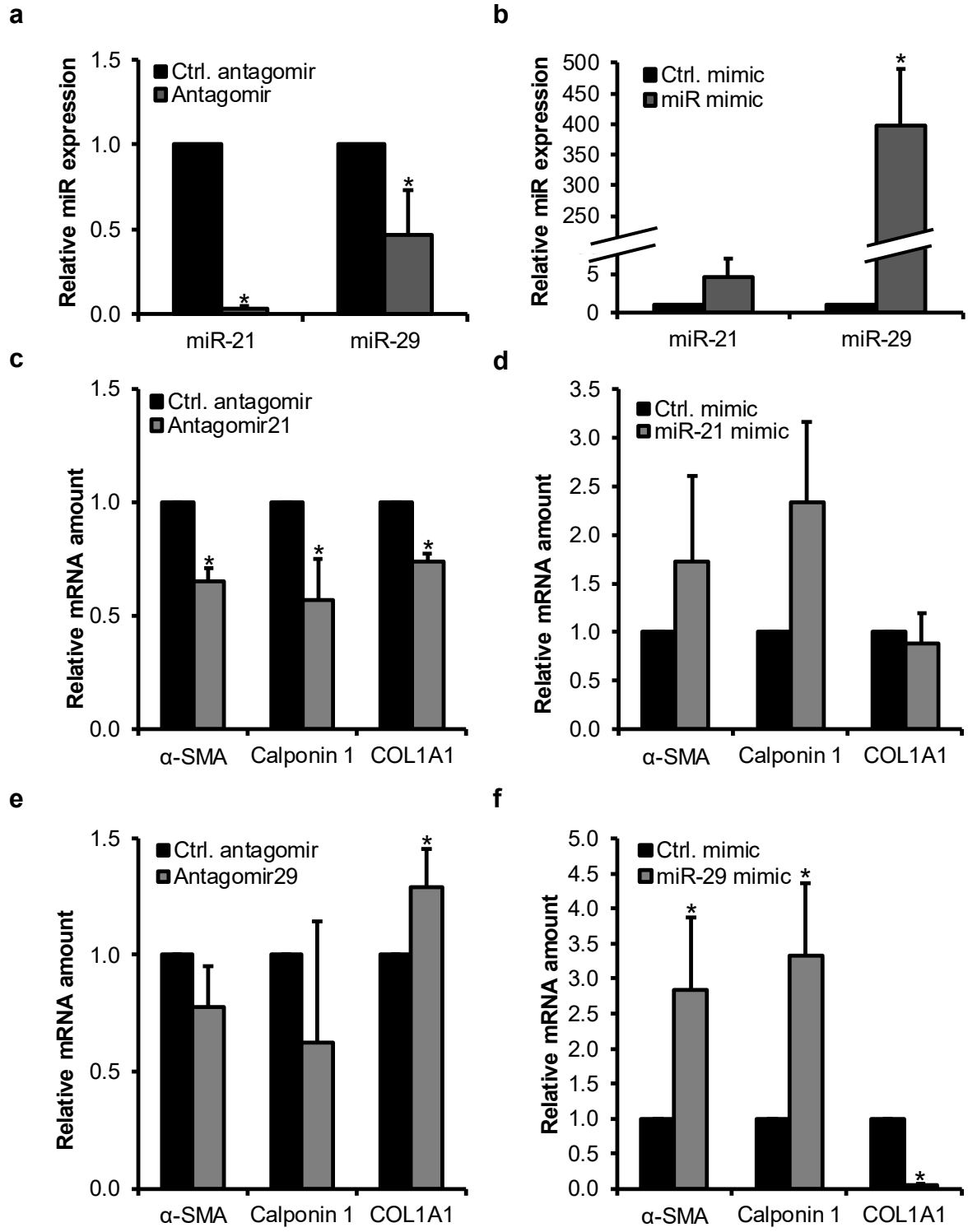


**Figure 16: Knockdown and overexpression of miR-21 and miR-29.**
MSC were transfected with miR-21 or miR-29 antagomirs or mimics for 48h. **(a)** miR-21 and miR-29 amounts are reduced upon antagomir transfection. **(b)** miR-21 and miR-29 amounts are increased after miR mimic transfection. The influence of miR-21 and miR-29 knockdown or overexpression on MRTF-A and myofibroblastic marker genes is shown in panels (c) to (f), respectively. **(c)** Knockdown of miR-21 causes significantly decreased levels of α-SMA, Calponin 1 and COL1A1 whereby overexpression **(d)** leads to increased α-SMA and Calponin 1 mRNA amounts. Knockdown of miR-29 by antagomir **(e)** leads to slightly diminished α-SMA and Calponin 1 amounts while COL1A1 expression was significantly elevated. **(f)** Overexpressed miR-29 by miR-29 mimic usage caused strikingly increased α-SMA and Calponin 1 whilst COL1A1 was significantly reduced. The relative miR amounts were determined by qPCR, normalised to the mean of SNORD61, SNORD72 and SNORD 95. For quantification Ctrl. antagomir or Ctrl. mimic were set to 1, respectively. Error bars correspond to SD (n=3). Asterisks indicate significant differences (*p≤0.05) according to an unpaired Student's t-test.

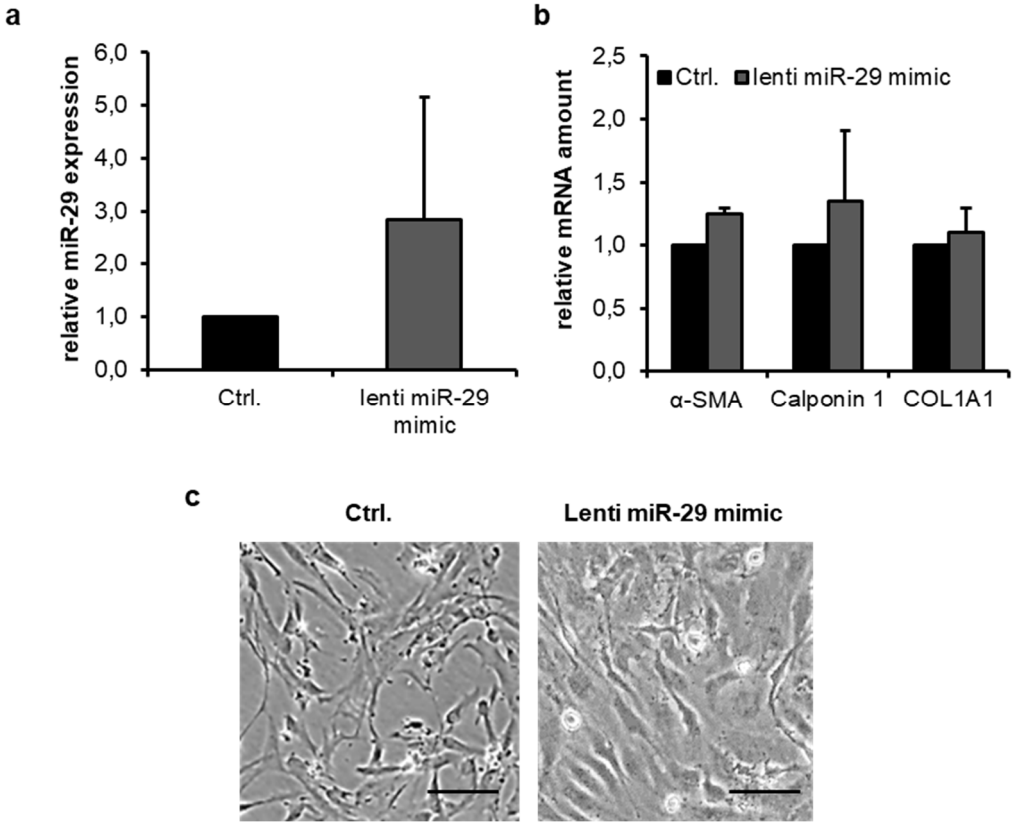


**Figure 17: Lentiviral miR-29 expression upon TGF-β1 stimulation and CAF differentiation.** MSC were transduced with lentiviral plasmid to overexpress miR-29. **(a)** miR29-amount is increased by lentiviral overexpression. **(b)** miR-29 lentiviral overexpression caused mildly increased α-SMA and Calponin 1 amounts whilst COL1A1 was not affected. The relative miR amounts were determined by qPCR, normalised to the mean of SNORD61, SNORD72 and SNORD 95. mRNA amounts were quantified by qPCR and normalised to the mean of ALAS and GAPDH. For quantification Ctrl. was set to 1. Error bars correspond to SD (n=3). Asterisks indicate significant differences (*p≤0.05) according to an unpaired Student's t-test. **(c)** Phase contrast images displaying the morphology of control transduced MSC (Ctrl.) and miR-29 overexpressing cells (Lenti miR-29 mimic), whereby the latter show increased cell detachment. 20 x magnification, scale bars 20 µm.

In contrast, miR-29 overexpression using miR mimics caused a significant upregulation of α-SMA and Calponin 1 (2.8-fold and 3.3-fold, respectively) and almost abolished COL1A1 mRNA expression (Figure 16 f). Since transient miR-29 mimic transfection caused severe effects on COL1A1 mRNA expression stable miR-29 overexpressing MSC (from three different donors) were created by lentiviral transduction.

It was aimed to analyse the effect of COL1A1 loss on MSC differentiation and its influence on HCT8 in spheroid co-culture. Lentiviral overexpression led to a mild 2.8-fold overexpression (Figure 17 a) compared to massive transient overexpression (Figure 16 b). The effect of stable miR-29 overexpression on myofibroblastic targets was very mild too. The α-SMA and Calponin 1 expression was increased to 1.2 or 1.3-fold respectively (Figure 17 b). Collagen expression remained unaffected whereby a massive downregulation was expected. Additionally, MSC underwent morphological changes after miR-29 lentiviral overexpression. Figure 17 c shows phase contrast images of control and miR-29 transduced cells 48 h after infection. MiR-29 overexpression led to increased cell detachment compared to control.

Taken together, these results suggest a critical role of miR-21 and especially miR-29 during MSC to CAF differentiation, triggered by recombinant TGF-β1 via the regulation of α-SMA, Calponin 1 and COL1A1. Especially the absence of COL1A1 mRNA after transfection of the miR-29 mimics may compromise differentiation.

## 3.6 MRTF-A is activated during myofibroblastic MSC differentiation

In further experiments, the MRTF-A activity was analysed. As described before MRTF-A is a transcriptional co-activator of the serum response factor (SRF) regulated by actin treadmilling (Miralles *et al.* 2003). In detail, in its inactive form, MRTF-A is bound to G-actin and thereby repressed. During actin polymerisation, the MRTF-actin complex dissociates and active MRTF-A can accumulate in the nucleus binding SRF (Olson and Nordheim 2010). Myofibroblastic processes, like the MSC to CAF differentiation, trigger actin polymerisation. It is thus hypothesised that MRTF-A translocates to the nucleus of MSC after TGF-β1 or TCM stimulus.

To evaluate this hypothesis, immunofluorescence assays in MSC (Figure 18 a) were performed. MSC of 3 independent donors were used for CAF differentiation by TGF-β1 and TCM (48 h) and stained for MRTF-A (red colour) and DNA (DAPI, blue) as described in 2.2.5.4. Cycling and starved cells showed an even distribution of the MRTF-A signal in the whole cell including the nucleus. In contrast, a slight increase of nuclear MRTF-A upon TGF-β1 and TCM stimulation was detected compared to the starved control. Quantifying the immunofluorescence staining's via ImageJ/Fiji revealed a significant 1.4-fold increase of nuclear MRTF-A after TGF-β1 and TCM stimulus (Figure 18 b).

To validate adjusted MRTF-A activity during myofibroblastic MSC differentiation, luciferase reporter MSC (3D.A-luc MSC) were created by lentiviral transduction (see 2.2.2.8). The reporter plasmid originated from a lentiviral shRNA plasmid (pLVX-shRNA2-Crimson-Puro) and was modified to meet the requirements of the present study, as described in 2.2.3.9. An increased amount of nuclear and active MRTF A correlates with increased luciferase synthesis measurable by luciferase activity. After the stable polyclonal 3D.A-luc reporter MSC have been created from three different donors, luciferase reporter assays were performed (see 2.2.5.5). Cells were pre-starved for 24 h and stimulated with TGF-β1 or TCM for 7 h, 24 h and 48 h afterwards. Increased MRTF-A activity was shown by TGF-β1 stimulation by 3.1-, 2.1- and 1.7-fold compared to the starved control at all three time points (Figure 18 c). TCM caused similar effects after stimulation for 7 h, 24 h and 48 h (2.6-, 2.5-, 1.6-fold, respectively). Comparing the immunofluorescence and luciferase studies the ratio of increased nuclear MRTF-A upon TGF-β1 and TCM stimulation (1.4-fold both) correlates with 1.7- and 1.6-fold increases in the luciferase assay.

Taken together the reporter assay and immunofluorescence findings demonstrate that in primary human MSC, the stimulation with TGF-β1 and TCM causes cytoplasmic MRTF-A to translocate to the nucleus. This event results in increased MRTF-A activity during the differentiation of myofibroblastic MSC into CAF, even though there are considerable amounts of nuclear MRTF-A levels under unstimulated conditions.

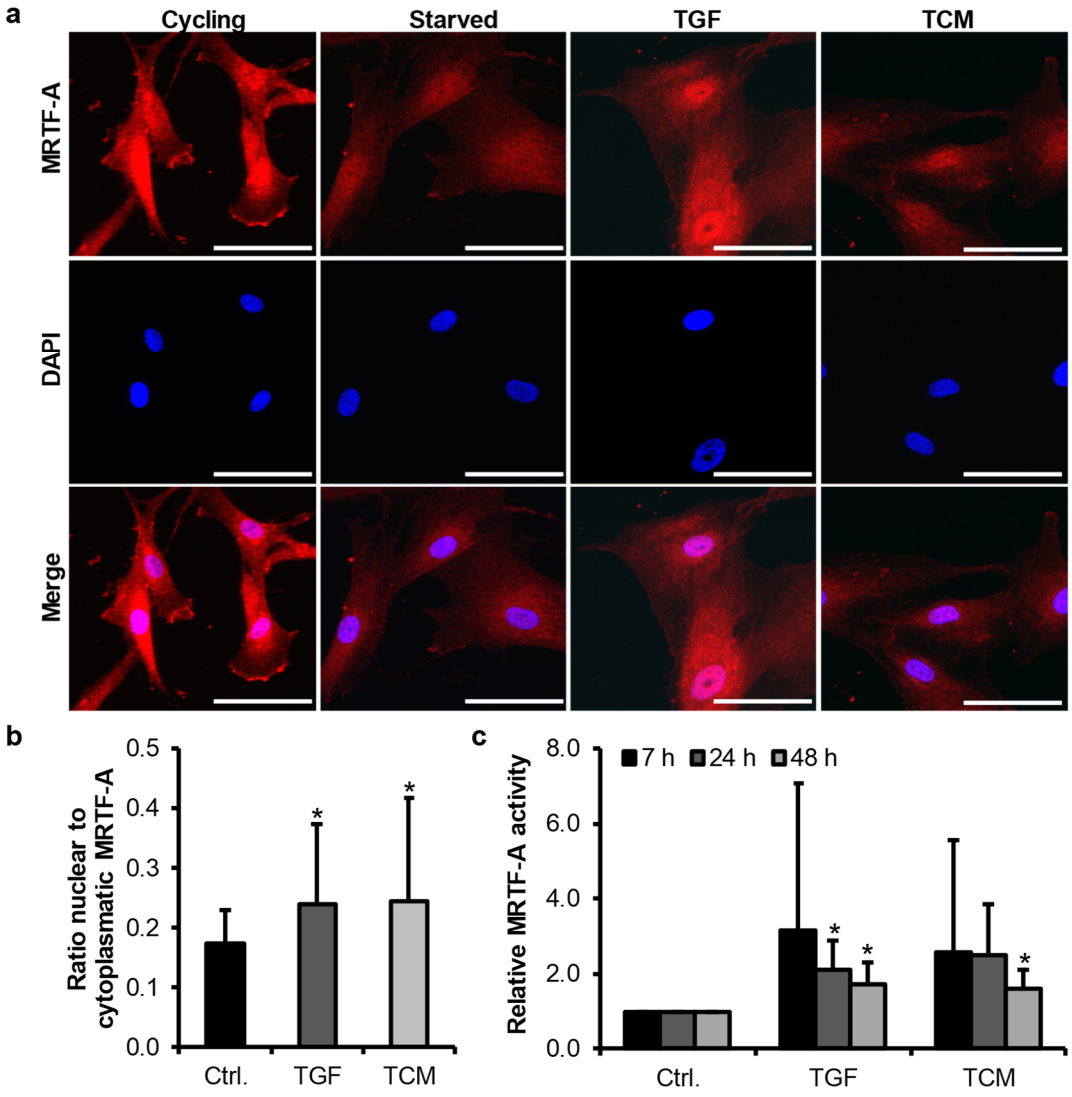


**Figure 18: Translocation and activation of MRTF-A during myofibroblastic MSC differentiation.** **(a)** Intracellular localisation of MRTF-A. Cells were immunostained with anti-MRTF-A (red) and DNA counterstained with DAPI (blue) following 48 h of treatment with TGF-β1 (TGF) or TCM. 20 x magnification, scale bars 20 µm. **(b)** Quantification of MRTF-A displaying the change of nuclear to cytoplasmatic MRTF-A signal in 30 cells (each) from three independent MSC donors. Asterisks indicate significant differences (*p≤0.05) according to an unpaired Student's t-test. **(c)** MSC stably infected with lentiviral MRTF-SRF dependent luciferase reporter constructs were analysed during MSC to CAF differentiation induced by TCM or TGF-β1 (TGF) for the indicated time points (7 h, 24 h, 48 h). Relative luciferase activities normalised to constitutive E2-Crimson expression are displayed. Error bars correspond to SD (n=4)

## 3.7 Impaired myofibroblastic marker expression upon MRTF-A knockdown by RNA interference

To further validate if MRTF-A is a supportive or limiting factor for MSC differentiation, knockdown studies were performed, using siRNA pools in combination with TGF treatment. Cells transfected with siRNA against MRTF-A (siMRTF-A) showed significant 83 % downregulation of MRTF-A (Figure 19). In addition, α-SMA and Calponin 1 mRNA expression were significantly affected by the MRTF-A knockdown resulting in expression levels reduced by 80 % and 86 %, respectively. In comparison, COL1A1 remained unaffected. SiCtrl. transfected and TGF-β1-stimulated MSC exhibit similar induction patterns of CAF marker genes (α-SMA, Calponin 1, COL1A1) as wild-type cells (Figure 7). Most importantly, the TGF-β1-induced α-SMA and Calponin 1 upregulations were effectively blocked by transient siRNA-mediated MRTF-A knockdown, whereas COL1A1 was still inducible under control conditions.

These results suggest that the TGF-β1 induced upregulation of α-SMA and Calponin 1 mRNA amount during MSC to CAF differentiation requires MRTF-A, whereas COL1A1 expression is regulated independently of MRTF-A in MSC.

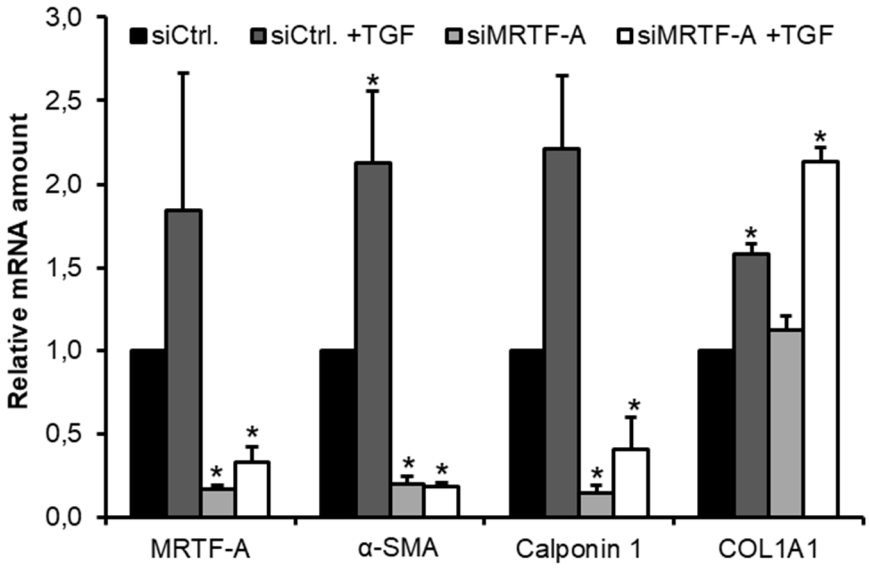


**Figure 19: Impaired MSC differentiation by transient MRTF-A knockdown.**
Expression of MRTF-A and myofibroblastic marker genes upon TGF-β1 treatment (24 h) following transient knockdown by MRTF-A siRNA (siMRTF-A) or control siRNA (siCtrl.). The relative mRNA abundance was determined by quantitative qPCR and normalised to ALAS and GAPDH. To display fold changes the starved siCtrl. was set to 1. Error bars correspond to SD (n=4). Asterisks indicate significant differences (*p≤0.05) according to an unpaired Student's t-test.

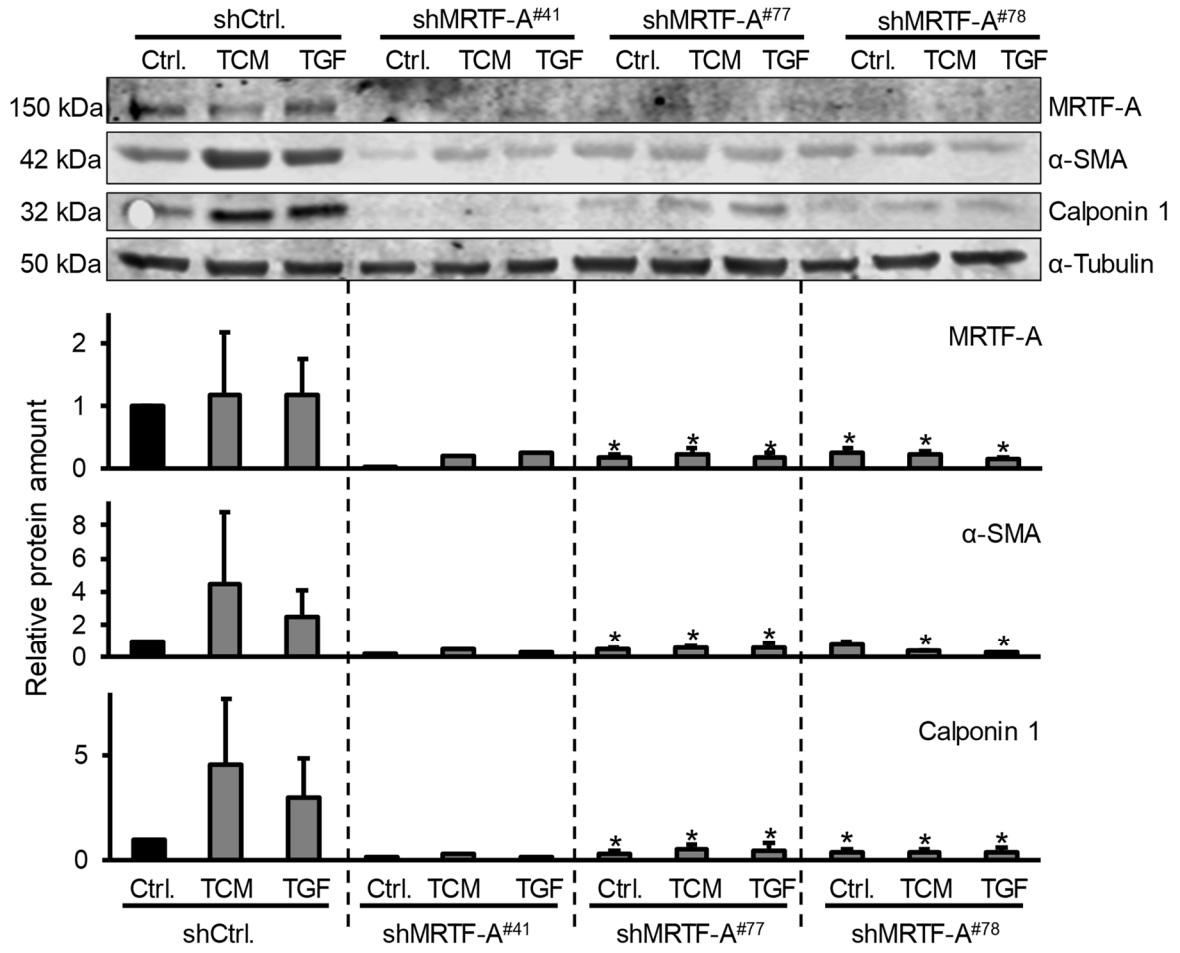


**Figure 20: Impaired MSC differentiation by stable MRTF-A knockdown.**
Representative Western Blot of MRTF A, α-SMA and Calponin 1 in lentiviral transduced MRTF-A knockdown MSC. Control infected cells (shCtrl.), as well as MRTF-A knockdown cells obtained by three independent shRNA constructs (#41, #77, #78), were treated with TCM or TGF-β1 (TGF) for 48 h. The relative protein amounts were normalised to α-tubulin signals. For quantification, data were normalised to the value for the starved shCtrl., which was set to 1. In the lower panels average results obtained for 3 individual donor MSC are displayed. Error bars correspond to SD (n=3). Asterisks indicate significant differences (*p≤0.05) according to a one-way ANOVA with Dunnett's multi comparison test (post-hoc).

By lentiviral transduction, stable MRTF-A knockdown MSC (shMRTF-A) were created using three different shRNA sequences targeting MRTF-A (indicated by #41, #77 and #78 in Figure 20). To reduce donor-specific effects, MSC of three different donors were transduced.The protein levels of MRTF-A, Calponin-1 and α-SMA were analysed compared to control MSC transduced with a non-targeting control shRNA (shCtrl.). Sh-MRTF-A and shCtrl. MSC were treated with TCM and TGF-β1 for 48 h and protein samples were analysed via Western Blotting. MRTF-A knockdown caused a >90 % MRTF-A reduction independent of the tested shRNA sequence. Furthermore MRTF-A knockdown caused a significant downregulation of basal α-SMA and Calponin 1 protein amount compared to shCtrl. MSC (Figure 20) to an average of 46 % and 27 % remaining protein, respectively. Stimulation of shCtrl. MSC with TCM and recombinant TGF-β1 led to increased α-SMA and Calponin 1 protein amounts,

comparable to unmodified MSC. This induction was, however, massively impaired after MRTF-A depletion. Only a minor increase of a mean of 3 % and 11 % of α-SMA and Calponin 1 could be detected in stimulated shMRTF-A MSC which did not even reach the level of endogenous α-SMA and Calponin 1 expression.

In summary, the transient and stable knockdown studies demonstrate that MRTF-A plays an important role during myofibroblastic MSC differentiation by regulating key elements of the myofibroblastic differentiation machinery.

## 3.8 MRTF-A knockdown affects the tumour-supporting role of MSC in HCT8 xenografts in nude mice

From the above knockdown studies, it became clear that the myofibroblastic MSC to CAF differentiation is disturbed by MRTF-A depletion. Additional *in vivo* studies were scheduled to gain further insights into the effects of MRTF-A knockdown on the tumour-supporting function of MSC and performed in collaboration with Dr. Jana Lützkendorf (Werner *et al.* 2019).

For xenograft experiments, Ds-Red-labelled HCT8 cells were mixed with MSC (shCtrl. or shMRTF A cells) in a ratio of 5:1. The cell mixture of HCT8 and MSC cells was injected subcutaneously into the flanks of male six- to eight-week-old athymic nude-fox n1 nu/nu mice. Seven days after injection, tumour formation was analysed using a calliper. As shown in Figure 21 a, HCT8 cells transplanted alone solely formed tiny tumours of 0.87 ± 1.49 $mm^3$ (mean volume ± SD) whereby transplantation of HCT8 cells mixed with shCtrl.-MSC caused a massive increase in tumour volume to 55.54 ± 29.73 $mm^3$. Comparing shCtrl.-MSC with shMRTF-MSC, a significant reduction in xenograft volume was detected (31.27 ± 10.98 $mm^3$), indicating an impairment of early tumour growth in the presence of MRTF-A-decimated MSC. Similar effects of MRTF-A knockdown were shown on xenograft weight at day 25 post-injection (Figure 21 b). The tumour mass of mixed xenografts harbouring shCtrl.-MSC increased to 557.3 ± 316.6 mg compared to HCT8 cells alone (28.3 ± 31.5 mg). Nevertheless, the weight of the MRTF-A knockdown xenografts was significantly reduced (359.7 ± 231.7 mg) in comparison to shCtrl.-MSC.

Moreover, the fluorescence of the Ds-Red-labelled HCT8 was imaged and allowed visualisation of tumour cell growth in anaesthetised mice (Figure 21 c). The Ds-Red signal was shown to directly correlate with the tumour cell number analysing the $R^2$ coefficient in several colorectal tumour cell lines (Caysa *et al.* 2012). Hence, the imaging results show that the decreased tumour size is directly connected to reduced HCT8 cell proliferation and not to failed stroma generation.

Taken as a whole, these results demonstrate that MRTF-A is not only controlling the myofibroblastic differentiation of MSC. MRTF-A is also necessary for the functional differentiation of MSC towards a tumour-promoting CAF phenotype *in vivo*.

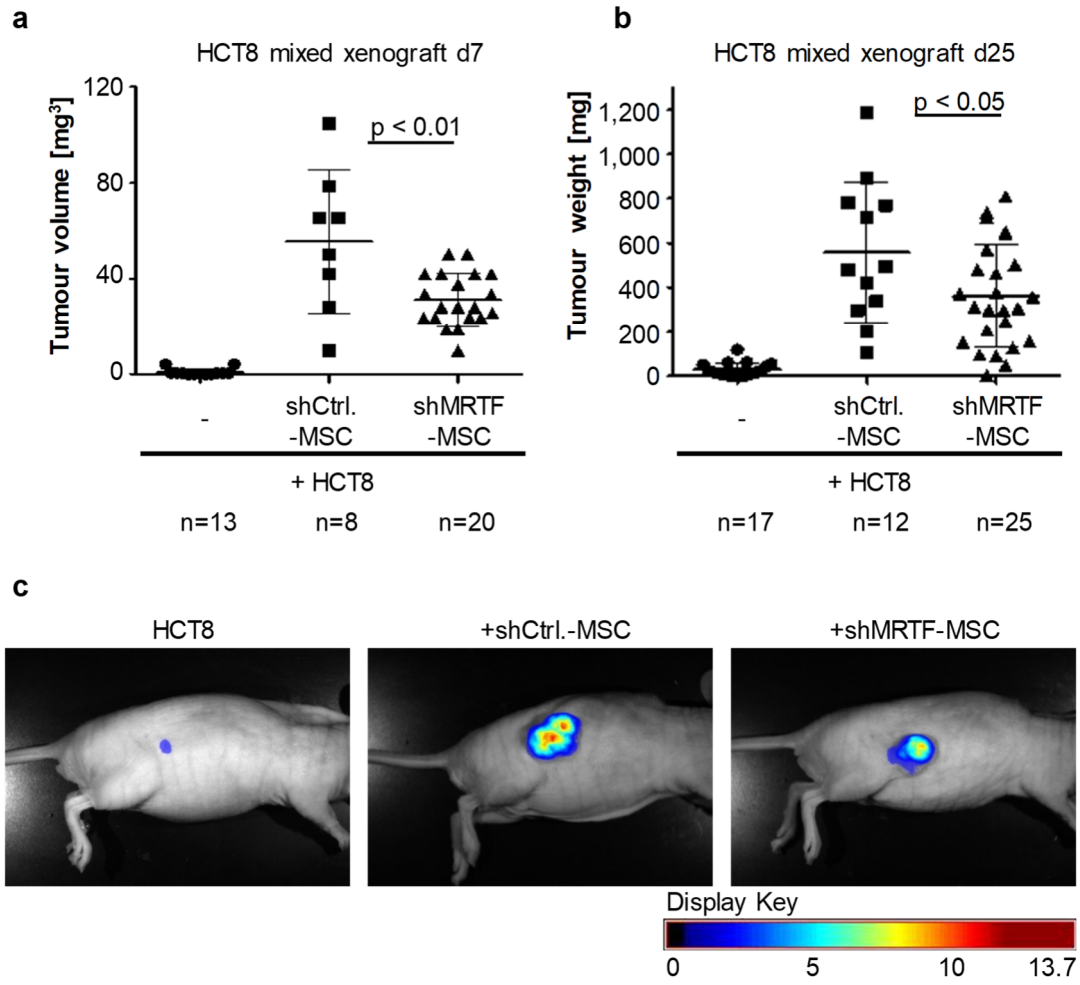


**Figure 21: MRTF-A knockdown partially impairs tumour-promoting effects of MSC on HCT8 xenograft growth in mice.**
3 x $10^6$ HCT8 cells were coinjected with or without 7.5x$10^5$ MSC s.c. in athymic nude mice. **(a)** Tumour volumes were determined using calliper measurement at day 7 (d7). **(b)** Mice were killed and the tumours were extracted and weighted after 25 days (d25). One-way ANOVA with Tukey's multiple comparison test (post-hoc) was applied to test for significance. **(c)** *In vivo* acquisition of multispectral images of DsRed expressing tumours in athymic nude mice on d25 post-injection. Pictures were taken via 2.2 CRi Maestro *in vivo* fluorescence imaging system (CRi, Woburn, MA, USA) with Maestro software (2.22). Representative grayscale images were overlayed with respective fluorescence images (intensity weighted pseudocolour mode, scale bar displayed beneath).
*Data presented in this Figure were produced and provided by the cooperating scientist and colleague Dr. Jana Lützkendorf (University Clinic of Internal Medicine IV).*

# 4 DISCUSSION AND PERSPECTIVE

The research conducted in this thesis aimed to investigate whether the transcription factor MRTF-A has an impact on the myofibroblastic differentiation of MSC into CAF. Additionally, the study explored the tumour-propagating capabilities of differentiated MSC.

## 4.1 TGF-β1 and TCM treatment induce MSC differentiation into CAF

Researchers in tumour biology increasingly realized the importance of stromal cells on tumour growth and progression. Stromal cells like CAF are well-known components of the tumour stroma and are directly connected to cancer initiation, progression and metastasis (Bhowmick *et al.* 2004, Li *et al.* 2013). But from what cell type can CAF arise?

MSC hold a lifelong presence in many tissues and their perivascular localisation led to the assumption that MSC are one possible source of CAF (Crisan *et al.* 2008). Thereby it is hypothesised that MSC-derived CAF can provide a pre-metastatic niche for tumour cells. Consistent with this, MSC were described to support colorectal tumour growth in colorectal cancer by β1-integrin-dependent mechanisms (Widder *et al.* 2016).

To prove the MSC to CAF differentiation in the current thesis two settings were designed to initiate the process: Incubation with recombinant TGF-β1 or TCM. These stimuli are widely recognised for inducing CAF differentiation in various precursor cells, including MSC, and are thus considered standard methods for this process. (Mishra *et al.* 2008, Shangguan *et al.* 2012b, Barcellos-de-Souza *et al.* 2016, Yoon *et al.* 2021).

CAF differentiation is characterised by morphological changes in the initial cell type (Kalluri and Zeisberg 2006b). In the current thesis, the altered morphology goes along with cytoskeleton reorganisation, especially characterised by an increased α-SMA signal. In cycling and starved MSC, the α-SMA staining is distributed over the whole cell, whereas in TGF-β1 or TCM-treated MSC, one can find distinct α-SMA fibres. In accordance with the literature, MSC show radical morphological changes upon TGF-β1 and TCM stimuli (Figure 9), leading to the assumption that indeed MSC undergo a myofibroblastic differentiation into CAF (Quante *et al.* 2011).

To further monitor the myofibroblastic MSC to CAF differentiation, three markers were analysed on protein and mRNA levels: α-SMA, Calponin 1 and Col1A1 which are described to be connected to myofibroblastic processes (Crider *et al.* 2011, Velasquez *et al.* 2013, Johnson *et al.* 2014). Increased α-SMA amounts were shown on protein level via western blot and elevated mRNA amounts were measured by qPCR (Figure 7 & Figure 8). These results are consistent with the immunofluorescence results (Figure 9). Together, these findings concur with other studies, proving α-SMA as a reliable CAF marker in the current experimental setting (Kalluri and Zeisberg 2006b, Hinz *et al.* 2007, Brentnall *et al.* 2012, Wang *et al.* 2018). Calponin

1, the second myofibroblastic CAF marker, showed significantly increased mRNA and protein amounts (Figure 7 & Figure 8) as described before (Martinez-Outschoorn *et al.* 2010, Guido *et al.* 2012). These results reproduce findings from former studies, which describe Calponin-1 as a myofibroblastic marker being upregulated upon TGF-β1 stimulation in connection to myofibroblastic CAF formation (Crider *et al.* 2011). Calponin 1, as well as α-SMA, belong to the contractile apparatus in smooth muscle cells, thus the results go along with the expectations to see those markers upregulated during the myofibroblastic differentiation of MSC to CAF (Hinz *et al.* 2001, Liu and Jin 2016).

Additionally, Col1A1 levels were examined during MSC differentiation. Col1A1 is described as an ECM protein and a typical marker of activated fibroblasts (Kojima *et al.* 2010). Moreover, myofibroblasts and hence CAF are known as the major cell type to secrete, synthesise, modify and assemble ECM (Yoshimura *et al.* 2015, Erdogan *et al.* 2017). The stroma of several human tumours shows elevated Col1A1 levels, and increased collagen amounts are associated with worse outcomes in CRC patients (Faouzi *et al.* 1999, Zhang *et al.* 2018, Liu *et al.* 2019). The results of the present thesis (Figure 7, Figure 8) correspond to the literature: upon TGF-β1 or TCM stimulation Col1A1 mRNA amounts were elevated to the same extent (Alkasalias *et al.* 2014). Due to the lack of a reliable Col1A1 antibody for western blot or immunofluorescence, the cooperating scientists Jana Lützkendorf used Picro-Sirius red staining in cell culture dishes, which is normally used for histological samples (Schmitz *et al.* 2010). This experiment was published in the joint paper and showed 50 % elevated collagen deposition upon 96 h of TGF-β1 stimulation (Werner *et al.* 2019). Nevertheless, a differentiation between the several collagens is not possible in this experimental setting.

To measure the TGF-β1 concentration in TCM, ELISA experiments were performed. Around 80 pg/ml TGF-β1 was detected in the medium conditioned for 72 h by 2,5 x $10^6$ HCT8 cells/ml. For TGF-β1-induced CAF differentiation, the cytokine concentration of 10 ng/ml was used as described before (Quante *et al.* 2011). Comparing the TGF-β1 concentrations between TCM and the recombinant cytokine it is evident that recombinant TGF-β1 was used at a 125-fold higher concentration. Regarding the experimental outcome, it seems like the TCM incubation is as effective as the recombinant TGF-β1 cytokine. In detail the increase of α-SMA, Calponin 1 and Col1A1 mRNA and protein levels is similar.

In the current thesis, there was no adjustment in recombinant TGF-β1 concentrations since the experimental outcome in both settings was comparable. In future experiments, one could try to directly compare the cytokine efficiencies, by using the recombinant TGF-β1 with a concentration of 80 pg/ml to resemble the medium concentration of TGF-β1 in TCM of HCT8 cells. On the other hand, recombinant cytokines are designed to mimic the natural proteins as closely as possible, but the activity of recombinant cytokines compared to their natural counterparts can vary based on several factors, including their production process, post-

translational modifications, and the presence of accessory proteins (Punnonen *et al.* 2019, Saxton *et al.* 2023).

Along with the detection of considerable amounts of TGF-β1 in TCM, the necessity of the TGFβ type I receptor kinase (ALK5) activity was shown (Figure 12) during the differentiation of MSC to CAF. pSMAD2 levels increased upon TGF-β1 and TCM stimuli whereby tSMAD2 levels remained unaffected. Additionally, the MSC to CAF differentiation is impaired by blocking TGF-β1 signalling via RepSox, shown by reduced protein amounts of α-SMA and Calponin 1 protein amounts (Figure 13). These findings agree with the literature, describing the importance of the canonical TGF-signalling during CAF generation (Hawinkels *et al.* 2014, Ringuette Goulet *et al.* 2018). Furthermore, MSC are described to be recruited to the tumour site by TGF-β1 and similar effects of TGF/SMAD inhibition on MSC-CAF differentiation was shown by independent researchers (Barcellos-de-Souza *et al.* 2016, Tan *et al.* 2019).

Taken together, it was successfully demonstrated that primary human bone marrow-derived MSC differentiated into CAF upon TGF-β1 or TCM stimulation characterised by increased α-SMA, Calponin 1 and Col1A1 mRNA and protein levels including Alk5 receptor kinase activity.

## 4.2 MSC to CAF differentiation and senescence

The elucidation of the MSC senescence during CAF differentiation in the present experimental setting was an important part of the thesis since senescent and activated myofibroblastic CAF can unite in a similar secretory phenotype (Schosserer *et al.* 2017). Both subpopulations of fibroblasts express α-SMA and promote tumour growth but differ in gene expression profiles regarding ECM deposition and organisation (Krtolica *et al.* 2001, Coppe *et al.* 2010, Goruppi and Dotto 2013). The differences in the ECM gene expression profiles suggest significantly different microenvironments during tumour development (Hanley *et al.* 2016). The TGF-β1 signalling pathway is described to play an important role in senescent and myofibroblastic CAF (Mellone *et al.* 2016). The induction of contractility and α-SMA expression after different senescence stimuli is dependent on TGF-β1/SMAD- or SMAD/Rho-signalling (Hinz *et al.* 2012). Several studies indicate that TGF-β1/SMAD-signalling is essential for senescence induction itself (Tremain *et al.* 2000, Vijayachandra *et al.* 2003, Hassona *et al.* 2013). Mellone and colleagues examined the difference in gene expression and ECM deposition in TGF-β1-treated myofibroblasts and senescent fibroblasts. Both cell types showed a contractile α-SMA positive phenotype, whereby the ECM deposition was reduced in senescent fibroblasts (Mellone *et al.* 2016). Obviously, there is an overlap between myofibroblastic differentiation and senescence induction. Therefore, it was necessary to clearly differentiate whether the TGF-β1 or TCM treatment induce myofibroblastic or the senescent CAF of MSC origin.

It is hypothesised that TGF-β1 treatment of MSC leads to an activated myofibroblastic but not senescent CAF in the present thesis. Back in 1995, a biomarker called ‘senescence-

associated β-galactosidase' (SA-βGal) was found to be expressed only in senescent cells (Dimri *et al.* 1995). To differentiate between senescent and cycling cells the β-galactosidase essay according to Debacq-Chainiaux was used (Debacq-Chainiaux *et al.* 2009). As a positive control, MSC were treated with a sublethal concentration of 5000 µM $H_2O_2$ for 48h in cultivation medium containing 10 % hPL. The $H_2O_2$ concentration was titrated in preliminary experiments. Comparing the 5000 µM $H_2O_2$ treated MSC with cycling cells, the first showed a significant 2,5-fold increase in the number of SA-βGal-positive cells compared to the negative control. This supports current research in bone marrow-derived MSC (Chang *et al.* 2017) and serves as a valid positive control. For TGF-β1 or TCM treatment, cells were cultivated in starvation medium to distinguish whether differentiation effects are induced by cytokines and growth factors independently from the protein components in the hPL. Comparing starved (Ctrl.) and cycling cells the first showed a slightly increased number of SA-βGal-positive cells (Figure 14 b). Since starvation may induce stress to the MSC, this could be the reason there are slightly more SA-βGal-positive detectable in starved cells than in cycling MSC (Petrenko *et al.* 2020). Both TGF-β1 and TCM slightly decreased the number of senescent MSC compared to the control, which is consistent with previous research indicating TGF-β1 is not a senescence inducer in MSC (Walenda *et al.* 2013).

Taken together, the senescence assay demonstrates that the effects of MSC to CAF differentiation - induced by TGF-β1 or TCM - is not connected to senescence. MSC originated CAF show an activated myofibroblastic phenotype.

## 4.3 The influence of miR during the CAF differentiation

MicroRNA (miR) are increasingly described to play a critical role in tumour microenvironment remodelling (Chou *et al.* 2013a, Suzuki *et al.* 2015). Furthermore, it's known that miR hold both tumour-promoting and tumour-supressing activities in the molecular context of tumour progression and CAF differentiation (Aprelikova *et al.* 2010). The current thesis focused on miR-21 and miR-29, since both are associated with TGF-β1 signalling, which plays an outstanding role in CAF development from MSC (Li *et al.* 2013, Bi *et al.* 2017).

miR-21 was the first oncogenic miR to be discovered and is overexpressed in many tumours. High miR-21 expression was associated with poor survival (Davis *et al.* 2008). MiR-21 is described to target SMAD 7, an inhibitory SMAD. Hence, miR-21 overexpression leads to decreased SMAD7 levels and SMAD2/3 can easily be activated by phosphorylation at the Alk5 receptor kinase (Li *et al.* 2013). Additionally, miR-21 expression was described to be induced by TGF-β1 (Wang *et al.* 2012).

miR-29 plays a significant role in various biological processes and is expressed in several tissues. Its expression levels can vary in different cell types and under different conditions (Kriegel *et al.* 2012). There is a controversial discussion, about whether miR-29 is either a tumour suppressor, documented in most studies, or an oncogene. The main reason to examine

miR-29 in this thesis was its role in ECM regulation and fibrosis (Bi *et al.* 2017, Kwon *et al.* 2019). In this context, miR-29 was described to be downregulated by TGF-β1 connected to increased expression of Col1A1 and other ECM proteins (Qin *et al.* 2011).

With reference to the literature, miR-21 and miR-29 showed expected expression patterns in MSC (Figure 15). miR-21 was slightly increased after 2 days of TGF-β1 stimulus which changed to significant 1,6-fold expression at 10 days of the stimulus. In the case of miR-29, the TGF-β1 stimulus caused a significant 20 % reduction after 2 days and an even more intense effect after 10 days: miR-29 expression was reduced to 0,6-fold. Figure 16 shows the miR-21 and -29 knockdown by antagomir and overexpression by miR mimics. Knockdown of both miR was significant, whereby overexpression of miR-21 showed 5-fold increase but remained without significance.

MiR are generally described to affect their targets through mRNA degradation or translational repression. When miR are overexpressed using miR mimics, an increased binding of miR target occurs. This often results in a stronger repression of target gene expression, leading to decreased levels of the target protein. Vice versa, the knockdown of miR generally results in enhanced expression of the target gene (Wienholds and Plasterk 2005). While most studies have shown that miR inhibit gene expression, there are also reports of miRNAs contributing to translational activation (Vasudevan and Steitz 2007, Ørom *et al.* 2008, Truesdell *et al.* 2012, Bukhari *et al.* 2016).

The effects of miR-21 overexpression and knockdown on the target genes SMA, Col1A1 and Calponin 1 can be classified into the current research status as follows. The knockdown of miR-21 (Figure 16 c) results in significant mRNA downregulation of all target genes. These findings align with former studies which show the same effects in different cell types than MSC (Yang *et al.* 2012, Jafarinejad-Farsangi *et al.* 2019). Overexpression of miR-21 (Figure 16 d) by specific mimics was previously described to result in increased α-SMA, Col1A1 and Calponin 1 levels in various cell types. (Davis *et al.* 2008, Zhou *et al.* 2017, Jafarinejad-Farsangi *et al.* 2019). These findings apply to α-SMA and Calponin1 but not fto Col1A1, as there is no effect on its mRNA levels upon miR-21 overexpression.

It is impossible to reliably state whether miR-21 directly or indirectly regulates α-SMA, Calponin 1 and Col1A1 in the given experimental setting. Only hypotheses can be formulated, suggesting that TGF/SMAD signalling is involved. This hypothesis arises from the fact that miR-21 is known to directly target SMAD 7, thereby influencing SMAD 2/3 signalling (Li *et al.* 2013). In keloids, miR-21 has been shown to enhance Col1A1 expression upon miR-21 knockdown, revealing a connection between the SMAD7-mediated fibroproliferative phenotype and Col1A1 (Zhou *et al.* 2017). Since Col1A1 was not affected by miR-21 overexpression, it can be hypothesised that an additional TGF-β1 stimulus is needed to initiate the SMAD7 pathway. It is possible that α-SMA and Calponin 1 gene expression are more

sensitive to reduced SMAD7 levels, and the basal TGF-β1 levels produced by MSC are sufficient to initiate gene expression. Another possibility of mir21 target gene regulation is an indirect pathway via the Programmed Cell Death 4 (PDCD4) protein. PDCD4 itself is a direct target of miR-21 and e.g. Calponin expression has been described to be induced by PDCD4 knockdown (Davis *et al.* 2008). It's important to note that miR-21's role in different cellular contexts can vary, and additional studies may provide further insights into its regulatory mechanisms.

Upon miR-29 antagomir knockdown, α-SMA and Calponin 1 show decreased mRNA amounts along with increased ColA1 mRNA levels (Figure 16 e). For Col1A1, similar results were achieved previously in primary rat myocytes and NRK52E (rat kidney cells) in two independent studies (van Rooij *et al.* 2008, Qin *et al.* 2011). Results for α-SMA and Calponin 1 are confirmable by a publication using Human fetal lung fibroblasts (IMR-90) and human pulmonary arterial smooth muscle cells (PASMC) (Cushing *et al.* 2015).

Overexpression of miR-29 showed matching results to the knockdown: α-SMA and Calponin 1 gene expression were induced by miR-29 overexpression and Col1A1 mRNA levels were nearly suppressed. Col1A1 is described to be directly targeted and inhibited by miR-29 in human lung fibroblasts, undergoing the classic regulatory pathway of miR (Li *et al.* 2009). Interestingly, miR-29 was found to directly target Myocardin (MYOCD) by affimetrix analysis (Cushing *et al.* 2015). MYOCD is one of the most important transcriptional factors in promoting SMC differentiation and belongs to the same family of transcription factors as MRTF-A (Wang *et al.* 2002). Eventually, mir-29 targets MYOCD in MSC thereby regulating Calponin and α-SMA. Further experiments could provide deeper insights in the connection of miR and MYOCD/MRTF-A signalling. For example, the mRNA levels of MRTF-A, MRTF-B, and MYOCD should be analysed after miR-29 overexpression and knockdown. Additionally, luciferase reporter assays could be performed to determine whether altered expression of miR-29 influences the activity of the myocardin family.

Col1A1 seems to be a crucial extracellular matrix protein in MSC to support tumour growth. It was described previously that spheroid formation of colorectal HCT8 cells with MSC *in vitro* depends on physiological amounts of Col1A1 secreted by MSC. Col1A1-knockdown MSC had relinquished their capacity to support the formation of spheroids in HCT8 cells. In contrast, mock-transduced MSC continued to stimulate spheroid formation in HCT8 cells like WT-MSC (Widder *et al.* 2016). Therefore, it was decided to switch from transient transfection to stable knockdown in MSC to perform similar experiments using miR-29 knockdown MSC in HCT8 spheroid formation experiments. Via lentiviral transduction, a construct harbouring the miR-29 sequence was used to ensure overexpression. In contrast to transient overexpression with a massive miR-29 amount, 400-fold higher than in the control cells, stable overexpression resulted in mild 2.8-fold overexpression of miR-29 levels, including a high standard deviation.

The effects on α-SMA and Calponin-1 were very subtle and could only be determined numerically. Col1A1 showed no change upon the mild miR-29 overexpression. It is also important to consider that the overexpression of miR-29 led to morphological changes in the MSC and resulted in increased cell detachment compared to the control group. It is hypothesised that MSC with extensive miR-29 overexpression and proper Col1A1 knockdown detach from the cell culture plastic losing them for further cultivation in connection with medium change. This results in an adherent MSC batch with mildly overexpressed miR-29 and physiological levels Col1A1. In conjunction with this, MSC with Col1A1 knockdown were described to exhibit significantly reduced proliferation (Widder *et al.* 2016). For future experiments, exploring alternative methods for culturing MSC is a viable option. Traditional plastic adherent cultivation presents several challenges: obtaining sufficient cell numbers for experimental purposes can be challenging, large-scale expansion can impact cell quality, MSC may lose their stem cell characteristics over time, and higher passages may potentially compromise both proliferation and differentiation potential (Bonab *et al.* 2006, Jung *et al.* 2012). Over the past few years, numerous publications have documented the extensive growth of MSC in suspension culture. Various methods of bioprocessing have been utilised to achieve this, such as bioreactors, spinner flasks, roller bottles, and multilayered flasks (reviewed in (Hassan *et al.* 2020)). Using one of those alternatives to culture MSC might support to maintain detached MSC created by miR-29 overexpression to perform further research.

Summarising, given the present circumstances, making a conclusive statement regarding the impact of miR-21 and miR-29 on MSC to CAF differentiation is not feasible. However, there are indications that both miRNAs play a role in regulating smooth muscle and extracellular matrix proteins in MSC, which are essential for the formation of CAF.

## 4.4 MRTF-A: Major regulator of MSC to CAF differentiation and tumour support?

As discussed in the previous chapters, the differentiation of MSC into CAF is a myofibroblastic process, marked by elevated expression of key target genes such as Calponin 1, α-SMA, and Col1A1. The transcriptional coactivator of SRF MRTF-A has been shown to regulate the expression of these genes across various cellular contexts (Small 2012). The results in Figure 18 show that endogenous MRTF-A activity is upregulated during myofibroblastic CAF differentiation in primary human bone marrow-derived MSC with both TCM and TGF-β1. In detail, two independent assays were conducted to examine whether MRTF-A is activated during MSC to CAF differentiation: A translocation assay using immunofluorescence staining and a promoter activity assay employing a luciferase reporter (Supplementary figure 1**Fehler! Verweisquelle konnte nicht gefunden werden.**), which was constructed as part of this thesis.

To evaluate the MRTF-A activity the murine cell line NIH3T3 historically served as the initial standard model to perform translocation assays. In NIH3T3, MRTF-A is inactive and located in the cytoplasm under starved conditions, thus it is excluded from the nucleus. By external stimuli like FCS, a common positive control, MRTF-A dissociates from G-actin in the cytoplasm and translocates to the nucleus (Miralles *et al.* 2003).

Interestingly, in starved MSC the translocation assay (Figure 18 a) demonstrated that MRTF-A was not excluded from the nucleus as expected. It was distributed over the whole cell. Preliminary experiments (Supplementary figure 3) demonstrated that FCS effectively induces MRTF-A translocation in MSC, altering the ratio between nuclear and cytoplasmic MRTF-A, while MRTF-A is not entirely excluded from the nucleus. In addition to the FCS positive control, TGF-β1 and TCM lead to equal nuclear translocation of MRTF-A after 48 h of incubation (Figure 18). MRTF-A activity in the promoter assay is equally upregulated in response to both, TGF-β and TCM stimuli (Figure 18 c).

These findings support the literature. Smooth muscle cells were described to express the majority of MRTF-A in the nucleus (Du *et al.* 2004, Hinson *et al.* 2007). It is hypothesised that the localisation of MRTF-A in starved cells depends on basal RhoA activity which influences the actin treadmilling. Studies have shown that NIH3T3 cells have a higher need for external stimulation to activate RhoA, whereas SMC and probably MSC naturally maintain higher RhoA activity under basal conditions (Błajecka *et al.* 2012, Fee *et al.* 2016). In addition, it was demonstrated that stiffer growth substrates, like standard cell culture dishes as used in the presented experiments, promote the translocation of MRTF-A to the nucleus (Foster *et al.* 2017). However, MRTF-A remains activatable by TGF-β1 and TCM thereby playing an active role in MSC during CAF differentiation.

As mentioned before, MRTF-A activity and localisation are highly dependent on actin dynamics. While a significant portion of actin dynamics occurs in the cytoplasm, actin-related processes also take place in the nucleus through nuclear actin. Actin is crucial both for regulating the localisation of MRTF-A and for modulating its activity within the nucleus.

Similar to the process in the cytoplasm, actin monomer-binding inhibits MRTF-A transcriptional activity within the nucleus (Vartiainen *et al.* 2007). Nuclear actin polymerisation in response to mechanotransduction relies on cell surface integrins, which relay signals to LINC proteins in the nuclear membrane (Plessner *et al.* 2015). Furthermore, external triggers like FCS, or TGF/TCM are transmitted to the nucleus by RhoA signalling pathway (Small 2012, Deshpande *et al.* 2022). Thereby, the described triggers might be able to activate mDia (mammalian Diaphanous-related formin) in the nucleus, initiating actin polymerisation, releasing MRTF-A from nuclear G-actin and leading to the activation of MRTF-A within the nucleus (Plessner and Grosse 2015). In human bone marrow-derived MSC, MRTF-A activation likely involves both

the nuclear translocation of cytoplasmic MRTF-A and the activation of MRTF-A that is predominantly located in the nucleus.

Calponin 1, α-SMA, and Col1A1 are well-established markers of myofibroblastic differentiation (Crider *et al.* 2011, Velasquez *et al.* 2013, Johnson *et al.* 2014). As demonstrated in Figures 7 and 8, their expression is significantly upregulated during the differentiation of MSC into CAF, driven by TGF-β1 and TCM. Additionally, the promoters of these genes are reported to be directly regulated by MRTF transcription factors and are sensitive to actin treadmilling, as observed in genome-wide expression studies (Descot *et al.* 2009, Esnault *et al.* 2014).

In fact, the induction of α-SMA and Calponin 1 during MSC differentiation by TGF-β1 and TCM is dependent on MRTF-A, as demonstrated by siRNA knockdown experiments in Figure 19, aligning with findings from other studies (Foster *et al.* 2017, Ge *et al.* 2018). These results go in line with the lentiviral knockdown experiments of MRTF-A shown in Figure 20. Using stable MRTF-A knockdown MSC generated in this thesis in HCT8 colorectal xenograft experiments, it was shown that tumour growth was significantly reduced but MRTF-A knockdown did not abolish it (Figure 21). Studies from 2016 have shown that collagen expression and synthesis are critical for the tumour-supporting function of MSC in colorectal cancer models like HCT8 (Widder *et al.* 2016). The lacking effect of MRTF-A on Col1A1 expression in MSC may explain the residual tumour growth observed in the xenograft experiments despite MRTF-A knockdown. This suggests that the lack of influence on Col1A1 could be a key factor allowing continued tumour progression, even when MRTF-A is silenced.

These outcomes on Col1A1 expression being regulated independently of MRTF-A are consistent with a previous study, which reported that MRTFs are not essential for COL1A1 induction in immortalized murine bone marrow MSC stimulated with TGF-β1 (Ge *et al.* 2018). In contrast, MRTF-A is crucial for the expression of all three collagen 1 genes in cardiac myofibroblasts, where their promoters are directly activated and bound by MRTFs (Small *et al.* 2010, Luchsinger *et al.* 2011, Novoyatleva *et al.* 2013). This suggests that in bone marrow-derived MSC, Col1A1 expression is effectively regulated through alternative pathways, independent of MRTF-A. Probably there is an interplay between micro-RNA like miR-29 and MRTF-A in MSC, since the first was found to effectively regulate Col1A1 expression in MSC to CAF differentiation in the current thesis. In contrast, MRTF-B and myocardin as myocardin family members could be in line to regulate Col1A1 since they are highly functional redundant to MRTF-A (Small 2012).

Although TGF-β1 is known to regulate MSC to CAF differentiation in MSC and has an impact on the translocation and activation of MRTF-A in MSC in the current studies, the precise mechanisms underlying its influence on actin-MRTF signalling remain unclear. Interestingly, the gene expression profiles induced by MRTF-A and TGF-β1 show significant overlaps (Esnault *et al.* 2014). To hypothesise one link between TGF-β1 and MRTF-A, one potential

mechanism involves the integration of the Hippo signalling pathway. TGF-β1 activates the receptor tyrosine kinase Alk5, which phosphorylates SMAD2. Phosphorylated SMAD2 then interacts with YAP (Yes-associated protein), facilitating its nuclear translocation and the subsequent activation of downstream genes (Pefani *et al.* 2016). Once in the nucleus, YAP has been shown to interact with the TEAD family of transcription factors (TEA Domain Transcription Factors), which binds to the promoter region of the *MRTF-A* gene, inducing its expression. The resulting increase in MRTF-A expression enhances the transcription of profibrotic genes such as *Col1A1*, *α-SMA*, *CTGF*, *Cyr61*, and *TGF-β1*. Notably, the TEAD-binding site in the *MRTF-A* gene appears to be evolutionarily conserved, as it is present in the *MRTF-A* genes of mice, rats, and humans (Francisco *et al.* 2020).

Although YAP-TEAD and MRTF-SRF signalling pathways are interconnected through cytoskeletal remodelling and linked by TGF-β1, the specific influence of "YAP-only" targets on the CAF-like functionality of MSC, especially under partial MRTF-A depletion, remains unclear. Col1A1 may be regulated as a "YAP-only" target in human bone marrow-derived MSC. To support this hypothesis, further studies involving knockdown of YAP and/or TEAD should be conducted to determine whether Col1A1 expression is indeed modulated by the Hippo pathway in MSC.

An additional connection between MRTF-A and TGF-β1 involves the Cdc42 signalling pathway. In murine mesenchymal stem cells (MSC), TGF-β1 induced myofibroblastic differentiation, like the findings in this thesis, and MRTF-A-driven α-SMA expression was reliant on the activity of the Rho GTPase Cdc42. Upon Cdc42 knockdown, α-SMA expression decreased. Although actin polymerisation and MRTF-A played essential roles in TGF-β1-induced α-SMA expression, this actin remodelling did not depend on standard processes like Arp2/3 or cofilin pathways. Instead, the levels of F-actin were linked to cell contraction, with TGF-β1-induced actin polymerisation correlating with enhanced cell contraction, driven by RhoA and Cdc42 activity (Ge *et al.* 2018). To gain deeper insights into MSC support of early tumour growth, further investigations into key signalling pathways, particularly those regulating Col1A1, are crucial. Chromatin Immunoprecipitation DNA sequencing (ChIP-seq), for instance, could be a valuable method to identify genes and signalling pathways upregulated during MSC to CAF differentiation.

In summary, the findings of this thesis, together with the discussed hypotheses on additional gene regulation pathways independent of MRTF-A, suggest a potential model for tumour support *in vivo* (Figure 22). In this model, colorectal cancer cells secrete TGF-like factors that attract and activate MSC, driving their differentiation into CAF. The differentiation process is strictly dependent on MRTF-A, while other mechanisms (miR), alternative gene regulation pathways (YAP/ CDC42) and supporting myocardin family members (MRTF-B/Myocardin) support the formation of the final CAF features. Supporting this model, increased TGF-β1

mRNA was detected in MSC (Supplementary figure 2) undergoing myofibroblastic differentiation, underscoring the interplay between tumour and stromal cells in the tumour microenvironment. Subsequently, MSC may establish an autocrine TGF-β1 signalling loop, which exerts paracrine effects on tumour cells.

In conclusion, MRTF-A plays a key role in supporting tumour formation by influencing the MSC to CAF differentiation and stromal environment.

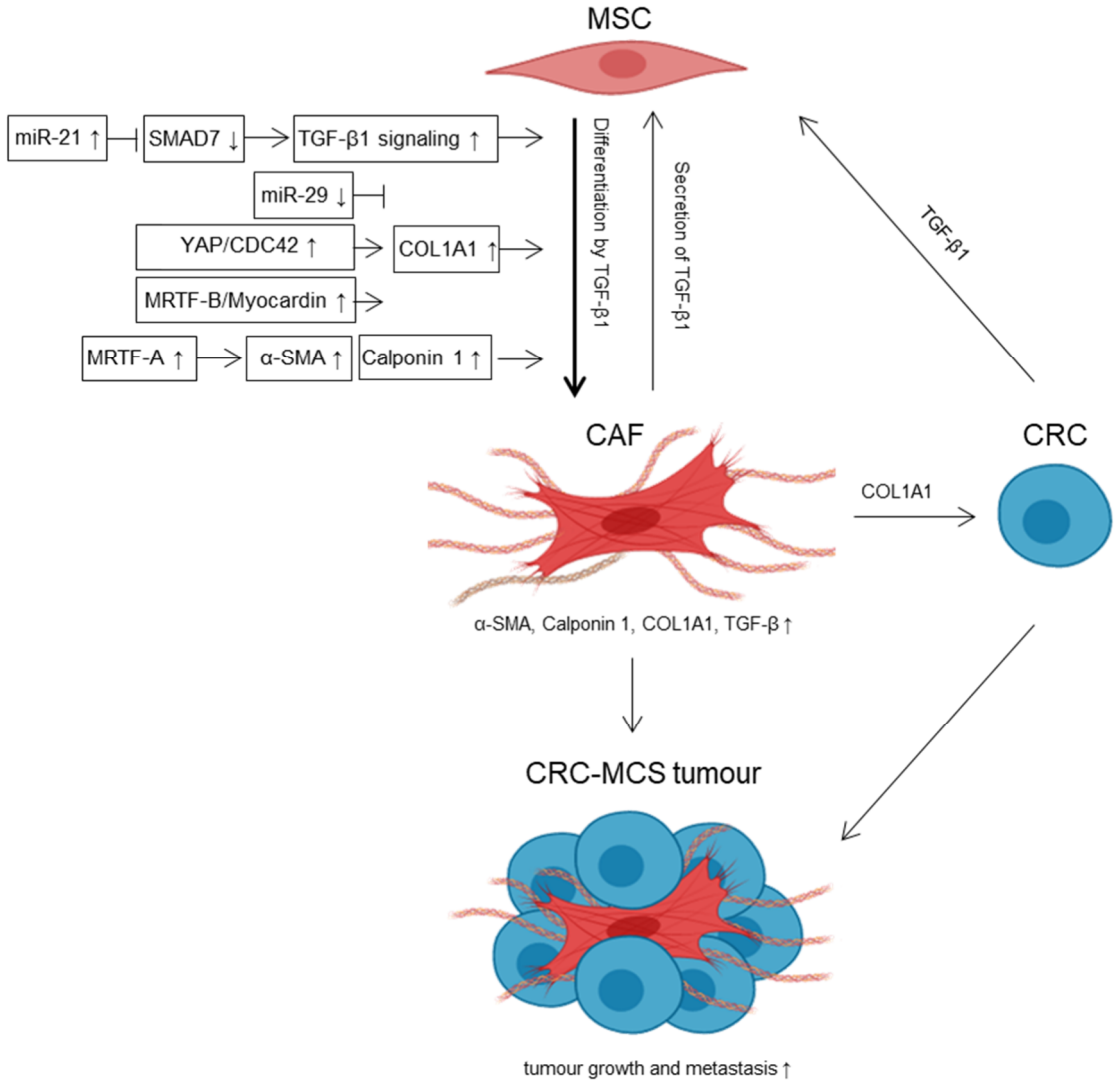


**Figure 22: Molecular regulation of MSC differentiation towards a CAF highlighting key signalling pathways and molecular markers.**
Mesenchymal stromal cells (MSC) are attracted from their perivascular niche to the tumour site by colorectal cancer (CRC) cells, such as HCT8, through TGF-β1 secretion. The transition from MSC to cancer-associated fibroblasts (CAF) is driven by TGF-β1, with miR-21 upregulation enhancing TGF-β signalling by inhibiting SMAD7. COL1A1 expression is regulated through various pathways, including miR-29, YAP, CDC42, or myocardin family members like MRTF-B and myocardin. During CAF differentiation, MRTF-A activity increases, leading to the upregulation of myofibroblastic markers α-SMA and Calponin 1. CAF exhibit elevated levels of α-SMA, Calponin 1, COL1A1, and TGF-β1. Additionally, CAF may establish an autocrine TGF-β1 signalling loop, which impacts HCT8 cells via paracrine mechanisms. In combination with CRC cells, CAF contribute to the formation of a solid tumour, promoting tumour growth and metastasis.

# BIBLIOGRAPHY

**AHRENDS, T. AND J. BORST (2018).** "The opposing roles of CD4(+) T cells in anti-tumour immunity." Immunology **154**(4): 582-592.

**AKIMOTO, K., K. KIMURA, M. NAGANO, S. TAKANO, G. TO'A SALAZAR, T. YAMASHITA AND O. OHNEDA (2013).** "Umbilical cord blood-derived mesenchymal stem cells inhibit, but adipose tissue-derived mesenchymal stem cells promote, glioblastoma multiforme proliferation." Stem Cells Dev **22**(9): 1370-1386.

**ALKASALIAS, T., E. FLABERG, V. KASHUBA, A. ALEXEYENKO, T. PAVLOVA, A. SAVCHENKO, L. SZEKELY, G. KLEIN AND H. GUVEN (2014).** "Inhibition of tumor cell proliferation and motility by fibroblasts is both contact and soluble factor dependent." PNAS **111**(48): 17188-17193.

**ALLINEN, M., R. BEROUKHIM, L. CAI, C. BRENNAN, J. LAHTI-DOMENICI, H. HUANG, D. PORTER, M. HU, L. CHIN, A. RICHARDSON, S. SCHNITT, W. R. SELLERS AND K. POLYAK (2004).** "Molecular characterization of the tumor microenvironment in breast cancer." Cancer Cell **6**(1): 17-32.

**ALSPACH, E., Y. FU AND S. A. STEWART (2013).** "Senescence and the pro-tumorigenic stroma." Crit Rev Oncog **18**(6): 549-558.

**APRELIKOVA, O., X. YU, J. PALLA, B.-R. WEI, S. JOHN, M. YI, R. STEPHENS, R. M. SIMPSON, J. I. RISINGER, A. JAZAERI AND J. NIEDERHUBER (2010).** "The role of miR-31 and its target gene SATB2 in cancer-associated fibroblasts." Cell Cycle **9**(21): 4387-4398.

**ARAS, S. AND M. R. ZAIDI (2017).** "TAMeless traitors: macrophages in cancer progression and metastasis." Br J Cancer **117**(11): 1583-1591.

**ARAVIND, L. AND E. V. KOONIN (2000).** "SAP - a putative DNA-binding motif involved in chromosomal organization." Trends Biochem Sci **25**(3): 112-114.

**ARINA, A., C. IDEL, E. M. HYJEK, M. L. ALEGRE, Y. WANG, V. P. BINDOKAS, R. R. WEICHSELBAUM AND H. SCHREIBER (2016).** "Tumor-associated fibroblasts predominantly come from local and not circulating precursors." Proc Natl Acad Sci U S A **113**(27): 7551-7556.

**ASANGANI, I. A., S. A. RASHEED, D. A. NIKOLOVA, J. H. LEUPOLD, N. H. COLBURN, S. POST AND H. ALLGAYER (2008).** "MicroRNA-21 (miR-21) post-transcriptionally downregulates tumor suppressor Pdcd4 and stimulates invasion, intravasation and metastasis in colorectal cancer." Oncogene **27**(15): 2128-2136.

**AYALA-CUELLAR, A. P., J. H. KANG, E. B. JEUNG AND K. C. CHOI (2019).** "Roles of Mesenchymal Stem Cells in Tissue Regeneration and Immunomodulation." Biomol Ther (Seoul) **27**(1): 25-33.

**BAGLEY, R. G., W. WEBER, C. ROULEAU, M. YAO, N. HONMA, S. KATAOKA, I. ISHIDA, B. L. ROBERTS AND B. A. TEICHER (2009).** "Human mesenchymal stem cells from bone marrow express tumor endothelial and stromal markers." Int J Oncol **34**(3): 619-627.

**BALKWILL, F. R., M. CAPASSO AND T. HAGEMANN (2012).** "The tumor microenvironment at a glance." J Cell Sci **125**(Pt 23): 5591-5596.

**BARCELLOS-DE-SOUZA, P., G. COMITO, C. PONS-SEGURA, M. L. TADDEI, V. GORI, V. BECHERUCCI, F. BAMBI, F. MARGHERI, A. LAURENZANA, M. DEL ROSSO AND P. CHIARUGI (2016).** "Mesenchymal Stem Cells are Recruited and Activated into Carcinoma-Associated Fibroblasts by Prostate Cancer Microenvironment-Derived TGF-beta1." Stem Cells **34**(10): 2536-2547.

**BARCELLOS-HOFF, M. H. AND T. A. DIX (1996).** "Redox-mediated activation of latent transforming growth factor-beta 1." Mol Endocrinol **10**(9): 1077-1083.

**BATISTA, F. D. AND N. E. HARWOOD (2009).** "The who, how and where of antigen presentation to B cells." Nat Rev Immunol **9**(1): 15-27.

**BAUM, J. AND H. S. DUFFY (2011).** "Fibroblasts and myofibroblasts: what are we talking about?" J Cardiovasc Pharmacol **57**(4): 376-379.

**BECKER BUSCAGLIA, L. E. AND Y. LI (2011).** "Apoptosis and the target genes of microRNA-21." Chin J Cancer **30**(6): 371-380.

**BELTRAO, P., G. CAGNEY AND N. J. KROGAN (2010).** "Quantitative genetic interactions reveal biological modularity." Cell **141**(5): 739-745.

**BENNETT, S. R., F. R. CARBONE, F. KARAMALIS, J. F. MILLER AND W. R. HEATH (1997).** "Induction of a CD8+ cytotoxic T lymphocyte response by cross-priming requires cognate CD4+ T cell help." The Journal of experimental medicine **186**(1): 65-70.

**BHOWMICK, N. A., E. G. NEILSON AND H. L. MOSES (2004).** "Stromal fibroblasts in cancer initiation and progression." Nature **432**(7015): 332-337.

**BI, S., C. CAO, L. L. CHAI, S. R. LI AND D. Y. YANG (2017).** "Regulatory mechanism of miR-29 over TGF-beta1 and COL1 in scar cells." Eur Rev Med Pharmacol Sci **21**(10): 2512-2517.

**BŁAJECKA, K., M. MARINOV, L. LEITNER, K. UTH, G. POSERN AND A. ARCARO (2012).** "Phosphoinositide 3-Kinase C2β Regulates RhoA and the Actin Cytoskeleton through an Interaction with Dbl." PLOS ONE **7**(9): e44945.

**BOCHON, B., M. KOZUBSKA, G. SURYGAŁA, A. WITKOWSKA, R. KUŹNIEWICZ, W. GRZESZCZAK AND G. WYSTRYCHOWSKI (2019).** "Mesenchymal Stem Cells-Potential Applications in Kidney Diseases." International journal of molecular sciences **20**(10): 2462.

**BONAB, M. M., K. ALIMOGHADDAM, F. TALEBIAN, S. H. GHAFFARI, A. GHAVAMZADEH AND B. NIKBIN (2006).** "Aging of mesenchymal stem cell in vitro." BMC Cell Biol **7**: 14.

**BORRIELLO, L., R. NAKATA, M. A. SHEARD, G. E. FERNANDEZ, R. SPOSTO, J. MALVAR, L. BLAVIER, H. SHIMADA, S. ASGHARZADEH, R. C. SEEGER AND Y. A. DECLERCK (2017).** "Cancer-Associated Fibroblasts Share Characteristics and Protumorigenic Activity with Mesenchymal Stromal Cells." Cancer Res **77**(18): 5142-5157.

**BOXER, L. M., R. PRYWES, R. G. ROEDER AND L. KEDES (1989).** "The sarcomeric actin CArG-binding factor is indistinguishable from the c-fos serum response factor." Mol Cell Biol **9**(2): 515-522.

**BRASSART-PASCO, S., S. BRÉZILLON, B. BRASSART, L. RAMONT, J.-B. OUDART AND J. C. MONBOISSE (2020).** "Tumor Microenvironment: Extracellular Matrix Alterations Influence Tumor Progression." Frontiers in oncology **10**: 397-397.

**BRENTNALL, T. A., L. A. LAI, J. COLEMAN, M. P. BRONNER, S. PAN AND R. CHEN (2012).** "Arousal of cancer-associated stroma: overexpression of palladin activates fibroblasts to promote tumor invasion." PLoS One **7**(1): e30219.

**BROUGHTON, J. P., M. T. LOVCI, J. L. HUANG, G. W. YEO AND A. E. PASQUINELLI (2016).** "Pairing beyond the Seed Supports MicroRNA Targeting Specificity." Mol Cell **64**(2): 320-333.

**BUKHARI, S. I. A., S. S. TRUESDELL, S. LEE, S. KOLLU, A. CLASSON, M. BOUKHALI, E. JAIN, R. D. MORTENSEN, A. YANAGIYA, R. I. SADREYEV, W. HAAS AND S. VASUDEVAN (2016).** "A Specialized Mechanism of Translation Mediated by FXR1a-Associated MicroRNP in Cellular Quiescence." Molecular Cell **61**(5): 760-773.

**CAMACHO, D. F. AND K. J. PIENTA (2012).** "Disrupting the networks of cancer." Clin Cancer Res **18**(10): 2801-2808.

**CAPLAN, A. I. (1991).** "Mesenchymal stem cells." J Orthop Res **9**(5): 641-650.

**CAYSA, H., S. HOFFMANN, J. LUETZKENDORF, L. P. MUELLER, S. UNVERZAGT, K. MÄDER AND T. MUELLER (2012).** "Monitoring of Xenograft Tumor Growth and Response to Chemotherapy by Non-Invasive In Vivo Multispectral Fluorescence Imaging." PLoS ONE **7**(10).

**CEN, B., A. SELVARAJ, R. C. BURGESS, J. K. HITZLER, Z. MA, S. W. MORRIS AND R. PRYWES (2003).** "Megakaryoblastic leukemia 1, a potent transcriptional coactivator for serum response factor (SRF), is required for serum induction of SRF target genes." Mol Cell Biol **23**(18): 6597-6608.

**CHANG, T. C., M. F. HSU, C. Y. SHIH AND K. K. WU (2017).** "5-methoxytryptophan protects MSC from stress induced premature senescence by upregulating FoxO3a and mTOR." Sci Rep **7**(1): 11133.

**CHEIFETZ, S., J. A. WEATHERBEE, M. L. TSANG, J. K. ANDERSON, J. E. MOLE, R. LUCAS AND J. MASSAGUÉ (1987).** "The transforming growth factor-beta system, a complex pattern of cross-reactive ligands and receptors." Cell **48**(3): 409-415.

**CHERNG, S., J. YOUNG AND H. MA (2008).** "Alpha-Smooth Muscle Actin (α -SMA)." The Journal of American Science **4**(4): 7-9.

**CHOO, K. B., Y. L. SOON, P. N. N. NGUYEN, M. S. Y. HIEW AND C.-J. HUANG (2014).** "MicroRNA-5p and -3p co-expression and cross-targeting in colon cancer cells." Journal of biomedical science **21**(1): 95-95.

**CHOU, J., J. H. LIN, A. BRENOT, J. W. KIM, S. PROVOT AND Z. WERB (2013A).** "GATA3 suppresses metastasis and modulates the tumour microenvironment by regulating microRNA-29b expression." Nat Cell Biol **15**(2): 201-213.

**CHOU, J., P. SHAHI AND Z. WERB (2013B).** "microRNA-mediated regulation of the tumor microenvironment." Cell cycle (Georgetown, Tex.) **12**: 3262-3271.

**CIHOVA, M., V. ALTANEROVA AND C. ALTANER (2011).** "Stem cell based cancer gene therapy." Mol Pharm **8**(5): 1480-1487.

**CIRRI, P. AND P. CHIARUGI (2011).** "Cancer associated fibroblasts: the dark side of the coin." Am J Cancer Res **1**(4): 482-497.

**COFFELT, S. B., M. D. WELLENSTEIN AND K. E. DE VISSER (2016).** "Neutrophils in cancer: neutral no more." Nat Rev Cancer **16**(7): 431-446.

**COPELAND, J. W. AND R. TREISMAN (2002).** "The diaphanous-related formin mDia1 controls serum response factor activity through its effects on actin polymerisation." Mol Biol Cell **13**(11): 4088-4099.

**COPPE, J. P., P. Y. DESPREZ, A. KRTOLICA AND J. CAMPISI (2010).** "The senescence-associated secretory phenotype: the dark side of tumor suppression." Annu Rev Pathol **5**: 99-118.

**CRAWFORD, S. E., V. STELLMACH, J. E. MURPHY-ULLRICH, S. M. RIBEIRO, J. LAWLER, R. O. HYNES, G. P. BOIVIN AND N. BOUCK (1998).** "Thrombospondin-1 is a major activator of TGF-beta1 in vivo." Cell **93**(7): 1159-1170.

**CRIDER, B. J., G. M. RISINGER, JR., C. J. HAAKSMA, E. W. HOWARD AND J. J. TOMASEK (2011).** "Myocardin-related transcription factors A and B are key regulators of TGF-beta1-induced fibroblast to myofibroblast differentiation." J Invest Dermatol **131**(12): 2378-2385.

**CRISAN, M., S. YAP, L. CASTEILLA, C. W. CHEN, M. CORSELLI, T. S. PARK, G. ANDRIOLO, B. SUN, B. ZHENG, L. ZHANG, C. NOROTTE, P. N. TENG, J. TRAAS, R. SCHUGAR, B. M. DEASY, S. BADYLAK, H. J. BUHRING, J. P. GIACOBINO, L. LAZZARI, J. HUARD AND B. PEAULT (2008).** "A perivascular origin for mesenchymal stem cells in multiple human organs." Cell Stem Cell **3**(3): 301-313.

**CUSHING, L., S. COSTINEAN, W. XU, Z. JIANG, L. MADDEN, P. KUANG, J. HUANG, A. WEISMAN, A. HATA, C. M. CROCE AND J. LÜ (2015).** "Disruption of miR-29 Leads to Aberrant Differentiation of Smooth Muscle Cells Selectively Associated with Distal Lung Vasculature." PLoS Genet **11**(5): e1005238.

**DALLAS, S. L., S. PARK-SNYDER, K. MIYAZONO, D. TWARDZIK, G. R. MUNDY AND L. F. BONEWALD (1994).** "Characterization and autoregulation of latent transforming growth factor beta (TGF

beta) complexes in osteoblast-like cell lines. Production of a latent complex lacking the latent TGF beta-binding protein." J Biol Chem **269**(9): 6815-6821.

**DAVIS, B. N., A. C. HILYARD, G. LAGNA AND A. HATA (2008).** "SMAD proteins control DROSHA-mediated microRNA maturation." Nature **454**(7200): 56-61.

**DE BOECK, A., A. HENDRIX, D. MAYNARD, M. VAN BOCKSTAL, A. DANIELS, P. PAUWELS, C. GESPACH, M. BRACKE AND O. DE WEVER (2013).** "Differential secretome analysis of cancer-associated fibroblasts and bone marrow-derived precursors to identify microenvironmental regulators of colon cancer progression." Proteomics **13**(2): 379-388.

**DE WEVER, O., M. VAN BOCKSTAL, M. MAREEL, A. HENDRIX AND M. BRACKE (2014).** "Carcinoma-associated fibroblasts provide operational flexibility in metastasis." Semin Cancer Biol **25**: 33-46.

**DEBACQ-CHAINIAUX, F., J. D. ERUSALIMSKY, J. CAMPISI AND O. TOUSSAINT (2009).** "Protocols to detect senescence-associated beta-galactosidase (SA-betagal) activity, a biomarker of senescent cells in culture and in vivo." Nat Protoc **4**(12): 1798-1806.

**DESCOT, A., R. HOFFMANN, D. SHAPOSHNIKOV, M. RESCHKE, A. ULLRICH AND G. POSERN (2009).** "Negative Regulation of the EGFR-MAPK Cascade by Actin-MAL-Mediated Mig6/Errfi-1 Induction." Molecular Cell **35**(3): 291-304.

**DESHPANDE, A., P. M. V. SHETTY, N. FREY AND A. Y. RANGREZ (2022).** "SRF: a seriously responsible factor in cardiac development and disease." J Biomed Sci **29**(1): 38.

**DESMOULIERE, A., M. REDARD, I. DARBY AND G. GABBIANI (1995).** "Apoptosis mediates the decrease in cellularity during the transition between granulation tissue and scar." Am J Pathol **146**(1): 56-66.

**DIMRI, G. P., X. LEE, G. BASILE, M. ACOSTA, G. SCOTT, C. ROSKELLEY, E. E. MEDRANO, M. LINSKENS, I. RUBELJ, O. PEREIRA-SMITH, M. PEACOCKE AND J. CAMPISI (1995).** "A biomarker that identifies senescent human cells in culture and in aging skin in vivo." Proceedings of the National Academy of Sciences **92**(September): 9363-9367.

**DINARELLO, C. A. (2007).** "Historical insights into cytokines." Eur J Immunol **37 Suppl 1**(Suppl 1): S34-45.

**DIREKZE, N. C., S. J. FORBES, M. BRITTAN, T. HUNT, R. JEFFERY, S. L. PRESTON, R. POULSOM, K. HODIVALA-DILKE, M. R. ALISON AND N. A. WRIGHT (2003).** "Multiple organ engraftment by bone-marrow-derived myofibroblasts and fibroblasts in bone-marrow-transplanted mice." Stem Cells **21**(5): 514-520.

**DIREKZE, N. C., K. HODIVALA-DILKE, R. JEFFERY, T. HUNT, R. POULSOM, D. OUKRIF, M. R. ALISON AND N. A. WRIGHT (2004).** "Bone marrow contribution to tumor-associated myofibroblasts and fibroblasts." Cancer Res **64**(23): 8492-8495.

**DOMINICI, M., K. LE BLANC, I. MUELLER, I. SLAPER-CORTENBACH, F. MARINI, D. KRAUSE, R. DEANS, A. KEATING, D. PROCKOP AND E. HORWITZ (2006).** "Minimal criteria for defining multipotent mesenchymal stromal cells. The International Society for Cellular Therapy position statement." Cytotherapy **8**(4): 315-317.

**DRANOFF, G. (2004).** "Cytokines in cancer pathogenesis and cancer therapy." Nat Rev Cancer **4**(1): 11-22.

**DU, K. L., M. CHEN, J. LI, J. J. LEPORE, P. MERICKO AND M. S. PARMACEK (2004).** "Megakaryoblastic leukemia factor-1 transduces cytoskeletal signals and induces smooth muscle cell differentiation from undifferentiated embryonic stem cells." J Biol Chem **279**(17): 17578-17586.

**DUBOIS, C. M., M. H. LAPRISE, F. BLANCHETTE, L. E. GENTRY AND R. LEDUC (1995).** "Processing of transforming growth factor beta 1 precursor by human furin convertase." J Biol Chem **270**(18): 10618-10624.

**DVORAK, H. F. (1986).** "Tumors: wounds that do not heal. Similarities between tumor stroma generation and wound healing." N Engl J Med **315**(26): 1650-1659.

**ERDOGAN, B., M. AO, L. M. WHITE, A. L. MEANS, B. M. BREWER, L. YANG, M. K. WASHINGTON, C. SHI, O. E. FRANCO, A. M. WEAVER, S. W. HAYWARD, D. LI AND D. J. WEBB (2017).** "Cancer-associated fibroblasts promote directional cancer cell migration by aligning fibronectin." The Journal of cell biology **216**(11): 3799-3816.

**ESNAULT, C., A. STEWART, F. GUALDRINI, P. EAST, S. HORSWELL, N. MATTHEWS AND R. TREISMAN (2014).** "Rho-actin signaling to the MRTF coactivators dominates the immediate transcriptional response to serum in fibroblasts." Genes and Development **28**(9): 943-958.

**FAOUZI, S., B. LE BAIL, V. NEAUD, L. BOUSSARIE, J. SARIC, P. BIOULAC-SAGE, C. BALABAUD AND J. ROSENBAUM (1999).** "Myofibroblasts are responsible for collagen synthesis in the stroma of human hepatocellular carcinoma: an in vivo and in vitro study." J Hepatol **30**(2): 275-284.

**FEE, T., S. SURIANARAYANAN, C. DOWNS, Y. ZHOU AND J. BERRY (2016).** "Nanofiber Alignment Regulates NIH3T3 Cell Orientation and Cytoskeletal Gene Expression on Electrospun PCL+Gelatin Nanofibers." PLOS ONE **11**(5): e0154806.

**FOSTER, C. T., F. GUALDRINI AND R. TREISMAN (2017).** "Mutual dependence of the MRTF-SRF and YAP-TEAD pathways in cancer-associated fibroblasts is indirect and mediated by cytoskeletal dynamics." Genes Dev **31**(23-24): 2361-2375.

**FOULDS, L. (1954).** "The experimental study of tumor progression: a review." Cancer Res **14**(5): 327-339.

**FOX, J. M., G. CHAMBERLAIN, B. A. ASHTON AND J. MIDDLETON (2007).** "Recent advances into the understanding of mesenchymal stem cell trafficking." Br J Haematol **137**(6): 491-502.

**FRANCISCO, J., Y. ZHANG, I. JEONG JAE, W. MIZUSHIMA, S. IKEDA, A. IVESSA, S. OKA, P. ZHAI, D. TALLQUIST MICHELLE AND P. DEL RE DOMINIC (2020).** "Blockade of Fibroblast YAP Attenuates Cardiac Fibrosis and Dysfunction Through MRTF-A Inhibition." JACC: Basic to Translational Science **5**(9): 931-945.

**FRANCOIS, S., B. USUNIER, M. E. FORGUE-LAFITTE, B. L'HOMME, M. BENDERITTER, L. DOUAY, N. C. GORIN, A. K. LARSEN AND A. CHAPEL (2019).** "Mesenchymal Stem Cell Administration Attenuates Colon Cancer Progression by Modulating the Immune Component within the Colorectal Tumor Microenvironment." Stem Cells Transl Med **8**(3): 285-300.

**FRANKEL, L. B., N. R. CHRISTOFFERSEN, A. JACOBSEN, M. LINDOW, A. KROGH AND A. H. LUND (2008).** "Programmed cell death 4 (PDCD4) is an important functional target of the microRNA miR-21 in breast cancer cells." J Biol Chem **283**(2): 1026-1033.

**FRIEDENSTEIN, A. J., R. K. CHAILAKHJAN AND K. S. LALYKINA (1970).** "The development of fibroblast colonies in monolayer cultures of guinea-pig bone marrow and spleen cells." Cell Tissue Kinet **3**(4): 393-403.

**FRIEDENSTEIN, A. J., J. F. GORSKAJA AND N. N. KULAGINA (1976).** "Fibroblast precursors in normal and irradiated mouse hematopoietic organs." Exp Hematol **4**(5): 267-274.

**FUKUMURA, D., R. XAVIER, T. SUGIURA, Y. CHEN, E. C. PARK, N. LU, M. SELIG, G. NIELSEN, T. TAKSIR, R. K. JAIN AND B. SEED (1998).** "Tumor induction of VEGF promoter activity in stromal cells." Cell **94**(6): 715-725.

**GABBIANI, G. (1992).** "The biology of the myofibroblast." Kidney Int **41**(3): 530-532.

**GABRILOVICH, D. I., S. OSTRAND-ROSENBERG AND V. BRONTE (2012).** "Coordinated regulation of myeloid cells by tumours." Nature reviews. Immunology **12**(4): 253-268.

**GALIE, M., C. SORRENTINO, M. MONTANI, L. MICOSSI, E. DI CARLO, T. D'ANTUONO, L. CALDERAN, P. MARZOLA, D. BENATI, F. MERIGO, F. ORLANDO, A. SMORLESI, C. MARCHINI, A. AMICI AND A.**

**SBARBATI (2005).** "Mammary carcinoma provides highly tumourigenic and invasive reactive stromal cells." Carcinogenesis **26**(11): 1868-1878.

**GAU, D. AND P. ROY (2018).** "SRF'ing and SAP'ing - the role of MRTF proteins in cell migration." J Cell Sci **131**(19).

**GE, J., L. BURNIER, M. ADAMOPOULOU, M. Q. KWA, M. SCHAKS, K. ROTTNER AND C. BRAKEBUSCH (2018).** "RhoA, Rac1, and Cdc42 differentially regulate alphaSMA and collagen I expression in mesenchymal stem cells." J Biol Chem **293**(24): 9358-9369.

**GELLIBERT, F., J. WOOLVEN, M. H. FOUCHET, N. MATHEWS, H. GOODLAND, V. LOVEGROVE, A. LAROZE, V. L. NGUYEN, S. SAUTET, R. WANG, C. JANSON, W. SMITH, G. KRYSA, V. BOULLAY, A. C. DE GOUVILLE, S. HUET AND D. HARTLEY (2004).** "Identification of 1,5-naphthyridine derivatives as a novel series of potent and selective TGF-beta type I receptor inhibitors." J Med Chem **47**(18): 4494-4506.

**GENESTE, O., J. W. COPELAND AND R. TREISMAN (2002).** "LIM kinase and Diaphanous cooperate to regulate serum response factor and actin dynamics." J Cell Biol **157**(5): 831-838.

**GENTRY, L. E. AND B. W. NASH (1990).** "The pro domain of pre-pro-transforming growth factor beta 1 when independently expressed is a functional binding protein for the mature growth factor." Biochemistry **29**(29): 6851-6857.

**GINEITIS, D. AND R. TREISMAN (2001).** "Differential usage of signal transduction pathways defines two types of serum response factor target gene." J Biol Chem **276**(27): 24531-24539.

**GINHOUX, F., J. L. SCHULTZE, P. J. MURRAY, J. OCHANDO AND S. K. BISWAS (2016).** "New insights into the multidimensional concept of macrophage ontogeny, activation and function." Nat Immunol **17**(1): 34-40.

**GLEIZES, P. E., J. S. MUNGER, I. NUNES, J. G. HARPEL, R. MAZZIERI, I. NOGUERA AND D. B. RIFKIN (1997).** "TGF-β latency: Biological significance and mechanisms of activation." Stem Cells **15**(3): 190-197.

**GONDA, T. A., A. VARRO, T. C. WANG AND B. TYCKO (2010).** "Molecular biology of cancer-associated fibroblasts: can these cells be targeted in anti-cancer therapy?" Semin Cell Dev Biol **21**(1): 2-10.

**GORUPPI, S. AND G. P. DOTTO (2013).** "Mesenchymal stroma: primary determinant and therapeutic target for epithelial cancer." Trends Cell Biol **23**(12): 593-602.

**GUALDRINI, F., C. ESNAULT, S. HORSWELL, A. STEWART, N. MATTHEWS AND R. TREISMAN (2016).** "SRF Co-factors Control the Balance between Cell Proliferation and Contractility." Mol Cell **64**(6): 1048-1061.

**GUIDO, C., D. WHITAKER-MENEZES, C. CAPPARELLI, R. BALLIET, Z. LIN, R. G. PESTELL, A. HOWELL, S. AQUILA, S. ANDÒ, U. MARTINEZ-OUTSCHOORN, F. SOTGIA AND M. P. LISANTI (2012).** "Metabolic reprogramming of cancer-associated fibroblasts by TGF-β drives tumor growth: connecting TGF-β signaling with "Warburg-like" cancer metabolism and L-lactate production." Cell cycle (Georgetown, Tex.) **11**(16): 3019-3035.

**GUILLEREY, C., N. D. HUNTINGTON AND M. J. SMYTH (2016).** "Targeting natural killer cells in cancer immunotherapy." Nat Immunol **17**(9): 1025-1036.

**GURBUZ, I., J. FERRALLI, T. ROLOFF, R. CHIQUET-EHRISMANN AND M. B. ASPARUHOVA (2014).** "SAP domain-dependent Mkl1 signaling stimulates proliferation and cell migration by induction of a distinct gene set indicative of poor prognosis in breast cancer patients." Mol Cancer **13**: 22.

**HAASTERS, F., W. C. PRALL, D. ANZ, C. BOURQUIN, C. PAUTKE, S. ENDRES, W. MUTSCHLER, D. DOCHEVA AND M. SCHIEKER (2009).** "Morphological and immunocytochemical characteristics indicate the yield of early progenitors and represent a quality control for human mesenchymal stem cell culturing." J Anat **214**(5): 759-767.

**HABIF, G., A. CRINIER, P. ANDRE, E. VIVIER AND E. NARNI-MANCINELLI (2019).** "Targeting natural killer cells in solid tumors." Cell Mol Immunol **16**(5): 415-422.

**HAN, I., B. S. KWON, H. K. PARK AND K. S. KIM (2017).** "Differentiation Potential of Mesenchymal Stem Cells Is Related to Their Intrinsic Mechanical Properties." Int Neurourol J **21**(Suppl 1): S24-31.

**HANAHAN, D. AND R. A. WEINBERG (2000).** "The hallmarks of cancer." Cell **100**(1): 57-70.

**HANAHAN, D. AND R. A. WEINBERG (2011).** "Hallmarks of cancer: the next generation." Cell **144**(5): 646-674.

**HANLEY, C. J., F. NOBLE, M. WARD, M. BULLOCK, C. DRIFKA, M. MELLONE, A. MANOUSOPOULOU, H. E. JOHNSTON, A. HAYDEN, S. THIRDBOROUGH, Y. LIU, D. M. SMITH, T. MELLOWS, W. J. KAO, S. D. GARBIS, A. MIRNEZAMI, T. J. UNDERWOOD, K. W. ELICEIRI AND G. J. THOMAS (2016).** "A subset of myofibroblastic cancer-associated fibroblasts regulate collagen fiber elongation, which is prognostic in multiple cancers." Oncotarget **7**(5): 6159-6174.

**HASSAN, M., M. D. YAZID, M. H. M. YUNUS, S. R. CHOWDHURY, Y. LOKANATHAN, R. B. H. IDRUS, A. M. H. NG AND J. X. LAW (2020).** "Large-Scale Expansion of Human Mesenchymal Stem Cells." Stem Cells Int **2020**: 9529465.

**HASSONA, Y., N. CIRILLO, K. P. LIM, A. HERMAN, M. MELLONE, G. J. THOMAS, G. N. PITIYAGE, E. K. PARKINSON AND S. S. PRIME (2013).** "Progression of genotype-specific oral cancer leads to senescence of cancer-associated fibroblasts and is mediated by oxidative stress and TGF-beta." Carcinogenesis **34**(6): 1286-1295.

**HASTINGS, J. F., J. N. SKHINAS, D. FEY, D. R. CROUCHER AND T. R. COX (2019).** "The extracellular matrix as a key regulator of intracellular signalling networks." Br J Pharmacol **176**(1): 82-92.

**HAWINKELS, L. J., M. PAAUWE, H. W. VERSPAGET, E. WIERCINSKA, J. M. VAN DER ZON, K. VAN DER PLOEG, P. J. KOELINK, J. H. LINDEMAN, W. MESKER, P. TEN DIJKE AND C. F. SIER (2014).** "Interaction with colon cancer cells hyperactivates TGF-β signaling in cancer-associated fibroblasts." Oncogene **33**(1): 97-107.

**HAY, E. D. (1995).** "An overview of epithelio-mesenchymal transformation." Acta Anat (Basel) **154**(1): 8-20.

**HAYASHI, H. AND T. SAKAI (2012).** "Biological Significance of Local TGF-β Activation in Liver Diseases." Frontiers in physiology **3**: 12-12.

**HILL, C. S., J. WYNNE AND R. TREISMAN (1995).** "The Rho family GTPases RhoA, Rac1, and CDC42Hs regulate transcriptional activation by SRF." Cell **81**(7): 1159-1170.

**HINSON, J. S., M. D. MEDLIN, K. LOCKMAN, J. M. TAYLOR AND C. P. MACK (2007).** "Smooth muscle cell-specific transcription is regulated by nuclear localisation of the myocardin-related transcription factors." American Journal of Physiology-Heart and Circulatory Physiology **292**(2): H1170-H1180.

**HINZ, B. (2007).** "Formation and function of the myofibroblast during tissue repair." J Invest Dermatol **127**(3): 526-537.

**HINZ, B., G. CELETTA, J. J. TOMASEK, G. GABBIANI AND C. CHAPONNIER (2001).** "Alpha-smooth muscle actin expression upregulates fibroblast contractile activity." Molecular biology of the cell **12**(9): 2730-2741.

**HINZ, B., S. H. PHAN, V. J. THANNICKAL, A. GALLI, M. L. BOCHATON-PIALLAT AND G. GABBIANI (2007).** "The myofibroblast: one function, multiple origins." Am J Pathol **170**(6): 1807-1816.

**HINZ, B., S. H. PHAN, V. J. THANNICKAL, M. PRUNOTTO, A. DESMOULIÈRE, J. VARGA, O. DE WEVER, M. MAREEL AND G. GABBIANI (2012).** "Recent developments in myofibroblast biology: paradigms for connective tissue remodeling." Am J Pathol **180**(4): 1340-1355.

**HOLSTEIN, I., A. K. SINGH, F. POHL, D. MISIAK, J. BRAUN, L. LEITNER, S. HÜTTELMAIER AND G. POSERN (2020).** "Post-transcriptional regulation of MRTF-A by miRNAs during myogenic differentiation of myoblasts." Nucleic Acids Research **48**(16): 8927-8942.

**HORWITZ, E. M. AND A. KEATING (2000).** "Nonhematopoietic mesenchymal stem cells: what are they?" Cytotherapy **2**(5): 387-388.

**HORWITZ, E. M., K. LE BLANC, M. DOMINICI, I. MUELLER, I. SLAPER-CORTENBACH, F. C. MARINI, R. J. DEANS, D. S. KRAUSE, A. KEATING AND T. INTERNATIONAL SOCIETY FOR CELLULAR (2005).** "Clarification of the nomenclature for MSC: The International Society for Cellular Therapy position statement." Cytotherapy **7**(5): 393-395.

**IORIO, M. V. AND C. M. CROCE (2012).** "MicroRNA dysregulation in cancer: diagnostics, monitoring and therapeutics. A comprehensive review." EMBO Mol Med **4**(3): 143-159.

**ISHII, G., T. SANGAI, T. ITO, T. HASEBE, Y. ENDOH, H. SASAKI, K. HARIGAYA AND A. OCHIAI (2005).** "In vivo andin vitro characterization of human fibroblasts recruited selectively into human cancer stroma." International Journal of Cancer **117**(2): 212-220.

**IWANO, M., D. PLIETH, T. M. DANOFF, C. XUE, H. OKADA AND E. G. NEILSON (2002).** "Evidence that fibroblasts derive from epithelium during tissue fibrosis." J Clin Invest **110**(3): 341-350.

**JACOBSOHN, D. A. AND G. B. VOGELSANG (2007).** "Acute graft versus host disease." Orphanet J Rare Dis **2**: 35.

**JAFARINEJAD-FARSANGI, S., F. GHARIBDOOST, A. FARAZMAND, H. KAVOSI, A. JAMSHIDI, E. KARIMIZADEH, F. NOORBAKHSH AND M. MAHMOUDI (2019).** "MicroRNA-21 and microRNA-29a modulate the expression of collagen in dermal fibroblasts of patients with systemic sclerosis." Autoimmunity **52**(3): 108-116.

**JEON, E. S., H. J. MOON, M. J. LEE, H. Y. SONG, Y. M. KIM, M. CHO, D.-S. SUH, M.-S. YOON, C. L. CHANG, J. S. JUNG AND J. H. KIM (2008).** "Cancer-derived lysophosphatidic acid stimulates differentiation of human mesenchymal stem cells to myofibroblast-like cells." Stem cells (Dayton, Ohio) **26**(3): 789-797.

**JIANG, H., G. ZHANG, J. H. WU AND C. P. JIANG (2014).** "Diverse roles of miR-29 in cancer (review)." Oncol Rep **31**(4): 1509-1516.

**JO, C. H., Y. G. LEE, W. H. SHIN, H. KIM, J. W. CHAI, E. C. JEONG, J. E. KIM, H. SHIM, J. S. SHIN, I. S. SHIN, J. C. RA, S. OH AND K. S. YOON (2014).** "Intra-articular injection of mesenchymal stem cells for the treatment of osteoarthritis of the knee: a proof-of-concept clinical trial." Stem Cells **32**(5): 1254-1266.

**JOHNSON, L. A., E. S. RODANSKY, A. J. HAAK, S. D. LARSEN, R. R. NEUBIG AND P. D. HIGGINS (2014).** "Novel Rho/MRTF/SRF inhibitors block matrix-stiffness and TGF-beta-induced fibrogenesis in human colonic myofibroblasts." Inflamm Bowel Dis **20**(1): 154-165.

**JOYCE, J. A. AND J. W. POLLARD (2009).** "Microenvironmental regulation of metastasis." Nat Rev Cancer **9**(4): 239-252.

**JUNG, S., K. M. PANCHALINGAM, R. D. WUERTH, L. ROSENBERG AND L. A. BEHIE (2012).** "Large-scale production of human mesenchymal stem cells for clinical applications." Biotechnol Appl Biochem **59**(2): 106-120.

**KALITA, K., G. KHAREBAVA, J. J. ZHENG AND M. HETMAN (2006).** "Role of megakaryoblastic acute leukemia-1 in ERK1/2-dependent stimulation of serum response factor-driven transcription by BDNF or increased synaptic activity." J Neurosci **26**(39): 10020-10032.

**KALLURI, R. (2016).** "The biology and function of fibroblasts in cancer." Nat Rev Cancer **16**(9): 582-598.

**KALLURI, R. AND E. G. NEILSON (2003).** "Epithelial-mesenchymal transition and its implications for fibrosis." J Clin Invest **112**(12): 1776-1784.

**KALLURI, R. AND M. ZEISBERG (2006A).** "Fibroblasts in cancer." Nat Rev Cancer **6**(5): 392-401.

**KALLURI, R. AND M. ZEISBERG (2006B).** "Fibroblasts in cancer." Nature Reviews Cancer **6**(5): 392-401.

**KARNOUB, A. E., A. B. DASH, A. P. VO, A. SULLIVAN, M. W. BROOKS, G. W. BELL, A. L. RICHARDSON, K. POLYAK, R. TUBO AND R. A. WEINBERG (2007).** "Mesenchymal stem cells within tumour stroma promote breast cancer metastasis." Nature **449**(7162): 557-563.

**KEHLET, S. N., R. SANZ-PAMPLONA, S. BRIX, D. J. LEEMING, M. A. KARSDAL AND V. MORENO (2016).** "Excessive collagen turnover products are released during colorectal cancer progression and elevated in serum from metastatic colorectal cancer patients." Scientific Reports **6**(1): 30599.

**KERN, S., H. EICHLER, J. STOEVE, H. KLUTER AND K. BIEBACK (2006).** "Comparative analysis of mesenchymal stem cells from bone marrow, umbilical cord blood, or adipose tissue." Stem Cells **24**(5): 1294-1301.

**KHAKOO, A. Y., S. PATI, S. A. ANDERSON, W. REID, M. F. ELSHAL, ROVIRA, II, A. T. NGUYEN, D. MALIDE, C. A. COMBS, G. HALL, J. ZHANG, M. RAFFELD, T. B. ROGERS, W. STETLER-STEVENSON, J. A. FRANK, M. REITZ AND T. FINKEL (2006).** "Human mesenchymal stem cells exert potent antitumorigenic effects in a model of Kaposi's sarcoma." J Exp Med **203**(5): 1235-1247.

**KHALIL, N. (1999A).** "TGF-beta: from latent to active." Microbes Infect **1**(15): 1255-1263.

**KHALIL, N. (1999B).** "TGF - beta : from latent to active." Microbes and Infection **1**(15): 1255-1263.

**KNAUPER, V., B. SMITH, C. LOPEZ-OTIN AND G. MURPHY (1997).** "Activation of progelatinase B (proMMP-9) by active collagenase-3 (MMP-13)." Eur J Biochem **248**(2): 369-373.

**KOJIMA, Y., A. ACAR, E. N. EATON, K. T. MELLODY, C. SCHEEL, I. BEN-PORATH, T. T. ONDER, Z. C. WANG, A. L. RICHARDSON, R. A. WEINBERG AND A. ORIMO (2010).** "Autocrine TGF-beta and stromal cell-derived factor-1 (SDF-1) signaling drives the evolution of tumor-promoting mammary stromal myofibroblasts." Proc Natl Acad Sci U S A **107**(46): 20009-20014.

**KOLACZKOWSKA, E. AND P. KUBES (2013).** "Neutrophil recruitment and function in health and inflammation." Nat Rev Immunol **13**(3): 159-175.

**KRIEGEL, A. J., Y. LIU, Y. FANG, X. DING AND M. LIANG (2012).** "The miR-29 family: genomics, cell biology, and relevance to renal and cardiovascular injury." Physiological Genomics **44**(January 2012): 237-244.

**KRTOLICA, A., S. PARRINELLO, S. LOCKETT, P. Y. DESPREZ AND J. CAMPISI (2001).** "Senescent fibroblasts promote epithelial cell growth and tumorigenesis: a link between cancer and aging." Proc Natl Acad Sci U S A **98**(21): 12072-12077.

**KRÜTZFELDT, J., S. KUWAJIMA, R. BRAICH, K. G. RAJEEV, J. PENA, T. TUSCHL, M. MANOHARAN AND M. STOFFEL (2007).** "Specificity, duplex degradation and subcellular localisation of antagomirs." Nucleic Acids Res **35**(9): 2885-2892.

**KUBICZKOVA, L., L. SEDLARIKOVA, R. HAJEK AND S. SEVCIKOVA (2012).** "TGF-β – an excellent servant but a bad master." Journal of Translational Medicine **10**(1): 183.

**KUIPERS, E. J., W. M. GRADY, D. LIEBERMAN, T. SEUFFERLEIN, J. J. SUNG, P. G. BOELENS, C. J. VAN DE VELDE AND T. WATANABE (2015).** "Colorectal cancer." Nat Rev Dis Primers **1**: 15065.

**KUROSE, K., K. GILLEY, S. MATSUMOTO, P. H. WATSON, X. P. ZHOU AND C. ENG (2002).** "Frequent somatic mutations in PTEN and TP53 are mutually exclusive in the stroma of breast carcinomas." Nat Genet **32**(3): 355-357.

**KURPINSKI, K., H. LAM, J. CHU, A. WANG, A. KIM, E. TSAY, S. AGRAWAL, D. V. SCHAFFER AND S. LI (2010).** "Transforming growth factor-beta and notch signaling mediate stem cell differentiation into smooth muscle cells." Stem Cells **28**(4): 734-742.

**KUWAHARA, K., T. BARRIENTOS, G. C. PIPES, S. LI AND E. N. OLSON (2005).** "Muscle-specific signaling mechanism that links actin dynamics to serum response factor." Mol Cell Biol **25**(8): 3173-3181.

**KWON, J. J., T. D. FACTORA, S. DEY AND J. KOTA (2019).** "A Systematic Review of miR-29 in Cancer." Mol Ther Oncolytics **12**: 173-194.

**LACERDA, L., B. G. DEBEB, D. SMITH, R. LARSON, T. SOLLEY, W. XU, S. KRISHNAMURTHY, Y. GONG, L. B. LEVY, T. BUCHHOLZ, N. T. UENO, A. KLOPP AND W. A. WOODWARD (2015).** "Mesenchymal stem cells mediate the clinical phenotype of inflammatory breast cancer in a preclinical model." Breast Cancer Res **17**: 42.

**LAEMMLI, U. K. (1970).** "Cleavage of structural proteins during the assembly of the head of bacteriophage T4." Nature **227**(5259): 680-685.

**LANZONI, G., F. ALVIANO, C. MARCHIONNI, L. BONSI, R. COSTA, L. FORONI, G. RODA, A. BELLUZZI, A. CAPONI, F. RICCI, P. LUIGI TAZZARI, P. PAGLIARO, R. RIZZO, F. LANZA, O. ROBERTO BARICORDI, G. PASQUINELLI, E. RODA AND G. PAOLO BAGNARA (2009).** "Isolation of stem cell populations with trophic and immunoregulatory functions from human intestinal tissues: potential for cell therapy in inflammatory bowel disease." Cytotherapy **11**(8): 1020-1031.

**LAWRENCE, D. A., R. PIRCHER, C. KRYCEVE-MARTINERIE AND P. JULLIEN (1984).** "Normal embryo fibroblasts release transforming growth factors in a latent form." J Cell Physiol **121**(1): 184-188.

**LEE, O. K., T. K. KUO, W. M. CHEN, K. D. LEE, S. L. HSIEH AND T. H. CHEN (2004A).** "Isolation of multipotent mesenchymal stem cells from umbilical cord blood." Blood **103**(5): 1669-1675.

**LEE, R. H., B. KIM, I. CHOI, H. KIM, H. S. CHOI, K. SUH, Y. C. BAE AND J. S. JUNG (2004B).** "Characterization and expression analysis of mesenchymal stem cells from human bone marrow and adipose tissue." Cell Physiol Biochem **14**(4-6): 311-324.

**LEI, X., Y. LEI, J. K. LI, W. X. DU, R. G. LI, J. YANG, J. LI, F. LI AND H. B. TAN (2020).** "Immune cells within the tumor microenvironment: Biological functions and roles in cancer immunotherapy." Cancer Lett **470**: 126-133.

**LI, C., P. JIANG, S. WEI, X. XU AND J. WANG (2020).** "Regulatory T cells in tumor microenvironment: new mechanisms, potential therapeutic strategies and future prospects." Mol Cancer **19**(1): 116.

**LI, H., X. FAN AND J. HOUGHTON (2007).** "Tumor microenvironment: the role of the tumor stroma in cancer." J Cell Biochem **101**(4): 805-815.

**LI, J., N. BOWENS, L. CHENG, X. ZHU, M. CHEN, S. HANNENHALLI, T. P. CAPPOLA AND M. S. PARMACEK (2012).** "Myocardin-like protein 2 regulates TGFbeta signaling in embryonic stem cells and the developing vasculature." Development **139**(19): 3531-3542.

**LI, J., X. ZHU, M. CHEN, L. CHENG, D. ZHOU, M. M. LU, K. DU, J. A. EPSTEIN AND M. S. PARMACEK (2005).** "Myocardin-related transcription factor B is required in cardiac neural crest for smooth muscle differentiation and cardiovascular development." Proc Natl Acad Sci U S A **102**(25): 8916-8921.

**LI, Q., D. ZHANG, Y. WANG, P. SUN, X. HOU, J. LARNER, X. WUJUN AND J. MI (2013).** "MiR-21/Smad 7 signaling determines TGF- b1-induced CAF formation." Scientific Reports **3**: 2038-2038.

**LI, S., S. CHANG, X. QI, J. A. RICHARDSON AND E. N. OLSON (2006).** "Requirement of a myocardin-related transcription factor for development of mammary myoepithelial cells." Mol Cell Biol **26**(15): 5797-5808.

**LI, S., D. Z. WANG, Z. WANG, J. A. RICHARDSON AND E. N. OLSON (2003).** "The serum response factor coactivator myocardin is required for vascular smooth muscle development." Proc Natl Acad Sci U S A **100**(16): 9366-9370.

**LI, Z., M. Q. HASSAN, M. JAFFERJI, R. I. AQEILAN, R. GARZON, C. M. CROCE, A. J. VAN WIJNEN, J. L. STEIN, G. S. STEIN AND J. B. LIAN (2009).** "Biological Functions of miR-29b Contribute to Positive Regulation of Osteoblast Differentiation*." Journal of Biological Chemistry **284**(23): 15676-15684.

**LIU, R. AND J. P. JIN (2016).** "Calponin isoforms CNN1, CNN2 and CNN3: Regulators for actin cytoskeleton functions in smooth muscle and non-muscle cells." Gene **585**(1): 143-153.

**LIU, T., L. ZHOU, D. LI, T. ANDL AND Y. ZHANG (2019).** "Cancer-Associated Fibroblasts Build and Secure the Tumor Microenvironment." Front Cell Dev Biol **7**: 60.

**LIU, Y., J. ZHANG, X. SUN, Q. SU AND C. YOU (2017).** "Down-regulation of miR-29b in carcinoma associated fibroblasts promotes cell growth and metastasis of breast cancer." Oncotarget **8**(24): 39559-39570.

**LONGO, P. A., J. M. KAVRAN, M. S. KIM AND D. J. LEAHY (2013).** "Transient mammalian cell transfection with polyethylenimine (PEI)." Methods Enzymol **529**: 227-240.

**LUCHSINGER, L. L., C. A. PATENAUDE, B. D. SMITH AND M. D. LAYNE (2011).** "Myocardin-related transcription factor-A complexes activate type I collagen expression in lung fibroblasts." J Biol Chem **286**(51): 44116-44125.

**LYU, Q., V. DHAGIA, Y. HAN, B. GUO, M. E. WINES-SAMUELSON, C. K. CHRISTIE, Q. YIN, O. J. SLIVANO, P. HERRING, X. LONG, S. A. GUPTE AND J. M. MIANO (2018).** "CRISPR-Cas9-Mediated Epitope Tagging Provides Accurate and Versatile Assessment of Myocardin-Brief Report." Arterioscler Thromb Vasc Biol **38**(9): 2184-2190.

**MA, Z., S. W. MORRIS, V. VALENTINE, M. LI, J. A. HERBRICK, X. CUI, D. BOUMAN, Y. LI, P. K. MEHTA, D. NIZETIC, Y. KANEKO, G. C. CHAN, L. C. CHAN, J. SQUIRE, S. W. SCHERER AND J. K. HITZLER (2001).** "Fusion of two novel genes, RBM15 and MKL1, in the t(1;22)(p13;q13) of acute megakaryoblastic leukemia." Nat Genet **28**(3): 220-221.

**MAIMELA, N. R., S. LIU AND Y. ZHANG (2018).** "Fates of CD8+ T cells in Tumor Microenvironment." Computational and structural biotechnology journal **17**: 1-13.

**MAREEL, M. AND S. CONSTANTINO (2011).** "Ecosystems of invasion and metastasis in mammary morphogenesis and cancer." Int J Dev Biol **55**(7-9): 671-684.

**MARTINEZ-OUTSCHOORN, U. E., S. PAVLIDES, D. WHITAKER-MENEZES, K. M. DAUMER, J. N. MILLIMAN, B. CHIAVARINA, G. MIGNECO, A. K. WITKIEWICZ, M. P. MARTINEZ-CANTARIN, N. FLOMENBERG, A. HOWELL, R. G. PESTELL, M. P. LISANTI AND F. SOTGIA (2010).** "Tumor cells induce the cancer associated fibroblast phenotype via caveolin-1 degradation: implications for breast cancer and DCIS therapy with autophagy inhibitors." Cell Cycle **9**(12): 2423-2433.

**MAZZIERI, R., J. S. MUNGER AND D. B. RIFKIN (2000).** "Measurement of active TGF-beta generated by cultured cells." Methods in molecular biology **142**(2): 13-27.

**MEDJKANE, S., C. PEREZ-SANCHEZ, C. GAGGIOLI, E. SAHAI AND R. TREISMAN (2009).** "Myocardin-related transcription factors and SRF are required for cytoskeletal dynamics and experimental metastasis." Nature cell biology **11**(3): 257-268.

**MELE, V., M. G. MURARO, D. CALABRESE, D. PFAFF, N. AMATRUDA, F. AMICARELLA, B. KVINLAUG, C. BOCELLI-TYNDALL, I. MARTIN, T. J. RESINK, M. HEBERER, D. OERTLI, L. TERRACCIANO, G. C. SPAGNOLI AND G. IEZZI (2014).** "Mesenchymal stromal cells induce epithelial-to-mesenchymal transition in human colorectal cancer cells through the expression of surface-bound TGF-beta." Int J Cancer **134**(11): 2583-2594.

**MELLONE, M., C. J. HANLEY, S. THIRDBOROUGH, T. MELLOWS, E. GARCIA, J. WOO, J. TOD, S. FRAMPTON, V. JENEI, K. A. MOUTASIM, T. D. KABIR, P. A. BRENNAN, G. VENTURI, K. FORD, N. HERRANZ, K. P. LIM, J. CLARKE, D. W. LAMBERT, S. S. PRIME, T. J. UNDERWOOD, P. VIJAYANAND, K. W. ELICEIRI, C. WOELK, E. V. KING, J. GIL, C. H. OTTENSMEIER AND G. J. THOMAS (2016).** "Induction of fibroblast senescence generates a non-fibrogenic myofibroblast phenotype that differentially impacts on cancer prognosis." Aging (Albany NY) **9**(1): 114-132.

**MELZER, C., J. VON DER OHE AND R. HASS (2018).** "Concise Review: Crosstalk of Mesenchymal Stroma/Stem-Like Cells with Cancer Cells Provides Therapeutic Potential." Stem cells **36**(7): 951-968.

**MERCHER, T., M. B. CONIAT, R. MONNI, M. MAUCHAUFFE, F. NGUYEN KHAC, L. GRESSIN, F. MUGNERET, T. LEBLANC, N. DASTUGUE, R. BERGER AND O. A. BERNARD (2001).** "Involvement of a human gene related to the Drosophila spen gene in the recurrent t(1;22) translocation of acute megakaryocytic leukemia." Proc Natl Acad Sci U S A **98**(10): 5776-5779.

**MIANO, J. M. (2015).** "Myocardin in biology and disease." J Biomed Res **29**(1): 3-19.

**MIANO, J. M., X. LONG AND K. FUJIWARA (2007).** "Serum response factor: master regulator of the actin cytoskeleton and contractile apparatus." Am J Physiol Cell Physiol **292**(1): C70-81.

**MICALLEF, L., N. VEDRENNE, F. BILLET, B. COULOMB, I. A. DARBY AND A. DESMOULIERE (2012).** "The myofibroblast, multiple origins for major roles in normal and pathological tissue repair." Fibrogenesis Tissue Repair **5**(Suppl 1): S5.

**MICHIELSEN, A. J., A. E. HOGAN, J. MARRY, M. TOSETTO, F. COX, J. M. HYLAND, K. D. SHEAHAN, D. P. O'DONOGHUE, H. E. MULCAHY, E. J. RYAN AND J. N. O'SULLIVAN (2011).** "Tumour tissue microenvironment can inhibit dendritic cell maturation in colorectal cancer." PloS one **6**(11): e27944-e27944.

**MILLS, C. D., K. KINCAID, J. M. ALT, M. J. HEILMAN AND A. M. HILL (2000).** "M-1/M-2 Macrophages and the Th1/Th2 Paradigm." The Journal of Immunology **164**(12): 6166.

**MIRALLES, F., G. POSERN, A.-I. ZAROMYTIDOU AND R. TREISMAN (2003).** "Actin Dynamics Control SRF Activity by Regulation of Its Coactivator MAL." Cell **113**(3): 329-342.

**MISHRA, P. J., P. J. MISHRA, R. HUMENIUK, D. J. MEDINA, G. ALEXE, J. P. MESIROV, S. GANESAN, J. W. GLOD AND D. BANERJEE (2008).** "Carcinoma-associated fibroblast-like differentiation of human mesenchymal stem cells." Cancer Res **68**(11): 4331-4339.

**MITTL, P. R., J. P. PRIESTLE, D. A. COX, G. MCMASTER, N. CERLETTI AND M. G. GRÜTTER (1996).** "The crystal structure of TGF-beta 3 and comparison to TGF-beta 2: implications for receptor binding." Protein Sci **5**(7): 1261-1271.

**MIYAZONO, K., A. OLOFSSON, P. COLOSETTI AND C. H. HELDIN (1991).** "A role of the latent TGF-beta 1-binding protein in the assembly and secretion of TGF-beta 1." Embo j **10**(5): 1091-1101.

**MOINFAR, F., Y. G. MAN, L. ARNOULD, G. L. BRATTHAUER, M. RATSCHEK AND F. A. TAVASSOLI (2000).** "Concurrent and independent genetic alterations in the stromal and epithelial cells of mammary carcinoma: implications for tumorigenesis." Cancer Res **60**(9): 2562-2566.

**MOREIRA, A., S. KAHLENBERG AND P. HORNSBY (2017).** "Therapeutic potential of mesenchymal stem cells for diabetes." Journal of molecular endocrinology **59**(3): R109-R120.

**MOUILLERON, S., S. GUETTLER, C. A. LANGER, R. TREISMAN AND N. Q. MCDONALD (2008).** "Molecular basis for G-actin binding to RPEL motifs from the serum response factor coactivator MAL." EMBO J **27**(23): 3198-3208.

**MRAZEK, A. A., J. R. CARMICAL, T. G. WOOD, M. R. HELLMICH, M. ELTORKY, F. J. BOHANON AND C. CHAO (2014).** "Colorectal Cancer-Associated Fibroblasts are Genotypically Distinct." Curr Cancer Ther Rev **10**(2): 97-218.

**MUELLER, L. P., J. LUETZKENDORF, T. MUELLER, K. REICHELT, H. SIMON AND H.-J. SCHMOLL (2006).** "Presence of mesenchymal stem cells in human bone marrow after exposure to chemotherapy: evidence of resistance to apoptosis induction." Stem cells **24**: 2753-2765.

**MUGURUMA, Y., T. YAHATA, H. MIYATAKE, T. SATO, T. UNO, J. ITOH, S. KATO, M. ITO, T. HOTTA AND K. ANDO (2006).** "Reconstitution of the functional human hematopoietic microenvironment derived from human mesenchymal stem cells in the murine bone marrow compartment." Blood **107**(5): 1878-1887.

**MULLIS, K., F. FALOONA, S. SCHARF, R. SAIKI, G. HORN AND H. ERLICH (1986).** "Specific enzymatic amplification of DNA in vitro: the polymerase chain reaction." Cold Spring Harb Symp Quant Biol **51 Pt 1**: 263-273.

**NATIONAL LIBRARY OF MEDICINE.** (2021, April 4th). "ClinicalTrials.gov." from https://www.clinicaltrials.gov/ct2/home.

**NISHIDA, N., H. YANO, T. NISHIDA, T. KAMURA AND M. KOJIRO (2006).** "Angiogenesis in cancer." Vasc Health Risk Manag **2**(3): 213-219.

**NOVOYATLEVA, T., Y. SCHYMURA, W. JANSSEN, F. STROBL, J. M. SWIERCZ, C. PATRA, G. POSERN, A. WIETELMANN, T. S. ZHENG, R. T. SCHERMULY AND F. B. ENGEL (2013).** "Deletion of Fn14 receptor protects from right heart fibrosis and dysfunction." Basic Research in Cardiology **108**(2): 1-13.

**NOWELL, P. C. (1976).** "The clonal evolution of tumor cell populations." Science **194**(4260): 23-28.

**O'BRIEN, J., H. HAYDER, Y. ZAYED AND C. PENG (2018).** "Overview of MicroRNA Biogenesis, Mechanisms of Actions, and Circulation." Frontiers in endocrinology **9**: 402-402.

**OH, J., J. A. RICHARDSON AND E. N. OLSON (2005).** "Requirement of myocardin-related transcription factor-B for remodeling of branchial arch arteries and smooth muscle differentiation." Proc Natl Acad Sci U S A **102**(42): 15122-15127.

**OLOFSSON, A., K. MIYAZONO, T. KANZAKI, P. COLOSETTI, U. ENGSTRÖM AND C. H. HELDIN (1992).** "Transforming growth factor-beta 1, -beta 2, and -beta 3 secreted by a human glioblastoma cell line. Identification of small and different forms of large latent complexes." J Biol Chem **267**(27): 19482-19488.

**OLSON, E. N. AND A. NORDHEIM (2010).** "Linking actin dynamics and gene transcription to drive cellular motile functions." Nature Reviews Molecular Cell Biology **11**(5): 353-365.

**ORIMO, A., P. B. GUPTA, D. C. SGROI, F. ARENZANA-SEISDEDOS, T. DELAUNAY, R. NAEEM, V. J. CAREY, A. L. RICHARDSON AND R. A. WEINBERG (2005).** "Stromal fibroblasts present in invasive human breast carcinomas promote tumor growth and angiogenesis through elevated SDF-1/CXCL12 secretion." Cell **121**(3): 335-348.

**ØROM, U. A., F. C. NIELSEN AND A. H. LUND (2008).** "MicroRNA-10a Binds the 5′UTR of Ribosomal Protein mRNAs and Enhances Their Translation." Molecular Cell **30**(4): 460-471.

**OTRANTO, M., V. SARRAZY, F. BONTE, B. HINZ, G. GABBIANI AND A. DESMOULIERE (2012).** "The role of the myofibroblast in tumor stroma remodeling." Cell Adh Migr **6**(3): 203-219.

**PAN, Z., Y. TIAN, G. NIU AND C. CAO (2020A).** "Role of microRNAs in remodeling the tumor microenvironment (Review)." International Journal of Oncology **56**(2): 407-416.

**PAN, Z., Y. TIAN, G. NIU AND C. CAO (2020B).** "Role of microRNAs in remodeling the tumor microenvironment (Review)." Int J Oncol **56**(2): 407-416.

**PAWLOWSKI, R., E. K. RAJAKYLA, M. K. VARTIAINEN AND R. TREISMAN (2010).** "An actin-regulated importin alpha/beta-dependent extended bipartite NLS directs nuclear import of MRTF-A." EMBO J **29**(20): 3448-3458.

**PEFANI, D.-E., D. PANKOVA, ASWIN G. ABRAHAM, ANNA M. GRAWENDA, N. VLAHOV, S. SCRACE AND E. O' NEILL (2016).** "TGF-β Targets the Hippo Pathway Scaffold RASSF1A to Facilitate YAP/SMAD2 Nuclear Translocation." Molecular Cell **63**(1): 156-166.

**PENG, Q., Z. FENG, Y. SHEN, J. ZHU, L. ZOU, Y. SHEN AND Y. ZHU (2019).** "Integrated analyses of microRNA-29 family and the related combination biomarkers demonstrate their widespread influence on risk, recurrence, metastasis and survival outcome in colorectal cancer." Cancer cell international **19**: 181-181.

**PERDIGUERO, E. G. AND F. GEISSMANN (2016).** "The development and maintenance of resident macrophages." Nat Immunol **17**(1): 2-8.

**PETERSEN, O. W., H. LIND NIELSEN, T. GUDJONSSON, R. VILLADSEN, L. RONNOV-JESSEN AND M. J. BISSELL (2001).** "The plasticity of human breast carcinoma cells is more than epithelial to mesenchymal conversion." Breast Cancer Res **3**(4): 213-217.

**PETERSEN, O. W., H. L. NIELSEN, T. GUDJONSSON, R. VILLADSEN, F. RANK, E. NIEBUHR, M. J. BISSELL AND L. RONNOV-JESSEN (2003).** "Epithelial to mesenchymal transition in human breast cancer can provide a nonmalignant stroma." Am J Pathol **162**(2): 391-402.

**PETRENKO, Y., I. VACKOVA, K. KEKULOVA, M. CHUDICKOVA, Z. KOCI, K. TURNOVCOVA, H. KUPCOVA SKALNIKOVA, P. VODICKA AND S. KUBINOVA (2020).** "A Comparative Analysis of Multipotent Mesenchymal Stromal Cells derived from Different Sources, with a Focus on Neuroregenerative Potential." Sci Rep **10**(1): 4290.

**PFAFFL, M. W. (2001).** "A new mathematical model for relative quantification in real-time RT-PCR." Nucleic Acids Res **29**(9): e45.

**PHILIPPAR, U., G. SCHRATT, C. DIETERICH, J. M. MULLER, P. GALGOCZY, F. B. ENGEL, M. T. KEATING, F. GERTLER, R. SCHULE, M. VINGRON AND A. NORDHEIM (2004).** "The SRF target gene Fhl2 antagonizes RhoA/MAL-dependent activation of SRF." Mol Cell **16**(6): 867-880.

**PIENTA, K. J., N. MCGREGOR, R. AXELROD AND D. E. AXELROD (2008).** "Ecological therapy for cancer: defining tumors using an ecosystem paradigm suggests new opportunities for novel cancer treatments." Transl Oncol **1**(4): 158-164.

**PIETRAS, K. AND A. OSTMAN (2010).** "Hallmarks of cancer: interactions with the tumor stroma." Exp Cell Res **316**(8): 1324-1331.

**PIPES, G. C., E. E. CREEMERS AND E. N. OLSON (2006).** "The myocardin family of transcriptional coactivators: versatile regulators of cell growth, migration, and myogenesis." Genes Dev **20**(12): 1545-1556.

**PITTENGER, M. F., D. E. DISCHER, B. M. PÉAULT, D. G. PHINNEY, J. M. HARE AND A. I. CAPLAN (2019).** "Mesenchymal stem cell perspective: cell biology to clinical progress." npj Regenerative Medicine **4**(1): 22.

**PITTENGER, M. F., A. M. MACKAY, S. C. BECK, R. K. JAISWAL, R. DOUGLAS, J. D. MOSCA, M. A. MOORMAN, D. W. SIMONETTI, S. CRAIG AND D. R. MARSHAK (1999).** "Multilineage potential of adult human mesenchymal stem cells." Science **284**(5411): 143-147.

**PLESSNER, M. AND R. GROSSE (2015).** "Extracellular signaling cues for nuclear actin polymerisation." Eur J Cell Biol **94**(7-9): 359-362.

**PLESSNER, M., M. MELAK, P. CHINCHILLA, C. BAARLINK AND R. GROSSE (2015).** "Nuclear F-actin formation and reorganization upon cell spreading." J Biol Chem **290**(18): 11209-11216.

**PONTE, A. L., E. MARAIS, N. GALLAY, A. LANGONNE, B. DELORME, O. HERAULT, P. CHARBORD AND J. DOMENECH (2007).** "The in vitro migration capacity of human bone marrow mesenchymal stem cells: comparison of chemokine and growth factor chemotactic activities." Stem Cells **25**(7): 1737-1745.

**POSERN, G. AND R. TREISMAN (2006).** "Actin' together: serum response factor, its cofactors and the link to signal transduction." Trends Cell Biol **16**(11): 588-596.

**POWELL, D. W., P. A. ADEGBOYEGA, J. F. DI MARI AND R. C. MIFFLIN (2005).** "Epithelial cells and their neighbors I. Role of intestinal myofibroblasts in development, repair, and cancer." Am J Physiol Gastrointest Liver Physiol **289**(1): G2-7.

**PROCKOP, D. J. (1997).** "Marrow stromal cells as stem cells for nonhematopoietic tissues." Science **276**(5309): 71-74.

**PSAILA, B. AND D. LYDEN (2009).** "The metastatic niche: adapting the foreign soil." Nat Rev Cancer **9**(4): 285-293.

**PUNNONEN, J., D. ROSEN, L. ZUNIGA, K. SPROGØE AND M. TABRIZI (2019).** "Cytokine Therapeutics in Cancer Immunotherapy: Design and Development." Current Pharmacology Reports **5**(5): 377-390.

**QIN, W., A. C. CHUNG, X. R. HUANG, X. M. MENG, D. S. HUI, C. M. YU, J. J. SUNG AND H. Y. LAN (2011).** "TGF-β/Smad3 signaling promotes renal fibrosis by inhibiting miR-29." J Am Soc Nephrol **22**(8): 1462-1474.

**QUANTE, M., S. P. TU, H. TOMITA, T. GONDA, S. S. WANG, S. TAKASHI, G. H. BAIK, W. SHIBATA, B. DIPRETE, K. S. BETZ, R. FRIEDMAN, A. VARRO, B. TYCKO AND T. C. WANG (2011).** "Bone marrow-derived myofibroblasts contribute to the mesenchymal stem cell niche and promote tumor growth." Cancer Cell **19**(2): 257-272.

**RADISKY, D. C., P. A. KENNY AND M. J. BISSELL (2007).** "Fibrosis and cancer: do myofibroblasts come also from epithelial cells via EMT?" J Cell Biochem **101**(4): 830-839.

**RADISKY, D. C., D. D. LEVY, L. E. LITTLEPAGE, H. LIU, C. M. NELSON, J. E. FATA, D. LEAKE, E. L. GODDEN, D. G. ALBERTSON, M. A. NIETO, Z. WERB AND M. J. BISSELL (2005).** "Rac1b and reactive oxygen species mediate MMP-3-induced EMT and genomic instability." Nature **436**(7047): 123-127.

**RASMUSSON, I. (2006).** "Immune modulation by mesenchymal stem cells." Exp Cell Res **312**(12): 2169-2179.

**REN, G., L. ZHANG, X. ZHAO, G. XU, Y. ZHANG, A. I. ROBERTS, R. C. ZHAO AND Y. SHI (2008).** "Mesenchymal stem cell-mediated immunosuppression occurs via concerted action of chemokines and nitric oxide." Cell Stem Cell **2**(2): 141-150.

**RINGUETTE GOULET, C., G. BERNARD, S. TREMBLAY, S. CHABAUD, S. BOLDUC AND F. POULIOT (2018).** "Exosomes Induce Fibroblast Differentiation into Cancer-Associated Fibroblasts through TGFβ Signaling." Mol Cancer Res **16**(7): 1196-1204.

**RØNNOV-JESSEN, L. AND O. W. PETERSEN (1993).** "Induction of alpha-smooth muscle actin by transforming growth factor-beta 1 in quiescent human breast gland fibroblasts. Implications for myofibroblast generation in breast neoplasia." Lab Invest **68**(6): 696-707.

**ROTTER, N., J. ODER, P. SCHLENKE, U. LINDNER, F. BOHRNSEN, J. KRAMER, J. ROHWEDEL, R. HUSS, S. BRANDAU, B. WOLLENBERG AND S. LANG (2008).** "Isolation and characterization of adult stem cells from human salivary glands." Stem Cells Dev **17**(3): 509-518.

**ROY, L. O., M. B. POIRIER AND D. FORTIN (2015).** "Transforming growth factor-beta and its implication in the malignancy of gliomas." Target Oncol **10**(1): 1-14.

**SAKURAI, T. AND M. KUDO (2011).** "Signaling pathways governing tumor angiogenesis." Oncology **81 Suppl 1**: 24-29.

**SANGER, F., S. NICKLEN AND A. R. COULSON (1977).** "DNA sequencing with chain-terminating inhibitors " Proc Natl Acad Sci U S A **74**(12): 5463-5467.

**SANTI, A., F. G. KUGERATSKI AND S. ZANIVAN (2018).** "Cancer Associated Fibroblasts: The Architects of Stroma Remodeling." Proteomics **18**(5-6): e1700167.

**SANTIBANEZ, J. F., M. QUINTANILLA AND C. BERNABEU (2011).** "TGF-beta/TGF-beta receptor system and its role in physiological and pathological conditions." Clin Sci (Lond) **121**(6): 233-251.

**SAXTON, R. A., C. R. GLASSMAN AND K. C. GARCIA (2023).** "Emerging principles of cytokine pharmacology and therapeutics." Nat Rev Drug Discov **22**(1): 21-37.

**SCHINDELIN, J., I. ARGANDA-CARRERAS, E. FRISE, V. KAYNIG, M. LONGAIR, T. PIETZSCH, S. PREIBISCH, C. RUEDEN, S. SAALFELD, B. SCHMID, J. Y. TINEVEZ, D. J. WHITE, V. HARTENSTEIN, K. ELICEIRI, P. TOMANCAK AND A. CARDONA (2012).** "Fiji: an open-source platform for biological-image analysis." Nat Methods **9**(7): 676-682.

**SCHMITZ, N., S. LAVERTY, V. B. KRAUS AND T. AIGNER (2010).** "Basic methods in histopathology of joint tissues." Osteoarthritis and Cartilage **18**: S113-S116.

**SCHOSSERER, M., J. GRILLARI AND M. BREITENBACH (2017).** "The Dual Role of Cellular Senescence in Developing Tumors and Their Response to Cancer Therapy." Front Oncol **7**: 278.

**SEIFERT, A. AND G. POSERN (2017).** "Tightly controlled MRTF-A activity regulates epithelial differentiation during formation of mammary acini." Breast Cancer Res **19**(1): 68.

**SELVARAJ, A. AND R. PRYWES (2004).** "Expression profiling of serum inducible genes identifies a subset of SRF target genes that are MKL dependent." BMC Mol Biol **5**: 13.

**SHANGGUAN, L., X. TI, U. KRAUSE, B. HAI, Y. ZHAO, Z. YANG AND F. LIU (2012A).** "Inhibition of TGF-beta/Smad signaling by BAMBI blocks differentiation of human mesenchymal stem cells to carcinoma-associated fibroblasts and abolishes their protumor effects." Stem Cells **30**(12): 2810-2819.

**SHANGGUAN, L., X. TI, U. KRAUSE, B. HAI, Y. ZHAO, Z. YANG AND F. LIU (2012B).** "Inhibition of TGF-β/Smad signaling by BAMBI blocks differentiation of human mesenchymal stem cells to carcinoma-associated fibroblasts and abolishes their protumor effects." Stem Cells **30**: 2810-2819.

**SHINAGAWA, K., Y. KITADAI, M. TANAKA, T. SUMIDA, M. KODAMA, Y. HIGASHI, S. TANAKA, W. YASUI AND K. CHAYAMA (2010).** "Mesenchymal stem cells enhance growth and metastasis of colon cancer." Int J Cancer **127**(10): 2323-2333.

**SHORE, P. AND A. D. SHARROCKS (1995).** "The MADS-box family of transcription factors." Eur J Biochem **229**(1): 1-13.

**SMALL, E. M. (2012).** "The Actin-MRTF-SRF gene regulatory axis and myofibroblast differentiation." Journal of Cardiovascular Translational Research **5**(6): 794-804.

**SMALL, E. M., J. E. THATCHER, L. B. SUTHERLAND, H. KINOSHITA, R. D. GERARD, J. A. RICHARDSON, J. M. DIMAIO, H. SADEK, K. KUWAHARA AND E. N. OLSON (2010).** "Myocardin-related transcription factor-a controls myofibroblast activation and fibrosis in response to myocardial infarction." Circulation research **107**(2): 294-304.

**SMITHERS, D. W. (1962).** "An attack on cytologism." Lancet **1**(7228): 493-499.

**SOCOVICH, A. M. AND A. NABA (2019).** "The cancer matrisome: From comprehensive characterization to biomarker discovery." Semin Cell Dev Biol **89**: 157-166.

**SOTIROPOULOS, A., D. GINEITIS, J. COPELAND AND R. TREISMAN (1999).** "Signal-regulated activation of serum response factor is mediated by changes in actin dynamics." Cell **98**(2): 159-169.

**SPAETH, E., A. KLOPP, J. DEMBINSKI, M. ANDREEFF AND F. MARINI (2008).** "Inflammation and tumor microenvironments: defining the migratory itinerary of mesenchymal stem cells." Gene Ther **15**(10): 730-738.

**SQUILLARO, T., G. PELUSO AND U. GALDERISI (2016).** "Clinical Trials With Mesenchymal Stem Cells: An Update." Cell Transplant **25**(5): 829-848.

**STRACK, R. L., B. HEIN, D. BHATTACHARYYA, S. W. HELL, R. J. KEENAN AND B. S. GLICK (2009).** "A rapidly maturing far-red derivative of DsRed-Express2 for whole-cell labeling." Biochemistry **48**(35): 8279-8281.

**SUDRES, M., F. NOROL, A. TRENADO, S. GREGOIRE, F. CHARLOTTE, B. LEVACHER, J. J. LATAILLADE, P. BOURIN, X. HOLY, J. P. VERNANT, D. KLATZMANN AND J. L. COHEN (2006).** "Bone marrow mesenchymal stem cells suppress lymphocyte proliferation in vitro but fail to prevent graft-versus-host disease in mice." J Immunol **176**(12): 7761-7767.

**SUN, B., K. H. ROH, J. R. PARK, S. R. LEE, S. B. PARK, J. W. JUNG, S. K. KANG, Y. S. LEE AND K. S. KANG (2009).** "Therapeutic potential of mesenchymal stromal cells in a mouse breast cancer metastasis model." Cytotherapy **11**(3): 289-298, 281 p following 298.

**SUN, Y., K. BOYD, W. XU, J. MA, C. W. JACKSON, A. FU, J. M. SHILLINGFORD, G. W. ROBINSON, L. HENNIGHAUSEN, J. K. HITZLER, Z. MA AND S. W. MORRIS (2006).** "Acute myeloid leukemia-associated Mkl1 (Mrtf-a) is a key regulator of mammary gland function." Mol Cell Biol **26**(15): 5809-5826.

**SUZUKI, H. I., A. KATSURA, H. MATSUYAMA AND K. MIYAZONO (2015).** "MicroRNA regulons in tumor microenvironment." Oncogene **34**(24): 3085-3094.

**TALMADGE, J. E. AND D. I. GABRILOVICH (2013).** "History of myeloid-derived suppressor cells." Nature reviews. Cancer **13**(10): 739-752.

**TAMPE, B. AND M. ZEISBERG (2014).** "Contribution of genetics and epigenetics to progression of kidney fibrosis." Nephrol Dial Transplant **29 Suppl 4**: iv72-79.

**TAN, H. X., Z. B. CAO, T. T. HE, T. HUANG, C. L. XIANG AND Y. LIU (2019).** "TGFβ1 is essential for MSC-CAFs differentiation and promotes HCT116 cells migration and invasion via JAK/STAT3 signaling." Onco Targets Ther **12**: 5323-5334.

**TAN, S., L. XIA, P. YI, Y. HAN, L. TANG, Q. PAN, Y. TIAN, S. RAO, L. OYANG, J. LIANG, J. LIN, M. SU, Y. SHI, D. CAO, Y. ZHOU AND Q. LIAO (2020).** "Exosomal miRNAs in tumor microenvironment." Journal of Experimental & Clinical Cancer Research **39**(1): 67.

**TANG, W., Y. ZHU, J. GAO, J. FU, C. LIU, Y. LIU, C. SONG, S. ZHU, Y. LENG, G. WANG, W. CHEN, P. DU, S. HUANG, X. ZHOU, J. KANG AND L. CUI (2014).** "MicroRNA-29a promotes colorectal cancer metastasis by regulating matrix metalloproteinase 2 and E-cadherin via KLF4." Br J Cancer **110**(2): 450-458.

**TAO, L., G. HUANG, H. SONG, Y. CHEN AND L. CHEN (2017).** "Cancer associated fibroblasts: An essential role in the tumor microenvironment." Oncol Lett **14**(3): 2611-2620.

**TARIN, D. AND C. B. CROFT (1969).** "Ultrastructural features of wound healing in mouse skin." J Anat **105**(Pt 1): 189-190.

**TAYLOR, M., R. TREISMAN, N. GARRETT AND T. MOHUN (1989).** "Muscle-specific (CArG) and serum-responsive (SRE) promoter elements are functionally interchangeable in Xenopus embryos and mouse fibroblasts." Development **106**(1): 67-78.

**TAYLOR, M. A., Y. H. LEE AND W. P. SCHIEMANN (2011).** "Role of TGF-beta and the tumor microenvironment during mammary tumorigenesis." Gene Expr **15**(3): 117-132.

**TIAN, M. AND W. P. SCHIEMANN (2009).** "The TGF-beta paradox in human cancer: an update." Future Oncol **5**(2): 259-271.

**TOMASEK, J. J., G. GABBIANI, B. HINZ, C. CHAPONNIER AND R. A. BROWN (2002).** "Myofibroblasts and mechano-regulation of connective tissue remodelling." Nat Rev Mol Cell Biol **3**(5): 349-363.

**TOMMELEIN, J., L. VERSET, T. BOTERBERG, P. DEMETTER, M. BRACKE AND O. DE WEVER (2015).** "Cancer-associated fibroblasts connect metastasis-promoting communication in colorectal cancer." Front Oncol **5**: 63.

**TOULLEC, A., D. GERALD, G. DESPOUY, B. BOURACHOT, M. CARDON, S. LEFORT, M. RICHARDSON, G. RIGAILL, M. C. PARRINI, C. LUCCHESI, D. BELLANGER, M. H. STERN, T. DUBOIS, X. SASTRE-GARAU, O. DELATTRE, A. VINCENT-SALOMON AND F. MECHTA-GRIGORIOU (2010).** "Oxidative stress promotes myofibroblast differentiation and tumour spreading." EMBO Mol Med **2**(6): 211-230.

**TREISMAN, R. (1985).** "Transient accumulation of c-fos RNA following serum stimulation requires a conserved 5' element and c-fos 3' sequences." Cell **42**(3): 889-902.

**TREISMAN, R. (1986).** "Identification of a protein-binding site that mediates transcriptional response of the c-fos gene to serum factors." Cell **46**(4): 567-574.

**TREMAIN, R., M. MARKO, V. KINNIMULKI, H. UENO, E. BOTTINGER AND A. GLICK (2000).** "Defects in TGF-beta signaling overcome senescence of mouse keratinocytes expressing v-Ha-ras." Oncogene **19**(13): 1698-1709.

**TRUESDELL, S. S., R. D. MORTENSEN, M. SEO, J. C. SCHROEDER, J. H. LEE, O. LETONQUEZE AND S. VASUDEVAN (2012).** "MicroRNA-mediated mRNA Translation Activation in Quiescent Cells and Oocytes Involves Recruitment of a Nuclear microRNP." Scientific Reports **2**(1): 842.

**TUHKANEN, H., M. ANTTILA, V. M. KOSMA, S. YLA-HERTTUALA, S. HEINONEN, A. KURONEN, M. JUHOLA, R. TAMMI, M. TAMMI AND A. MANNERMAA (2004).** "Genetic alterations in the peritumoral stromal cells of malignant and borderline epithelial ovarian tumors as indicated by allelic imbalance on chromosome 3p." Int J Cancer **109**(2): 247-252.

**URIBE-QUEROL, E. AND C. ROSALES (2015).** "Neutrophils in Cancer: Two Sides of the Same Coin." J Immunol Res **2015**: 983698.

**VALKENBURG, K. C., A. E. DE GROOT AND K. J. PIENTA (2018).** "Targeting the tumour stroma to improve cancer therapy." Nat Rev Clin Oncol **15**(6): 366-381.

**VALTIERI, M. AND A. SORRENTINO (2008).** "The mesenchymal stromal cell contribution to homeostasis." J Cell Physiol **217**(2): 296-300.

**VAN DER VEEKEN, J., A. J. GONZALEZ, H. CHO, A. ARVEY, S. HEMMERS, C. S. LESLIE AND A. Y. RUDENSKY (2016).** "Memory of Inflammation in Regulatory T Cells." Cell **166**(4): 977-990.

**VAN ROOIJ, E., L. B. SUTHERLAND, J. E. THATCHER, J. M. DIMAIO, R. H. NASEEM, W. S. MARSHALL, J. A. HILL AND E. N. OLSON (2008).** "Dysregulation of microRNAs after myocardial infarction reveals a role of miR-29 in cardiac fibrosis." Proceedings of the National Academy of Sciences of the United States of America **105**(35): 13027-13032.

**VARTIAINEN, M. K., S. GUETTLER, B. LARIJANI AND R. TREISMAN (2007).** "Nuclear actin regulates dynamic subcellular localisation and activity of the SRF cofactor MAL." Science **316**(5832): 1749-1752.

**VASUDEVAN, S. (2012).** "Posttranscriptional upregulation by microRNAs." Wiley Interdiscip Rev RNA **3**(3): 311-330.

**VASUDEVAN, S. AND J. A. STEITZ (2007).** "AU-Rich-Element-Mediated Upregulation of Translation by FXR1 and Argonaute 2." Cell **128**(6): 1105-1118.

**VEGLIA, F., M. PEREGO AND D. GABRILOVICH (2018).** "Myeloid-derived suppressor cells coming of age." Nat Immunol **19**(2): 108-119.

**VELASQUEZ, L. S., L. B. SUTHERLAND, Z. LIU, F. GRINNELL, K. E. KAMM, J. W. SCHNEIDER, E. N. OLSON AND E. M. SMALL (2013).** "Activation of MRTF-A-dependent gene expression with a small molecule promotes myofibroblast differentiation and wound healing." Proc Natl Acad Sci U S A **110**(42): 16850-16855.

**VIJAYACHANDRA, K., J. LEE AND A. B. GLICK (2003).** "Smad3 regulates senescence and malignant conversion in a mouse multistage skin carcinogenesis model." Cancer Res **63**(13): 3447-3452.

**VOLINIA, S., G. A. CALIN, C. G. LIU, S. AMBS, A. CIMMINO, F. PETROCCA, R. VISONE, M. IORIO, C. ROLDO, M. FERRACIN, R. L. PRUEITT, N. YANAIHARA, G. LANZA, A. SCARPA, A. VECCHIONE, M. NEGRINI, C. C. HARRIS AND C. M. CROCE (2006).** "A microRNA expression signature of human solid tumors defines cancer gene targets." Proc Natl Acad Sci U S A **103**(7): 2257-2261.

**VONG, S. AND R. KALLURI (2011).** "The role of stromal myofibroblast and extracellular matrix in tumor angiogenesis." Genes Cancer **2**(12): 1139-1145.

**VOSKOBOINIK, I., M. J. SMYTH AND J. A. TRAPANI (2006).** "Perforin-mediated target-cell death and immune homeostasis." Nat Rev Immunol **6**(12): 940-952.

**WAGNER, W., F. WEIN, A. SECKINGER, M. FRANKHAUSER, U. WIRKNER, U. KRAUSE, J. BLAKE, C. SCHWAGER, V. ECKSTEIN, W. ANSORGE AND A. D. HO (2005).** "Comparative characteristics of mesenchymal stem cells from human bone marrow, adipose tissue, and umbilical cord blood." Exp Hematol **33**(11): 1402-1416.

**WALENDA, G., K. ABNAOF, S. JOUSSEN, S. MEURER, H. SMEETS, B. RATH, K. HOFFMANN, H. FRÖHLICH, M. ZENKE, R. WEISKIRCHEN AND W. WAGNER (2013).** "TGF-beta1 does not induce senescence of multipotent mesenchymal stromal cells and has similar effects in early and late passages." PloS one **8**(10): e77656-e77656.

**WANG, D., P. S. CHANG, Z. WANG, L. SUTHERLAND, J. A. RICHARDSON, E. SMALL, P. A. KRIEG AND E. N. OLSON (2001).** "Activation of cardiac gene expression by myocardin, a transcriptional cofactor for serum response factor." Cell **105**(7): 851-862.

**WANG, D. Z., S. LI, D. HOCKEMEYER, L. SUTHERLAND, Z. WANG, G. SCHRATT, J. A. RICHARDSON, A. NORDHEIM AND E. N. OLSON (2002).** "Potentiation of serum response factor activity by a family of myocardin-related transcription factors." Proceedings of the National Academy of Sciences **99**(23): 14855-14860.

**WANG, Q., T. LI, W. WU AND G. DING (2020).** "Interplay between mesenchymal stem cell and tumor and potential application." Hum Cell.

**WANG, T., F. NOTTA, R. NAVAB, J. JOSEPH, E. IBRAHIMOV, J. XU, C. Q. ZHU, A. BORGIDA, S. GALLINGER AND M. S. TSAO (2017).** "Senescent Carcinoma-Associated Fibroblasts Upregulate IL8 to Enhance Prometastatic Phenotypes." Mol Cancer Res **15**(1): 3-14.

**WANG, T., L. ZHANG, C. SHI, H. SUN, J. WANG, R. LI, Z. ZOU, X. RAN AND Y. SU (2012).** "TGF-β-induced miR-21 negatively regulates the antiproliferative activity but has no effect on EMT of TGF-β in HaCaT cells." Int J Biochem Cell Biol **44**(2): 366-376.

**WANG, X., W. ZHANG, X. SUN, Y. LIN AND W. CHEN (2018).** "Cancer-associated fibroblasts induce epithelial-mesenchymal transition through secreted cytokines in endometrial cancer cells." Oncol Lett **15**(4): 5694-5702.

**WANG, Y., X. CHEN, W. CAO AND Y. SHI (2014).** "Plasticity of mesenchymal stem cells in immunomodulation: pathological and therapeutic implications." Nat Immunol **15**(11): 1009-1016.

**WANG, Z., D. Z. WANG, G. C. PIPES AND E. N. OLSON (2003).** "Myocardin is a master regulator of smooth muscle gene expression." Proc Natl Acad Sci U S A **100**(12): 7129-7134.

**WERNER, S., J. LÜTZKENDORF, T. MÜLLER, L. P. MÜLLER AND G. POSERN (2019).** "MRTF-A controls myofibroblastic differentiation of human multipotent stromal cells and their tumour-supporting function in xenograft models." Scientific Reports **9**.

**WHO.** (2021). "Cancer." Retrieved 03.01., 2021, from https://www.who.int/health-topics/cancer#tab=tab_1.

**WIDDER, M., J. LÜTZKENDORF, H. CAYSA, S. UNVERZAGT, C. WICKENHAUSER, R. A. BENNDORF, H. J. SCHMOLL, C. MÜLLER-TIDOW, T. MÜLLER AND L. P. MÜLLER (2016).** "Multipotent mesenchymal stromal cells promote tumor growth in distinct colorectal cancer cells by a beta1-integrin-dependent mechanism." Int J Cancer **138**(4): 964-975.

**WIENHOLDS, E. AND R. H. PLASTERK (2005).** "MicroRNA function in animal development." FEBS Lett **579**(26): 5911-5922.

**WINKLER, J., A. ABISOYE-OGUNNIYAN, K. J. METCALF AND Z. WERB (2020).** "Concepts of extracellular matrix remodelling in tumour progression and metastasis." Nature Communications **11**(1): 5120.

**WINTER, J., S. JUNG, S. KELLER, R. I. GREGORY AND S. DIEDERICHS (2009).** "Many roads to maturity: microRNA biogenesis pathways and their regulation." Nature cell biology **11**(3): 228-234.

**WONG, S. P., J. E. ROWLEY, A. N. REDPATH, J. D. TILMAN, T. G. FELLOUS AND J. R. JOHNSON (2015).** "Pericytes, mesenchymal stem cells and their contributions to tissue repair." Pharmacol Ther **151**: 107-120.

**WYNN, T. A., A. CHAWLA AND J. W. POLLARD (2013).** "Macrophage biology in development, homeostasis and disease." Nature **496**(7446): 445-455.

**YANG, S., S. BANERJEE, A. FREITAS, H. CUI, N. XIE, E. ABRAHAM AND G. LIU (2012).** "miR-21 regulates chronic hypoxia-induced pulmonary vascular remodeling." Am J Physiol Lung Cell Mol Physiol **302**(6): L521-529.

**YANG, Z., Z. MU, B. DABOVIC, V. JURUKOVSKI, D. YU, J. SUNG, X. XIONG AND J. S. MUNGER (2007).** "Absence of integrin-mediated TGFbeta1 activation in vivo recapitulates the phenotype of TGFbeta1-null mice." J Cell Biol **176**(6): 787-793.

**YAO, Q., S. CAO, C. LI, A. MENGESHA, B. KONG AND M. WEI (2011).** "Micro-RNA-21 regulates TGF-??-induced myofibroblast differentiation by targeting PDCD4 in tumor-stroma interaction." International Journal of Cancer **128**: 1783-1792.

**YOON, H., C.-M. TANG, S. BANERJEE, A. L. DELGADO, M. YEBRA, J. DAVIS AND J. K. SICKLICK (2021).** "TGF-β1-mediated transition of resident fibroblasts to cancer-associated fibroblasts promotes cancer metastasis in gastrointestinal stromal tumor." Oncogenesis **10**(2): 13.

**YOSHIDA, T., K. KAWAI-KOWASE AND G. K. OWENS (2004).** "Forced expression of myocardin is not sufficient for induction of smooth muscle differentiation in multipotential embryonic cells." Arterioscler Thromb Vasc Biol **24**(9): 1596-1601.

**YOSHIDA, T., S. SINHA, F. DANDRE, B. R. WAMHOFF, M. H. HOOFNAGLE, B. E. KREMER, D. Z. WANG, E. N. OLSON AND G. K. OWENS (2003).** "Myocardin is a key regulator of CArG-dependent transcription of multiple smooth muscle marker genes." Circ Res **92**(8): 856-864.

**YOSHIMURA, H., M. MICHISHITA, K. OHKUSU-TSUKADA, Y. MATSUDA, T. ISHIWATA, Z. NAITO AND K. TAKAHASHI (2015).** "Cellular sources of tenascin-C in canine mammary carcinomas." Vet Pathol **52**(1): 92-96.

**YU, Q. AND I. STAMENKOVIC (2000).** "Cell surface-localized matrix metalloproteinase-9 proteolytically activates TGF-beta and promotes tumor invasion and angiogenesis." Genes Dev **14**(2): 163-176.

**ZEISBERG, E. M. AND M. ZEISBERG (2013).** "The role of promoter hypermethylation in fibroblast activation and fibrogenesis." J Pathol **229**(2): 264-273.

**ZEISBERG, M., J. HANAI, H. SUGIMOTO, T. MAMMOTO, D. CHARYTAN, F. STRUTZ AND R. KALLURI (2003).** "BMP-7 counteracts TGF-beta1-induced epithelial-to-mesenchymal transition and reverses chronic renal injury." Nat Med **9**(7): 964-968.

**ZEISBERG, M. AND R. KALLURI (2004).** "The role of epithelial-to-mesenchymal transition in renal fibrosis." J Mol Med (Berl) **82**(3): 175-181.

**ZHANG, Z., Y. WANG, J. ZHANG, J. ZHONG AND R. YANG (2018).** "COL1A1 promotes metastasis in colorectal cancer by regulating the WNT/PCP pathway." Molecular medicine reports **17**(4): 5037-5042.

**ZHOU, J., Y. NEFEDOVA, A. LEI AND D. GABRILOVICH (2018).** "Neutrophils and PMN-MDSC: Their biological role and interaction with stromal cells." Seminars in immunology **35**: 19-28.

**ZHOU, R., C. WANG, C. WEN AND D. WANG (2017).** "miR-21 promotes collagen production in keloid via Smad7." Burns **43**(3): 555-561.

**ZHU, W., W. XU, R. JIANG, H. QIAN, M. CHEN, J. HU, W. CAO, C. HAN AND Y. CHEN (2006).** "Mesenchymal stem cells derived from bone marrow favor tumor cell growth in vivo." Exp Mol Pathol **80**(3): 267-274.

**ZIOGAS, D. E., C. KATSIOS AND D. H. ROUKOS (2011).** "From traditional molecular biology to network oncology." Future Oncol **7**(2): 155-159.

# LIST OF FIGURES

# LIST OF TABLES

# LIST OF ABBREVIATIONS

| Abbreviation | Meaning |
|---|---|
| °C | Degree Celsius |
| 3'UTR | 3' untranslated region |
| 5'UTR | 5' untranslated region |
| Ag | Antigen |
| ALAS | Delta-aminolevulinate synthase 1 |
| ATP | Adenosine triphosphate |
| BCA | Bicinchoninic acid |
| BMPs | Bone morphogenetic proteins |
| bp | Base pair |
| BSA | Albumin fraction from bovine serum |
| CAF | Carcinoma-associated fibroblasts |
| CArG box | Consensus SRF-binding site (CC(A/T)6GG) |
| CDC42 | Cell division control protein 42 homolog |
| cDNA | Complementary DNA |
| CFU-F | Colony-forming unit fibroblasts |
| ChIP-seq | Chromatin immunoprecipitation DNA sequencing |
| CNN1 | Calponin 1 |
| Col1A1 | Collagen 1A1 |
| CRC | Colorectal cancer |
| CTGF | Connective tissue growth factor |
| CYR61 | Cysteine-rich angiogenic inducer 61 |
| DMEM | Dubelcco's modified Eagle medium |
| DMF | N,N-dimethylformamide |
| DMSO | Dimethyl sulfoxide |
| DNA | Deoxyribonucleic acid |
| ECM | Extracellular matrix |
| EDTA | Ethylene-diamine-tetra-acetic acid |
| EGF | Epidermal growth factor |
| EMT | Epithelial-mesenchymal transition |
| FCS | Fetal calf serum |
| GAPDH | Glyceraldehyde 3-phosphate dehydrogenase |
| GDNF | Glial cell line-derived neurotrophic factor |
| GFP | Green fluorescent protein |
| GvHD | Graft-versus-host disease |
| $H_2O$ | Water |
| $H_2O_2$ | Hydrogen peroxide |
| HCT8 | Human colorectal epithelial cells |
| HGF | Hepatocyte growth factor |
| HPL | Human platelet lysate |
| HRP | Horseradish peroxidase |
| IL-10 | Interleukin10 |
| IL-2 | Interleukin 2 |
| IL-6 | Interleukin 6 |

| | |
|---|---|
| IMR-90 | Human fetal lung fibroblasts |
| kb | Kilobase |
| KD | Knockdown |
| kDa | Kilodalton |
| KLF4 | Kruppel-like factor 4 |
| KO | Knockout |
| LAP | Latency-associated peptide |
| LB | Lysogeny broth |
| LLC | Large latent complex |
| LTBP | Latent TGF-β binding protein |
| LTR | Long terminal repeat |
| LZ | Leucine zipper |
| MADS | MCM1, Agamous, Deficiens, SRF |
| mDia | Mammalian Diaphanous-related formin |
| MDSCs | Myeloid-derived suppressor cells |
| MHC I | Major histocompatibility complex class I molecules |
| miR | MicroRNA |
| MKL1 | Megakaryoblastic leukaemia 1 |
| M-MDSCs | Monocytic myeloid-derived suppressor cells |
| MMP | Matrix metalloproteinases |
| mRNA | Messenger RNA |
| MRTF | Myocardin-related transcription factor |
| MRTF-A | Myocardin-related transcription factor A |
| MRTF-b | Myocardin-related transcription factor B |
| MSC | Multipotent mesenchymal stromal cells |
| MYOCD | Myocardin |
| NAF | Normally activated fibroblasts |
| NK | Natural killer |
| NRK52E | NRK52E |
| PAGE | Polyacrylamide gel electrophoresis |
| PASMC | Human pulmonary arterial smooth muscle cells |
| PBS | Phosphate buffered saline |
| PCR | Polymerase chain reaction |
| PDCD4 | Programmed Cell Death 4 |
| PEI | Polyethylenimine |
| PMN-MDSCs | Polymorphonuclear myeloid-derived suppressor cells |
| pre-miR | Precursor hairpin |
| pri-miR | Primary miR |
| pSMAD2 | Phosphorylated SMAD2 |
| PTEN | Phosphatase and Tensin homolog |
| PVDF | Polyvinylidene fluoride |
| qPCR | Quantitative real-time PCR |
| RAC1 | Ras-related C3 botulinum toxin substrate 1 |
| rcf | Relative centrifugal force |
| RhoA | Ras homolog family member A |
| RNA | Ribonucleic acid |
| RNAi | RNA interference |
| RPEL | Actin-binding domain with consensus sequence RPxxxEL |
| RPM | Rounds per minute |
| RPMI | Roswell Park Memorial Institute |

| | |
|---|---|
| RRE | Rev response element |
| SAP | SAF-A/B, Acinus and PIAS |
| SDF-1 | Stromal cell-derived factor 1 |
| SDS | Sodium dodecyl sulphate |
| SEM | Standard error of the mean |
| SEM | Standard error of the mean |
| siRNA | Small interfering RNA |
| SLC | Small latent complex |
| SMAD | Mothers against decapentaplegic homolog |
| SMAD2 | Mothers against decapentaplegic homolog 2 |
| SMAD7 | Mothers against decapentaplegic homolog 7 |
| SMC | Smooth-muscle cells |
| SNORD | Small Nucleolar RNA |
| SRE | Serum response element |
| SRF | Serum response factor |
| TAD | Transcriptional activation domain |
| TAM | Tumour-associated macrophages |
| TAN | Tumour-associated neutrophils |
| TBS | Tris-buffered saline |
| TBS-T | Tris-buffered saline with Tween20 |
| TCF | Ternary complex factors |
| TCM | Tumour conditioned medium |
| TEAD | TEA Domain Transcription Factors |
| TEMED | N,N,N,N-Tetramethylethylenediamine |
| TGF | Transforming Growth Factor |
| TGF-β1 | Transforming Growth Factor β 1 |
| TME | Tumour microenvironment |
| TNF | Tumour necrosis factor |
| Tregs | Regulatory T cells |
| tSMAD2 | Total SMAD2 |
| V/V | Volume to volume, percentage by volume |
| VGEF | Vascular endothelial growth factor |
| WPRE | Woodchuck hepatitis virus posttranscriptional regulatory element |
| YAP | Yes-associated protein |
| α-SMA | Alpha smooth muscle actin |

# APPENDIX

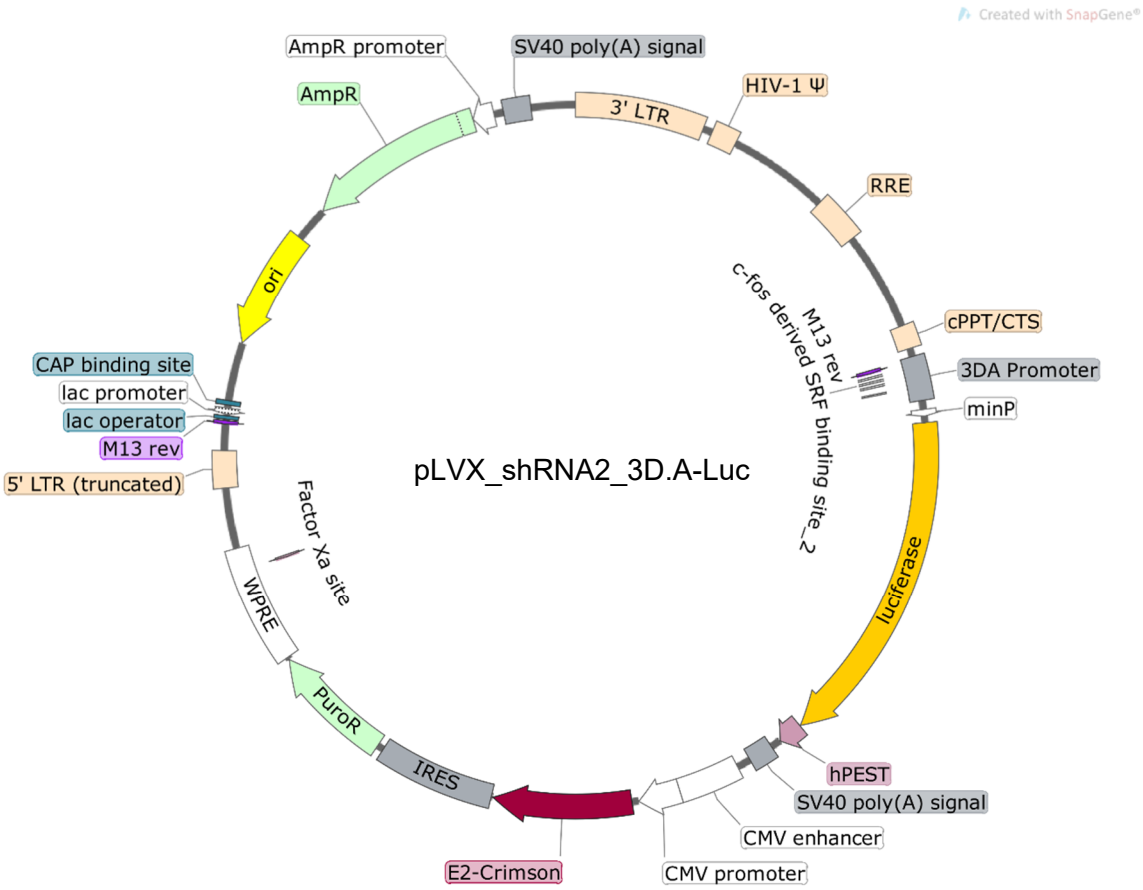


**Supplementary figure 1: Full plasmid card of pLVX_shRNA2_3D.A-Luc**
The different parts of the luciferase reporter plasmid are listed below: 3'LTR (3' long terminal repeat (LTR) from HIV-1), HIV-1ψ (packaging signal of human immunodeficiency virus type 1), RRE (Rev response element of HIV-1; allows Rev-dependent mRNA export from the nucleus to the cytoplasm), cPPT/CTS [central polypurine tract and central termination sequence of HIV-1 (lacking the first T)], 3D.A Promoter (consisting of 3 c-fos derived SRF binding sites, Xenopus laevis type 5 actin TATA-Box and M13 primer binding site for sequencing), minP (minimal TATA-box promoter with low basal activity), hPEST (PEST degradation sequence from mouse ornithine decarboxylase, human codon-optimized), SV50 poly(A) signal (SV40 polyadenylation signal), CMV enhancer (human cytomegalovirus immediate-early enhancer), CMV promoter [constitutive human cytomegalovirus (CMV) immediate early promoter], E2-Crimson (far-red noncytotoxic tetrameric variant of DsRed fluorescent protein), IRES (internal ribosome entry site of the encephalomyocarditis virus), WPRE (woodchuck hepatitis virus posttranscriptional regulatory element, enhances expression of transgenes from retroviral vectors), 5'LTR (truncated 5' long terminal repeat from HIV-1), lac operator (DNA sequence element that binds the lac repressor), lac promoter (promoter for the E. coli lac operon), CAP binding site (catabolite activator protein binding site), Ori (high-copy-number ColE1/pMB1/pBR322/pUC origin of replication) AmpR (β-lactamase), AmpR promoter (β-lactamase promoter).

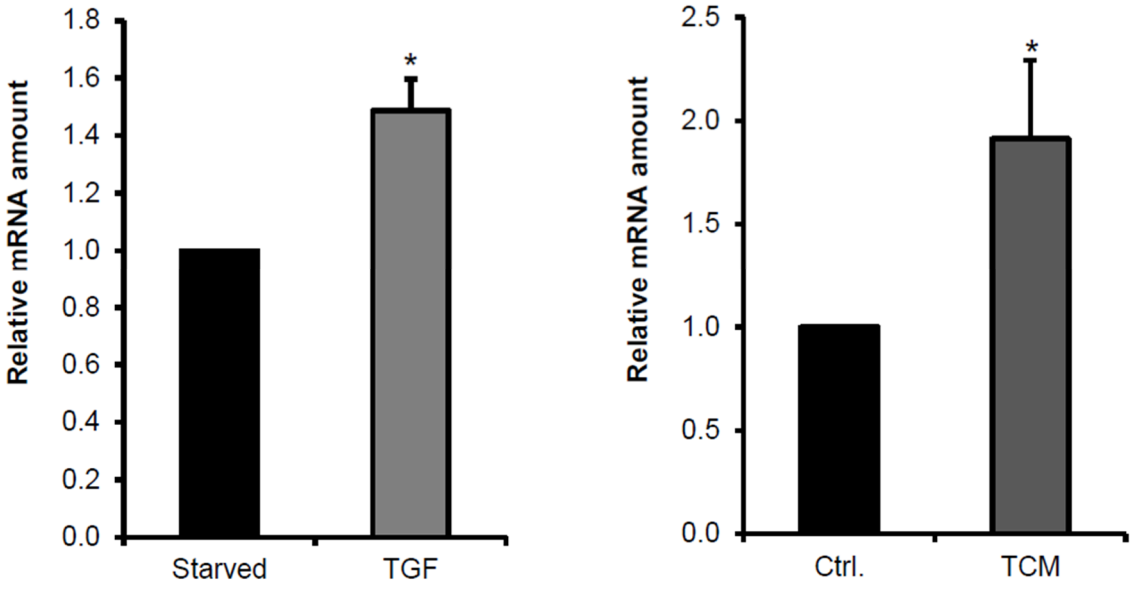


**Supplementary figure 2: TGF β 1 mRNA induction upon TGF β 1 and TCM treatment**
MSC were treated with TGF β 1 (left panel) or tumour cell conditioned medium (TCM right panel) for 24 h Relative mRNA of TGF β 1 was quantified by qPCR and normalised to ALAS and GAPDH Data were normalised to the value for the starved control or TCM Control medium (Ctrl. which was set to 1 Error bars correspond to SD (n=3) Asterisks indicate significant differences * p≤0 05 according to an unpaired Student's t test

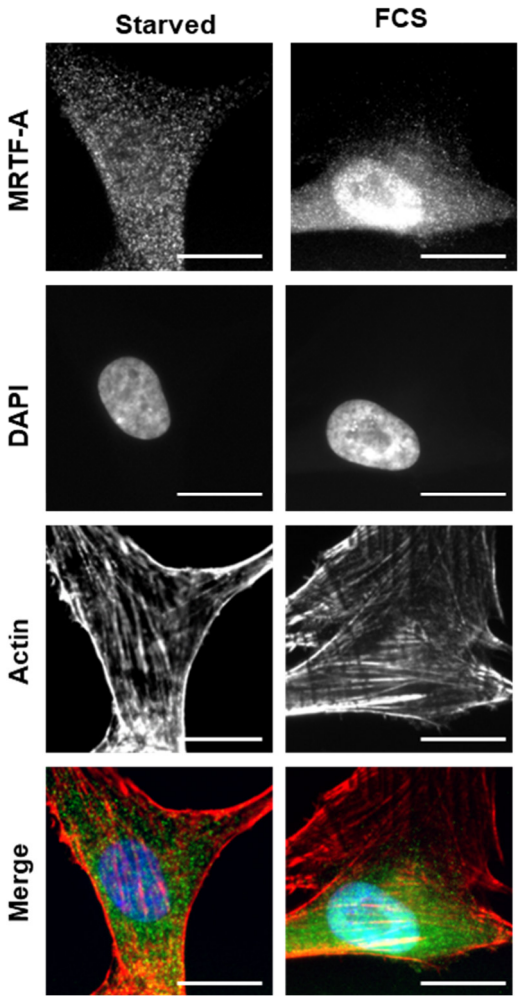


**Supplementary figure 3: Translocation of MRTF-A in MSC induced by FCS.**
Intracellular localisation of MRTF-A. Cells were immunostained with anti-MRTF-A (green), Phalloidin to display actin (red) and DNA counterstained with DAPI (blue) following 2 h of treatment with 20% FCS. 63 x magnification, scale bars 5 µm.

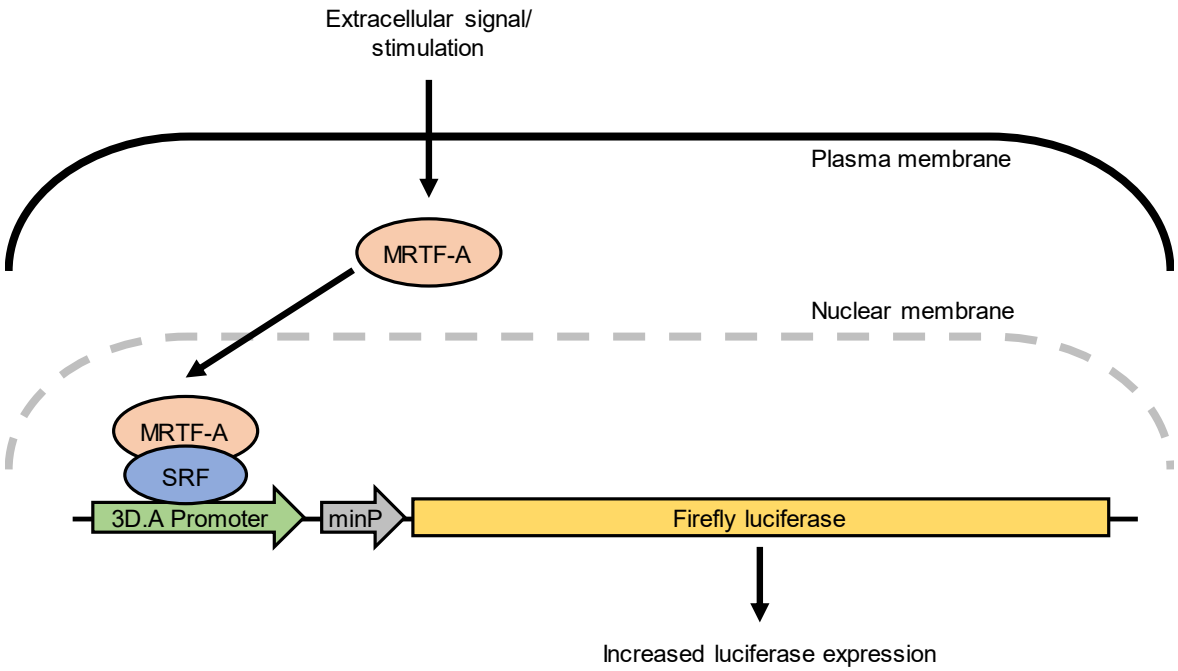


**Supplementary figure 4: Schematic diagram of the luciferase assay.**
Extracellular signals and stimuli like TGF-β1 and TCM trigger MRTF-A to translocate into the nucleus. Nuclear MRTF-A will bind to SRF as a coactivator increasing MRTF/SRF-dependent gene expression. Regarding the luciferase assay, increased nuclear MRTF-A leads to increased luciferase expression whereby the translated protein can be measured via luciferase assay after cell lysis.

# LIST OF PUBLICATIONS

Werner S, Lützkendorf J, Müller T, Müller LP, Posern G. **MRTF-A controls myofibroblastic differentiation of human multipotent stromal cells and their tumour-supporting function in xenograft models.** Sci Rep. 2019 Aug 13;9(1):11725. doi: 10.1038/s41598-019-48142-z. PMID: 31409840; PMCID: PMC6692381.

# ACKNOWLEDGEMENTS

First, I would like to express my sincere gratitude to Prof. Dr. Guido Posern for giving me the opportunity to work in his laboratory on such an interesting project. His support, especially over the extended time it took to complete this thesis, has been remarkable. I also thank him for his scientific input, general mentoring and his continued willingness to engage in thoughtful discussions.

I am also grateful to PD Dr. Lutz P. Müller and Dr. Jana Lützkendorf from the University Hospital in Halle for their collaboration, valuable input during regular meetings, and support with the animal experiments. A special thanks to Lutz for kindly agreeing to serve as my second proofreader.

I want to extend my thanks to all former and current members of the Posern group, particularly Anja Weber, Astrid Vess, Anurag Singh, Franziska Schikora, Julia Weißbach, Robert Torka, and Ingo Holstein. Thank you for creating such a warm and collegial working atmosphere, for our scientific and personal exchanges and for making each lab day memorable. You were incredible lab mates, and I am deeply thankful for the time we shared. A special thanks to Robert for proofreading my thesis.

I also want to acknowledge Herbert Neuhaus, whose support, feedback and valuable advice have been a constant source of help throughout this journey.

Thank you to all the members of the Institute for Physiological Chemistry in Halle for their collaboration and support.

To my family and friends, your encouragement throughout my life and this PhD journey have meant the world to me. A special thanks to Tina and Hendrik for your advice, and most importantly, your friendship.

Mom and Dad YOU have shaped me into who I am today.

Thank you for everything. I love you.

And to my wonderful husband, Basti—thank you for reminding me every day of my worth and for your promise to always love me. You, me, Tiga, Suri, and Krümel—together, we have everything I need for a lifetime of happiness.

.

# STATUTORY DECLARATION

I hereby declare that I wrote the present dissertation with the topic:

**Mechanisms of the MRTF-A Controlled Myofibroblastic Differentiation and its Influence on the Tumour Propagating Function of Mesenchymal Stromal Cells**

independently and used no other aids than those cited. In each individual case, I have clearly identified the source of the passages that are taken word for word or paraphrased from other works.

I apply for the doctoral degree with this thesis for the first time.

Zörbig, 25.10.2024

Sara Werner

# CURRICULUM VITAE

## Persönliche Daten:

| | |
|---|---|
| Name | Sara Werner |
| Geburtsdatum | [redacted] |
| Adresse | |
| Geburtsort | |
| Familienstand | |

## Beruflicher Werdegang:

| | |
|---|---|
| 03/2022-heute | **Regionalleiterin (Santis im Auftrag von AstraZeneca)**<br>Sachsen (Dresden und Ostsachsen)<br><br>Mitarbeiter Entwicklung, Umsatzanalyse, Businessplan Präsentation, Planung strategische Ausrichtung des Teams<br><br>Indikationen: COPD, Asthma, Diabetes, Herzinsuffizienz, Niereninsuffizienz<br>Betreute Arztgruppen: Hausärzte, Internisten, Diabetologen, Kardiologen, Nephrologen, Pneumologen |
| 10/2019-03/2022 | **Pharmareferentin (Santis im Auftrag von AstraZeneca)**<br>Sachsen-Anhalt (Halle und Umgebung)<br><br>Indikationen: COPD, Asthma, Diabetes, Herzinsuffizienz, Niereninsuffizienz<br>Betreute Arztgruppen: Hausärzte, Internisten, Diabetologen |
| 05/2014-02/2019 | **Promotion**<br><br>**Martin-Luther-Universität Halle-Wittenberg**<br><br>*Schwerpunkte:*<br>· Genregulation und Molekulare Medizin<br>· Doktorthesis: „Die Rolle von MRTF-A bei der Differenzierung tumorfördernder Stromazellen“<br>Institut für Physiologische Chemie, Abteilung Genregulation<br>(Leitung und Betreuung Prof. Dr. Guido Posern) |

## Studium & Schulausbildung:

| | |
|---|---|
| 10/2011-12/2013 | **Master-Studium im Fach Biologie**<br><br>**Martin-Luther-Universität Halle-Wittenberg**<br><br>*Schwerpunkte:*<br>· Molekulare und Allgemeine Mikrobiologie<br>· Masterthesis: „Die Charakterisierung des Magnesium-Transporters MgtE aus *Caldalkalibacillus thermarum*“<br>Institut für Mikrobiologie, Abteilung Molekulare Mikrobiologie (Leitung Prof. Dr. Dietrich H. Nies),<br>Betreut durch Dr. Falk Kalamorz |

| | |
|---|---|
| 10/2007 – 06/2011 | **Bachelor of Science im Fach Biologie**<br>**Martin-Luther-Universität Halle-Wittenberg**<br>*Schwerpunkte:*<br>· Pflanzenphysiologie/Zellphysiologie, Molekulare und Allgemeine Mikrobiologie<br>· Bachelorthesis: „Die Erstellung von *Chlamydomonas reinhardtii* Mutanten zur Untersuchung der pD1-Prozessierung“<br>Institut für Pflanzenphysiologie, Abteilung Zellphysiologie (Leitung Prof. Dr. Udo Johanningmeier)<br>Betreut durch Ivo Bertalan |
| 06/07/2007 | **Erlangen der Allgemeinen Hochschulreife**<br>**(Gymnasium Delitzsch)** |

Sara Werner Zörbig, 25.10.2024

[redacted]